SYNTHESIS OF LARGE-AREA FEW LAYER GRAPHENE FILMS BY RAPID HEATING AND COOLING IN A MODIFIED APCVD FURNACE

by

LAMUEL ABRAHAM DAVID

B. E., Anna University, 2010

A THESIS

submitted in partial fulfillment of the requirements for the degree

MASTER OF SCIENCE

Department of Mechanical and Nuclear Engineering
College of Engineering

KANSAS STATE UNIVERSITY
Manhattan, Kansas

2011

Approved by:

Major Professor
Gurpreet Singh

Copyright

Abstract

Graphene because of its unique electrical (electron mobility = 2 x 10^5 cm^{-2} V^{-1} s^{-1}), mechanical (E = 1 TPa), optical, thermal and chemical properties has generated a lot of interest among the research community in recent years. One of the most notable methods of synthesizing large area pristine graphene sheets, which are several 100 micrometers wide, is through thermal chemical vapor deposition (CVD). But very little has been known about the effects of heating and cooling rate of the substrate on the quality of graphene produced. Hence we varied various growth parameters to understand the process of graphene growth on Cu and Ni substrates when subjected to fast heating and quenching. This allowed optimization of the CVD process to achieve large-area graphene films consistently and repeatedly.

This work provides new insights on synthesis of graphene at atmospheric pressures and the effect of (a) fast heating and fast cooling of substrates, (b) catalyst type and (c) gas flow rates on quality of the graphene produced. A carbon nanotube CVD furnace was restored and modified to accommodate graphene synthesis.

We started with synthesis of graphene on Cu substrate following procedures already available in the literature (heating rate ~ 15 °C/min and cooling rate ~ 5 °C/min; total processing time 7 hours). This provided a good reference point for the particular furnace and the test setup. The best results were obtained for 15 minutes of growth at a CH_4:H_2 ratio of 1:30 at 950 °C. SEM images showed full coverage of the substrate by few layer graphene (FLG), which was indicated by the relatively high I_{2D}/I_G ratio of 0.44.

The furnace was further modified to facilitate fast cooling (~4 °C/sec) of substrate while still being in inert atmosphere (Argon). The effect of growth time and concentration of CH_4 was

studied for this modified procedure (at H_2 flow rate of 300 SCCM). SEM images showed full coverage for a CH_4 flow rate of 10 SCCM in as little as 6 minutes of growth time. This coupled with the fast cooling cycle effectively reduced the overall time of graphene synthesis by 7 times. The I_{2D}/I_G ratio in Raman spectrum was 0.4 indicating that the quality of graphene synthesized was similar to that obtained in conventional CVD.

This modification also facilitated introduction of catalyst substrate after the furnace has reached growth temperature (fast heating ~8 °C/sec). Hence, the overall time required for graphene synthesis was reduced to ~6 % (30 minutes) when compared to the traditional procedure. SEM images showed formation of high concentration few layer graphene islands. This was attributed to the impurities on the catalyst surface, which in the traditional procedure would have been etched away during the long heating period. The optimum process parameters were 30 minutes of growth with 20 SCCM of CH_4 and 300 SCCM of H_2 at 950 °C. The Raman spectrum for this condition showed a relatively high I_{2D}/I_G ratio of 0.66.

We also studied the effect of Ni as a catalyst. Similar to Cu, for Ni also, traditional procedure found in the literature was used to optimize the graphene growth for this particular furnace. Best results were obtained for 10 minutes of growth time with 120 SCCM of CH_4 in 300 SCCM of H_2 at 950 °C. SEM images showed large grain growth (~50 μm) with full coverage. The Raman spectrum showed formation of bi-layer graphene with a I_{2D}/I_G ratio of 1.03.

Later the effect of growth time and concentration of the hydrocarbon precursor for Ni substrate subjected to fast heating (~ 8 °C/sec) was studied. It was found that because the process of graphene synthesis on Ni is by segregation, growth period or gas flow rate had little effect on the

quality and size of the graphene sheets because of the presence of impurities on the substrate. This procedure yielded multilayer graphite instead of graphene under all conditions.

Future work will involve study of changing several other parameters like type of hydrocarbon precursor and pressure in the chamber for graphene synthesis. Also various other substrates like Cu or Ni based alloys will be studied to identify the behavior of graphene growth using this novel procedure.

Table of Contents

List of Figures

List of Tables

Acknowledgements

I would like to express my deep appreciation for all who helped me to complete this dissertation. First, I would like to thank my advisor, Dr. Gurpreet Singh for providing me with vital guidance as well as detailed instructions on my research projects. I also appreciate his encouragement and help on developing the right thinking and attitude towards academic research.

Special thanks to Dr. Elisabeth Mansfield (NIST, Boulder) and Dr. Stephanie Hooker (NIST, Boulder) for providing us with the CVD furnace. And also to Jim Hodgson, senior scientific glassblower for providing valuable technical advice and helping me to modify the quartz tube without which this work would not be complete.

My deepest gratitude to Dr. Qiang (KU, Lawrence) and Dr. Scott Bunch (CU, Boulder) for Raman usage.

I would like to thank my lab mate Romil Bhandavat and other engineering students for their help and support during my studies at KSU.

Financial support from National Science Foundation and Mechanical and Nuclear Engineering Department, KSU is also appreciated.

Finally, thanks to my sister, parents and relatives for their endless support all through my Masters.

Dedication

I dedicate this to my parents for their unconditional love and a constant source of encouragement and inspiration in all my academic endeavors.

Chapter 1 - Introduction

Nanotechnology is defined as the study of engineering functional systems at the molecular scale. The term nanotechnology deals with a size range between 1 to 100 nm. Nano comes from "*nanos*", a Greek word meaning dwarf. Although this is a relatively new concept, the development of the core concept happened over a longer period of time. The development of nanotechnology was guided by the invention of scanning tunneling microscope in 1981 and the discovery of fullerenes in 1985 by Harry Kroto, Richard Smalley and Robert Curl, who together won the 1996 Nobel Prize in chemistry.

The field of nanotechnology is divided into three major categories, (i) zero-dimensional (0D) nanostructures (e.g., quantum dots); (ii) one dimensional (1D) nanostructures (e.g., nano-tubes, nano-wires, nano-rods); and two-dimensional (2D) structures (e.g., graphene, boron nitride, molybdenum sulfide and tungsten sulfide nanosheets). Carbon emerges as one of the most remarkable elements found in a significant number of compounds. Nanostructures of carbon are the most studied of all other elements due to the ease in synthesizing these thermodynamically stable carbon structures. Graphene, a single atomic layer of carbon, has attracted considerable interest after the material was isolated in 2004 by Novoselov *et al.*[1]

1.1 Morphology of graphene

Graphene is a mono layer of sp^2-bonded carbon atoms tightly packed in a two dimensional honeycomb lattice. The carbon bond length in graphene is about 0.142 nm. Graphene layers stacked together forms graphite with an inter-planar spacing of 0.335 nm, which means that a

stack of three million sheets would be only one millimeter thick. Bilayer and few layer graphene consist of 2 and 3 to 10 layers of these 2D sheets, respectively. These carbon atoms can be arranged in a Bernal (AB) stacking or ABC stacking. Each carbon atom is bonded in-plane together with σ bonds, providing a solid hexagonal network while the out-of-plane π bonds accomplish the weak interaction between different graphene layers.

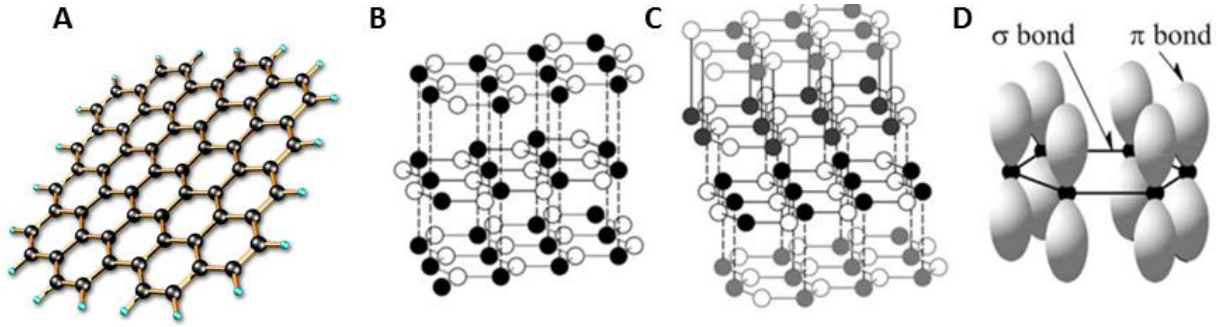

Figure 1.1 (A) Artistic representation of graphene. The image clearly shows the hexagonal structure of graphene. It more or less looks like a chicken mesh with the nodes made of carbon atoms. Each carbon atom is covalently bonded with three other carbon atoms forming this very high strength structure. Graphene can be stacked in two possible arrangements: (B) Bernal or AB stacking and (C) rhombohedral or ABC stacking. (D) Schematic of in-plane σ bonds and π orbitals perpendicular to the plane of graphene sheets [Source: Ref no.55].

1.2 Discovery of graphene

Graphite is the most common form of carbon, which consists of stacked layers of carbon which are covalently bonded in a hexagonal structure. It had been known to exist for centuries. In1996 Nobel Prize in chemistry was awarded for the discovery of C60 otherwise called as Bucky balls. It is made up from 20 hexagons and 12 pentagons which along the surface to form a sphere. Another form of carbon the nanotubes were known to exist for several decades and the Single Walled Carbon nanotubes (SWCNT) since 1993.

It is well known that stable three-dimensional graphite crystals are composed of stacked graphene layers that are weakly coupled by van der Waals forces. However, it was proved theoretically and experimentally that it becomes thermodynamically unstable at finite temperatures when the thickness of the crystal was brought down to a few layers[2-5] as it decomposed and segregated into islands as the melting temperature of thin films rapidly decreases with thickness. This theory was disproved when free-standing graphene was created in 2004 by Novoselov *et al.,* [1] through the "micromechanical cleavage" of highly-oriented pyrolytic graphite (HOPG).

The technique involved repeated peeling of HOPG with scotch tape until atomically thin sheets are obtained. The reason why this was not discovered earlier because of the inability to locate the monolayers even thought they were tried many times unsuccessfully by other groups [6, 7]. The breakthrough that made it possible to locate it was the discovery that monolayers of graphene give good optical contrast when they are deposited on a SiO_2 substrate with a specific oxide thickness of 300 nm. Graphene was detected when AFM was used to scan

regions on substrates where this optical effect occurred. The isolation of graphene led to significant amount of interest in the study of graphene because of its remarkable properties.

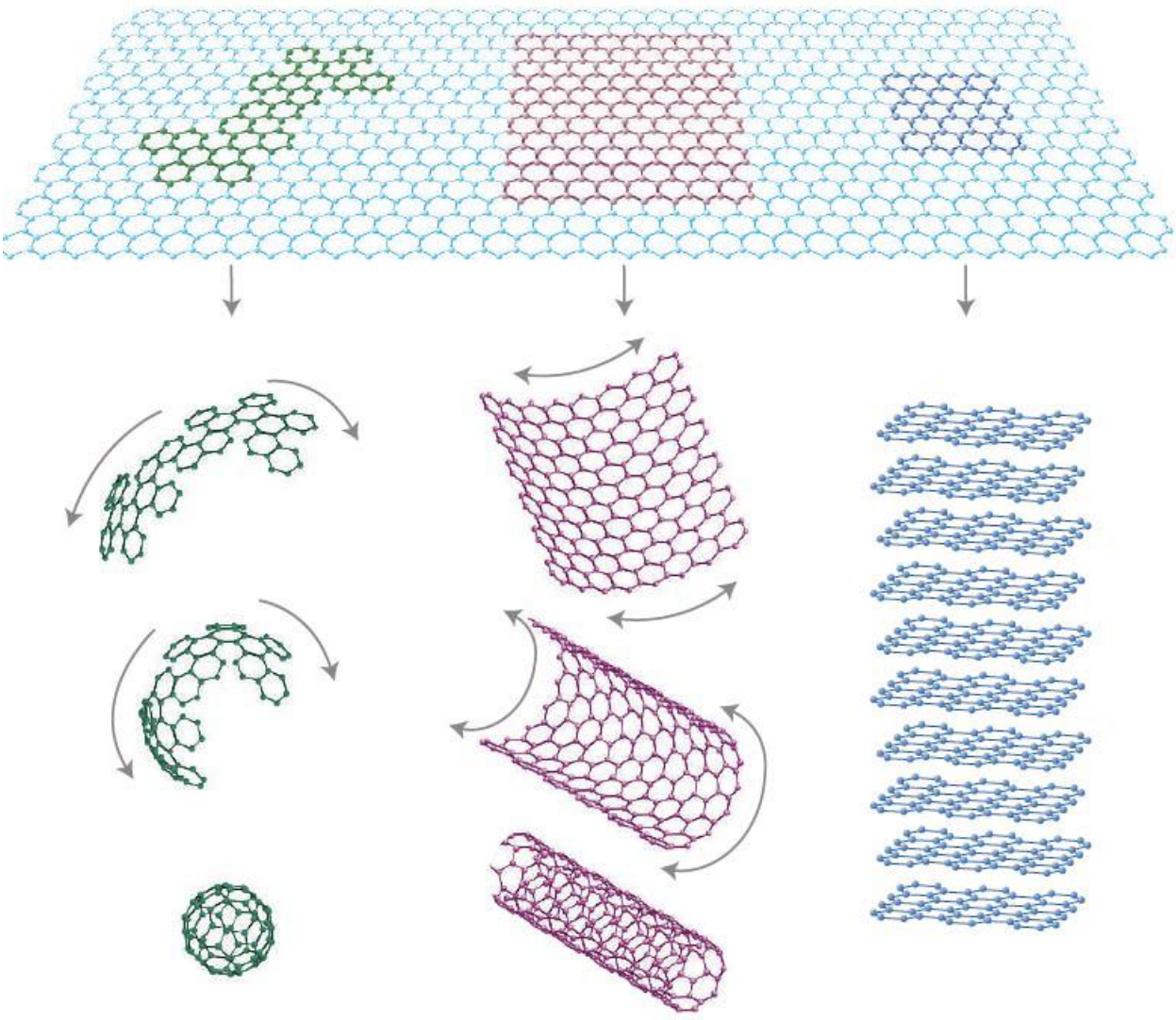

Figure 1.2 A single sheet of graphene can be rolled up to form C60 (Bucky balls) and carbon nanotubes. Multiple layers of this single sheet can form graphite [Source: Ref no.5].

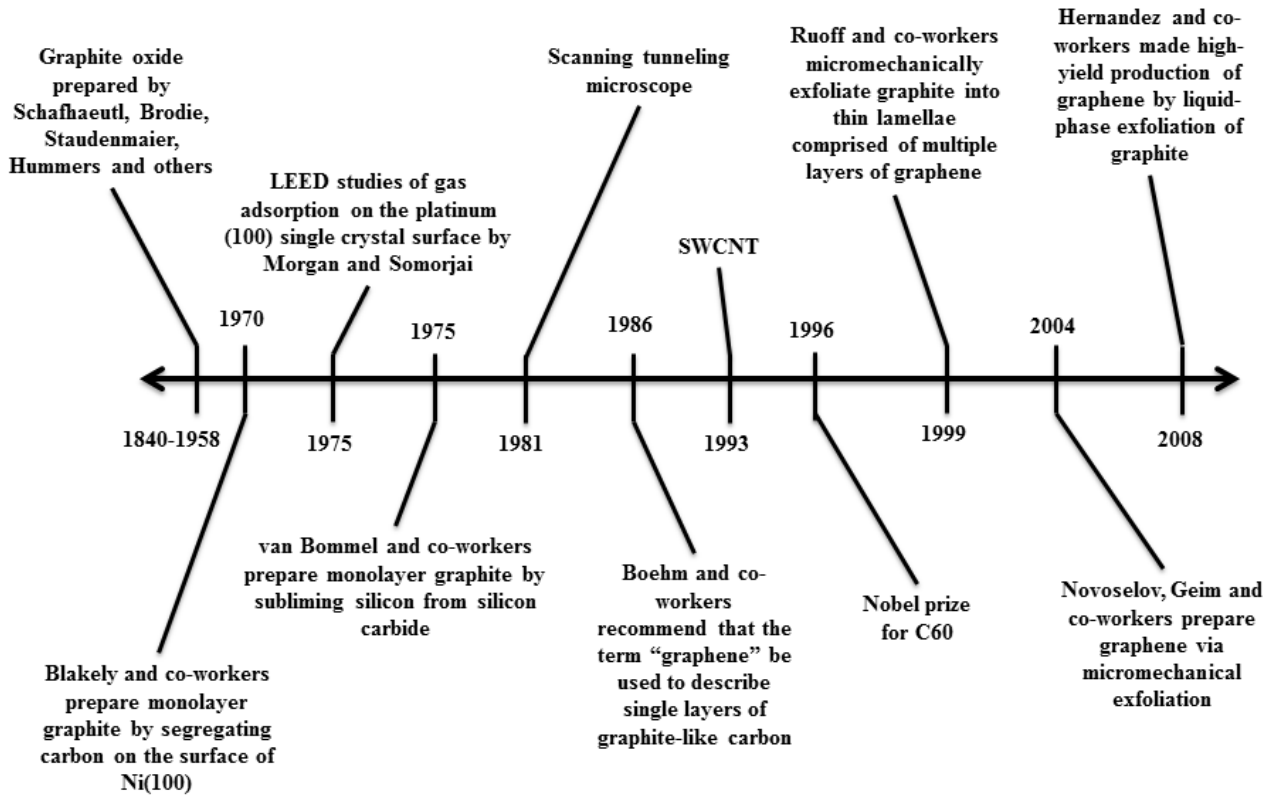

Figure 1.3 Timeline showing the occurrence of different events in the history of graphene

It is surprising to know that every one of us have synthesized graphene some time or the other. Whenever we draw a line using a pencil, which is made of graphite, we end up cleaving the graphite crystals into little flakes of graphite. A small fraction of these thin layers may even contain single layers of graphene.

Thus it is understood that it is not difficult to fabricate the graphene structures but it is the isolation of these structures in large quantities in order to study and characterize the graphene and verify its amazing two dimensional properties.

1.3 Properties of graphene

Graphene possesses a number of unique electronic properties. Electrons travel sub-micron distances without scattering, even at room temperature[5, 8, and 10]; on the surface of graphene electrons behave mass less, thus they can move through space near the speed of light[5, 8-10]. Due to this, charge carriers in graphene have exhibited mobility of 2 x 10^5 cm^2 V^{-1} s^{-1}. For comparison, electrons travel through Si and GaAs at 1500 and 8500 cm^2 V^{-1} s^{-1} respectively[9]. The corresponding resistivity of graphene is 10^{-6} Ω cm. This is less than the resistivity of silver, the lowest resistivity substance known at room temperature. The mobility is nearly independent of temperature which implies that the dominant scattering mechanism is defect scattering. Furthermore, charge carriers can be tuned continuously between electrons and holes in concentrations[5] up to 10^{13} cm^{-2}. Graphene also possesses superior mechanical and thermal properties; defect-free graphene exhibits a Young's modulus of 1 TPa, a third-order elastic stiffness of -2 TPa, and an intrinsic strength of 130 GPa, making it the strongest material ever measured[11]. The breaking strength of graphene is 200 times greater than steel. It is also unique because it is highly pliable but fractures like glass at high strains, and it is also impermeable to gases (including He) [9]. The material exhibits an extremely high room temperature thermal conductivity[12] of 5300 W m^{-1} K^{-1}, which is superior to that of single-walled carbon nanotubes (3500 W m^{-1} K^{-1}) and diamond (2000 W m^{-1} K^{-1}), which is the best bulk crystalline thermal conductor[12]. Graphene's unique optical properties produce an unexpectedly high opacity for an atomic monolayer, with a startlingly simple value: it absorbs $\pi\alpha \approx 2.3\%$ of white light. This is because of the unusual electronic structure of monolayer graphene where the electron and hole conical bands meet each other at the Dirac point.

1.4 Potential applications of graphene

Numerous electronic applications have been envisioned for graphene. The electronic property of graphene and the size makes it a suitable candidate for replacing silicon in the semiconductor industry[5]. Other materials like GaAs and InP[5, 8, 9], which are currently used in making ultrahigh-frequency transistors could be replaced by graphene. Graphene being one atomic layer thick is flexible, which makes it a potential candidate for electronic appliances like touchscreens and transparent sensors[13]. Other proposed electronic applications for graphene include super-capacitors, batteries, interconnects, and field emitters[8].

Researchers are studying the possibility of making composites using graphene to create electrically-conducting plastics[14] and sensors capable of detecting individual gas molecules[15] and DNA[16]. There has been growing interest in the use of graphene as a base material for nano-electromechanical systems, since graphene-based resonators offer low inertial masses, ultrahigh frequencies, and low resistance contacts . Graphene can be utilized as a supporting membrane for bacteria and other living microbes in transmission electron microscope (TEM) because the material is highly transparent and wraps around it thus protecting it from ultrahigh vacuum[17].

1.5 Synthesis techniques

Graphene was first synthesized by chemical vapor deposition in 1975 by Morgan *et al.,* [18] who used single crystal platinum as the metal substrate. Unfortunately, this process was abandoned because of lack of reproducibility in the results and unavailability of methods to transfer graphene onto an insulating substrate. In the same year van Bommel *et al.,* [19] described the epitaxial sublimation of silicon from single crystal of silicon carbide (0001). At high temperature

and high vacuum monolayer flakes of carbon consistent with the structure of graphene were obtained. No further investigation was done. There were many other attempts to synthesize pristine graphene by chemically exfoliating graphite to transform it into graphite oxide[19]. Graphite oxide consists of oxidized graphene sheets, which have epoxide and hydroxyl groups attached on the surface and carboxyl and carbonyl groups attached at the edges. Thus functionalization of graphite makes individual layers hydrophilic, and thus water can readily intercalate into the layers and sonication of the intercalated sheets exfoliates the bulk material into individual graphene oxide layers. But this material comes with a lot of inherent defects and disorders. And also the functional groups are not completely removes which makes the sheets to behave non- metallic[20].

A more repeatable and pristine graphene yielding process was realized by Novoselov *et al.,* [1] in 2004. This technique has been applied since then, along with efforts to produce large scale graphene. A few physical and chemical methods to produce graphene are presented here.

1.5.1 Mechanical exfoliation

There are several mechanical methods for synthesis of graphene. In 2004 Novoselov *et al.,* [1] used Highly Oriented Pyrolytic Graphene (HOPG), which consists of many layers of graphene bonded weakly together by Van der Waals force. HOPG was crushed and the small flakes were attached to a scotch tape and repeated sticking and peeling with another piece of tape yields graphene. Afterwards, the tape is gently rubbed on top of a substrate with a soft tweezers to prevent damaging the graphene flakes and the tape is removed carefully.

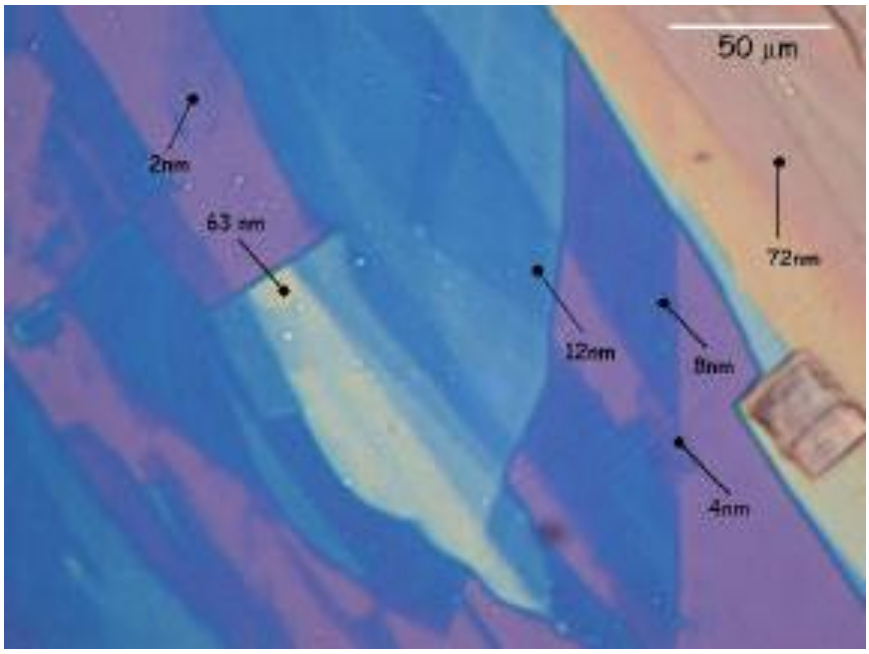

Figure 1.4 Optical image showing graphene transferred onto SiO_2 substrate. The varying thickness of graphene can be identified by the contrast in color of the optical image. On the silicon wafer with an oxide thickness of 300 nm a monolayer of graphene will a faint violet-blue color. But as the thickness increases the color shifts towards blue [Source: Ref no.1].

This process is highly efficient in producing monolayers of graphene but the size and the yield that this process produces has to be compromised to the high structural and electronic quality flakes. The other method is intercalating graphite with lithium and on introduction of water the intercalated lithium ions forms hydrogen gas which in-turn rips open the layers of graphite into layers of graphene[24].

1.5.2 Epitaxial growth

Some of the important properties of graphene were identified in graphene produced by this method. For example, the electronic band-structure (so-called Dirac cone structure) has been first visualised in this material. Very large and temperature independent mobilities have been observed in SiC epitaxial graphene. The limitation of this method is the cost of the source material. In this method SiC is annealed to a high temperature (>1250 °C) in ultra-high vacuum (UHV) [19] or argon atmosphere [23].

Due to the intense heat the silicon evaporates off the surface to leave behind a carbon rich surface, resulting in the growth of high quality graphene. There are two factors which determine the number of layers: decomposition temperature and the amount of Si evaporated. Three layers of carbon needs to collapse to form a single layer of graphene. The major drawbacks of this process is the cost of the base material and the strong interaction between graphene and SiC makes it difficult to transfer onto another substrate. Also the difference in the thermal expansion coefficient makes it difficult to make exact electrical measurements[18].

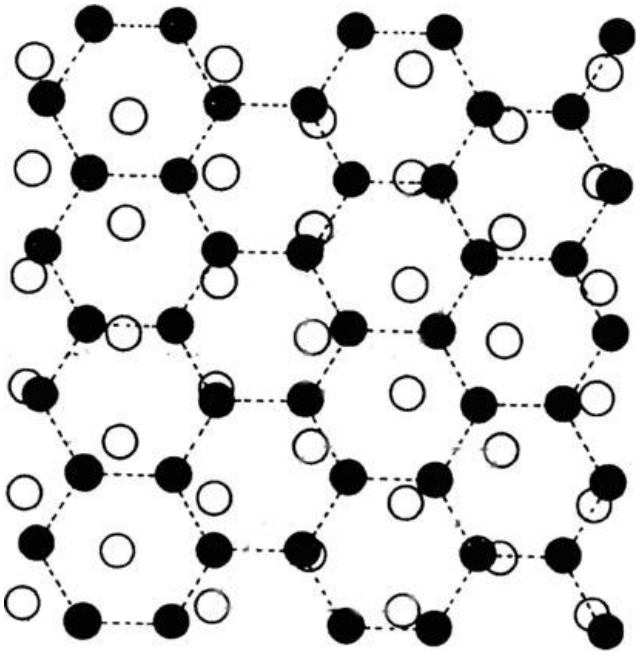

Figure 1.5 Schematic of a silicon carbide structure in which three carbon layers of SiC have collapsed upon the evaporation of Si to form a single layer; ● C atoms of monocrystalline graphite top layer; ○ C atoms resulting for the collapse of three layers of SiC [Source: Ref no.19].

1.5.3 Unzipping carbon nanotubes

Most recently graphene nano-ribbons are made by opening up a multi-walled carbon nanotube (MWCNT) in the longitudinal direction. This has been realized in different approaches[24-26]. The more easy approach is to partially coat the nanotube with polymer and expose it to plasma etchant which unzips the carbon nanotubes into graphene nanoribbons[26]. The high quality and well-controlled widths of graphene nano-ribbons can be used for device fabrication purposes. This method is particularly useful because of a number of reasons: (1) It gives a larger yield than any other synthesis methods, (2) the process is fast and there is no lack for availability of

nanotubes, (3) It does not have any residue or solvent like liquid phase exfoliation which requires more processes to eliminate, (4) The quality of graphene obtained is pristine. But a drawback is that the graphene sheets with only a certain width can be obtained. Sheets with all large dimensions cannot be obtained.

Another method is to suspend MWCNT in a concentrated solution of sulfuric acid followed by treatment with 500 wt% $KMnO_4$ [25].The mechanism is the oxidation of alkenes by permanganate in acid. The first step is the manganate ester formation which oxidizes the alkenes in the acid medium. Juxtaposition of the oxide distorts the β, γ-alkenes thus making them prone to further attack. Thus once an opening has been initiated the tubes just opens up or unzips. This could occur in a longitudinal cut or in a spiral manner depending upon the initial site of attack and the chirality of the nanotube.

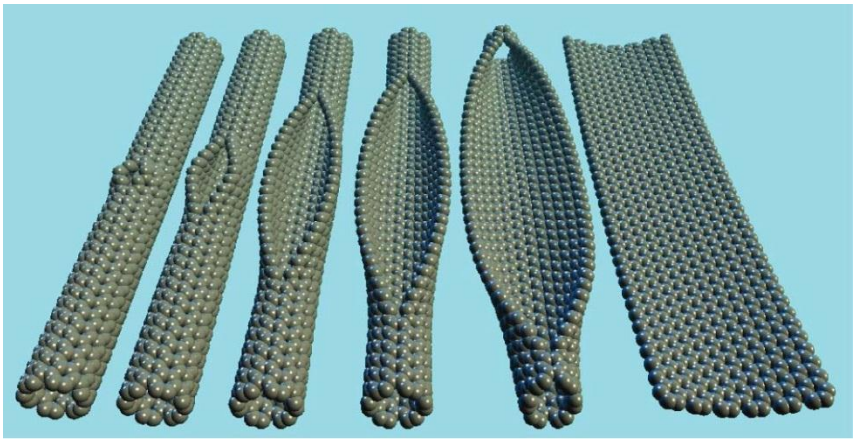

Figure 1.6 Graphical representation of the method of initiation and propagation of the unzipping process that happens when nanotubes are treated by sulfuric acid and $KMnO_4$ as proposed by Novoselov *et al.*, [Source: Ref no.25].

1.5.4 Liquid phase exfoliation

Recently, carbon nanotubes have been successfully exfoliated in a small number of solvents such N-methylpyrrolidone (NMP) [27-33]. Such exfoliation occurs because the strong interaction between solvent and nanotube sidewall means that the energetic penalty for exfoliation and subsequent solvation becomes small. Similar effects occur between these solvents and graphene. Hernandez *et al.,* [32] made a detailed study of the effect of these solvents on graphene. They made dispersions of graphite powder in NMP by sonication. After sonication a grey solution consisting of a homogeneous phase and large number of macroscopic particles.

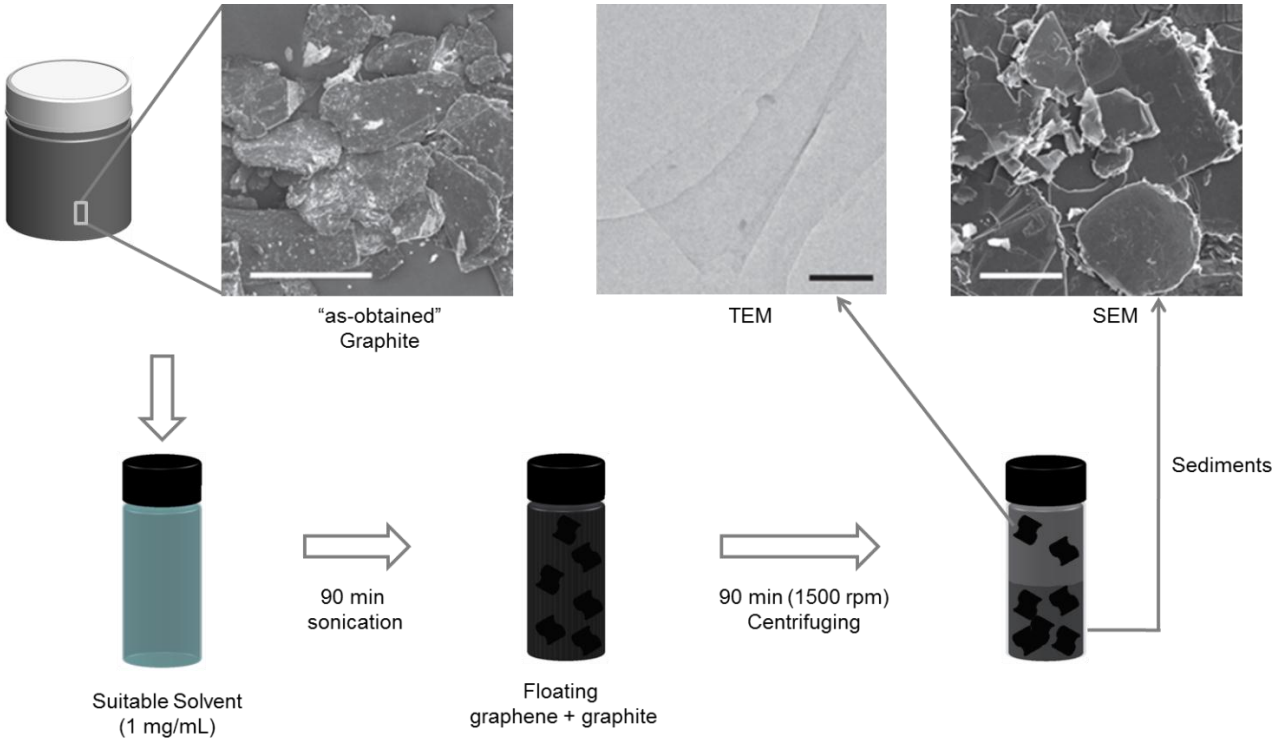

Figure 1.7 Shows the procedure for liquid phase exfoliation of graphite in suitable solvents. After sonication a homogeneous mixture is obtained which is centrifuged so that the large graphitic particles get settled down.

Table 1.1 Solvents sorted by the fraction of graphene/graphite remaining after centrifugation [Ref. no. 33].

Solvent	Surface tension (mJ/m^2)	Percentage remaining after Centrifugation
Benzyl Benzonate	45.95	8.3
NMP (1-Methyl1-2-pyrrolidinone)	40.1	7.6
GBL (γ-Butyrolactone)	46.5	7.6
DMA (N,N-Dimethylacetamide)	36.7	7.2
DMEU (1,3-Dimethyl-2-Imidazolidinone)	42.5	7.2
NVP (1-Vinyl-2-pyrrolidinone)	42.7	6.6
N12P (1-Dodecyl-2-pyrrolidinone)	34.5	5.4
DMF (n,n-Dimethylformamide)	37.1	4.5
DMSO (dimethyl sulfoxide)	42.98	4.1
IPA (isopropanol)	21.66	3.4
N8P (1-Octyl-2-pyrrolidone)	34.5	2.6
Acetone	25.2	2.5

.As with any dispersion these aggregates was removed by centrifugation, giving a homogeneous dark dispersion. It was observed by them that only a slight amount of sedimentation occurred in the solution which on the longer period of time remained as a good dispersed liquid. They postulated that the reason for the successful dispersion of graphite in the solvent was the difference in net energetic cost for the exfoliation process is expressed in enthalpy. Enthalpy of mixing depends on the graphene and solvent surface energies. The surface energy is defined as the energy per unit area required to overcome the Van Der Waals forces when peeling off two sheets. Enthalpy of mixing is minimized when the surface energies of flake and solvent match.

The same procedure were repeated by Coleman *et al.,* [33] for other solvents known to successfully disperse nanotubes: N, N-Dimethylacetamide (DMA), γ-butyrolactone (GBL), 1,3-dimethyl-2-imidazolidinone (DMEU) and more. The twelve best solvents were characterized by the fraction of graphite/graphene remaining after centrifugation. This was calculated by measuring the absorbance after centrifugation and using the measured absorption coefficient, $<\alpha_{660}>=2460$ $Lg^{-1}m^{-1}$, to give concentration after centrifugation. The drawback of this method is that the size and position of the graphene sheets is uncontrollable. Also the graphene sheets are in a solution from which it is hard to separate off and deposit on the required substrate.

1.5.5 Chemical vapor deposition (CVD)

Graphene monolayers can be synthesized on surface of transition metals using Chemical Vapor Deposition (CVD) process. It is the most inexpensive and readily available method for graphene synthesis is chemical vapor deposition (CVD) onto transition metal substrates like Ni[34], Pd[35], Ru[36], Ir[37] or Cu[38]. The first method for synthesis of graphene using CVD was realized by Morgan

and Somorjai in 1975[18] who used low-energy electron diffraction (LEED) to investigate the adsorption of various gases like CO, C_2H_2, C_2H_4 onto a platinum (100) surface at elevated temperatures. In the later year May *et al.,* [39] deduced the data from the experiment and postulated that layers of a material that features a graphitic structure were present as a result of these adsorption processes. It was shown that the first monolayer of graphene reduces the energy of adsorption on each of the studied faces of platinum. Later studies by Blakely and co-workers reported an extensive series of adsorption of mono- and multilayer graphene on various metal surfaces including Ni (100) and (111), Pt (111), Pd (100) and Co (0001)[40-46].

Of the other synthesis methods available metal-assisted thermal CVD method is most promising because of a number of reasons: (1) it allows large area graphene synthesis with a high level of uniformity and low defects, (2) it facilitates discovery of large variety of transition metals as catalysts thus exploring the possibility of producing large area graphene in large scale and (3) it allows the integration with the high volume semiconductor industry. This method generally involves introduction of carbonaceous gaseous species at high temperatures (900-1100 °C) in the presence of metal thin films/foils, which serves the purpose of being a catalyst for the decomposition of carbonaceous gas to carbon and also in acting as a site for nucleation for the growth of graphene lattice. The mechanism of growth depends on several factors: (1) solubility of carbon in the metal, (2) the crystal structure of the metal, (3) the metals lattice plane and (4) other thermodynamic parameters like the temperature, cooling rate, pressure of the system and the amount of flow of gasses in the system. The main factor of them is the carbon solubility in metals. In case of very low carbon solubility metals (<0.001 atomic %) such as Cu, the mechanism of synthesis of graphene is limited to the interaction to the surface of the catalyst, and in the case of intermediate-high solubility (>0.1 atomic %) metal catalysts like Co and Ni,

graphene synthesis is due to a combination of diffusion into the metal thin film at growth temperature, and segregation of carbon at the surface of the metal upon cooling after CVD synthesis.

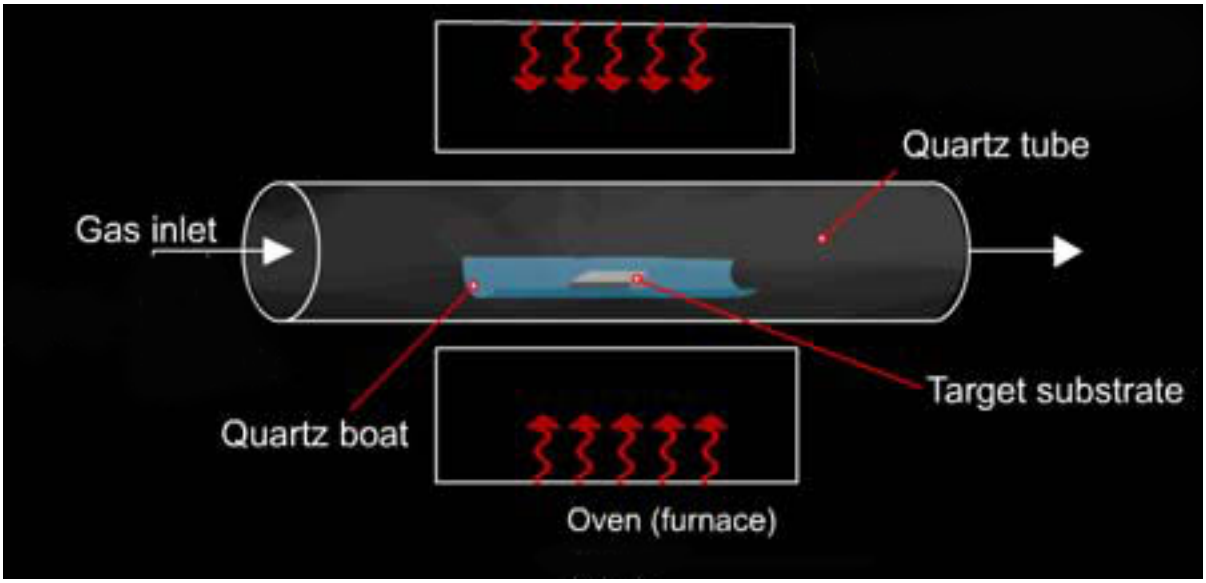

Figure 1.8 Schematic of a CVD furnace. The major components are: (1) gas controller which precisely measures the amount of gas to supply as instructed by the controller, (2) heating element which heats up the quartz tube that is inside the furnace to required temperature and (3) loader which is used to load the sample into the core of the furnace.

The epitaxial growth of graphene layer is possible on Ru (0001)[36] substrates by using the phenomenon of temperature-dependent solubility of interstitial carbon in transition metals. Carbon gets absorbed into Ru at around 1200 °C and when it is cooled slowly to 800 °C the carbon solubility lowers which brings it out to the surface. This result in formation of very large islands of graphene with domains over 100 µm. Large area graphene can be synthesized using this process. But graphene on Ru is hard to separate as the carbon forms a strong bond with the

metal. Graphene grown on iridium on the other hand is very weakly bonded, uniform in thickness, and can be made highly ordered. Like on many other substrates, graphene on Iridium is slightly rippled. Due to the long range of ripples, generation of mini-gaps in the electronic band-structure (Dirac cone) becomes visible[47].

Graphene segregation at surfaces and grain boundaries of metal has been studied in detail for a long time[48]. There are several methods which showed that mono-layered or few layered graphene films can be segregated on the surface of metals and metal carbides[49, 50] held at high temperatures in an equilibrium segregation process[51, 41]. But this cannot be preserved because of the non-equilibrium segregation of carbon while cooling down. The cooling rate determines if the graphene is synthesized or not. Fast cooling rejects carbon atoms from the substrate. Very slow cooling rate causes the carbon to be diffused into the metal[52]. So Nickel substrate requires very accurate cooling rate. However the synthesis is dependent on the quality of the underlying Ni film, and the graphene thus produced had non-uniform number of layers and large number of patches which was primarily due to the irregularity of the underlying Ni layer.

Initially for synthesizing graphene with nickel as substrate involves the e-beam evaporation of Ni onto SiO_2/Si substrates, which is then followed by annealing thus making a thin Ni film with microstructures consisting of single-crystalline grains with sizes from 1 to 20 μm[22, 34]. This is then placed in a CVD furnace where a the substrate is subjected to a highly dilute mixture of hydrocarbon flow under ambient pressure at 1000 °C, which results in the formation of monolayer graphene films or graphene with few layers. However the synthesis is dependent on the quality of the underlying Ni film, and the graphene thus produced had non-uniform number

of layers and large number of patches which was primarily due to the irregularity of the underlying Ni layer. Thin nickel sheets can also be used to synthesize graphene.

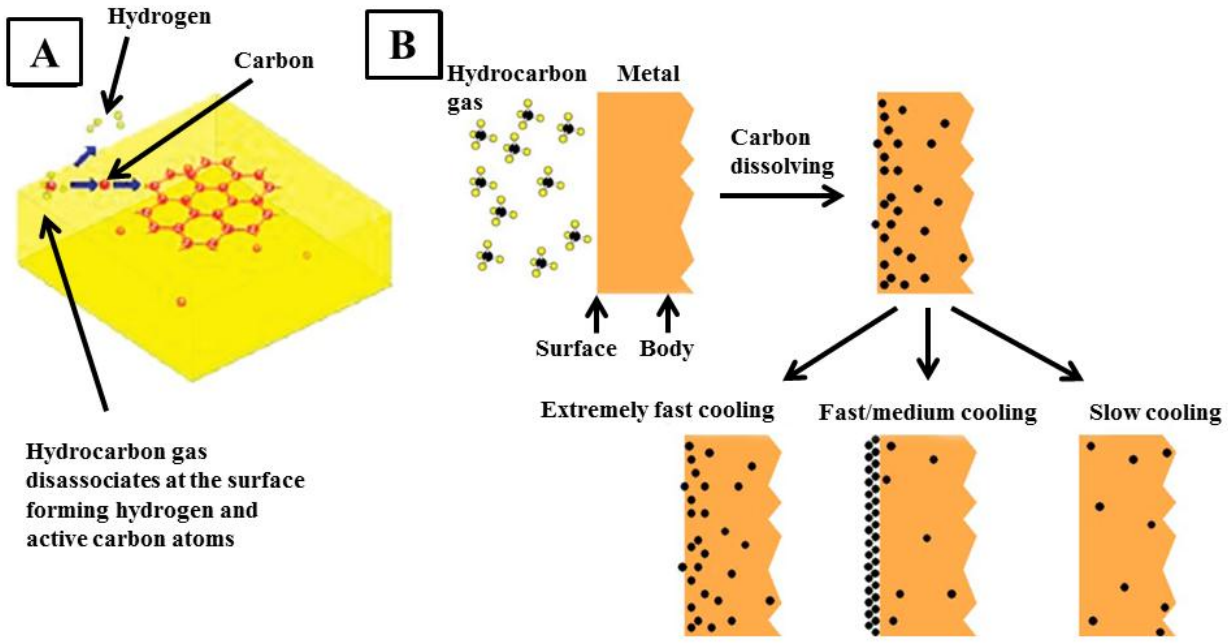

Figure 1.9 Graphical representation of the different mechanisms in which carbon forms graphene layers: (A) surface adsorption process at Cu surface (B) segregation process at Ni surface [Source: Ref no.54 and 51].

Recently, lots of study has been carried on graphene synthesis on copper foil. At very low pressure, the growth automatically stops after a single graphene layer forms, and arbitrarily large graphene films can be created. But in atmospheric pressure CVD growth, multilayer graphene may form on copper[52]. Large are graphene synthesis using Cu catalyst in a LPCVD process has attracted widespread attention since it was first reported in 2009 [38]. The mechanism of graphene growth on Cu is a surface phenomenon as discussed earlier. Copper acts as a catalyst and disassociates the carbonaceous gas to from carbon atoms which then are attracted by the

substrate surface. The growth begins with the nucleation of growth sites on the surface and then growing with the addition of carbon to the edge of these growth domains. This is the reason why this mechanism provides a uniform mono-layer of graphene on the surface which is not true in the case in which segregation occurs. The domains keep growing till it joins with other domains thus forming a large graphene sheet. The temperature plays an important role in the growth process. Results shows that increasing the temperature while holding the growth time constant results in larger domains when compared to graphene grown at lower temperature[53]. It also showed that complete coverage of high quality graphene was achieved due to the high temperature.

The pressure of the gas was also found to affect the growth mechanism of graphene[52]. They assumed that there is a stagnant boundary layer due to the steady state gas flow close to the surface of the catalyst. So the carbon species first has to (1) diffuse through the boundary layer and reach the surface and the (2) get adsorbed on the surface, (3) disassociates to form active species, (4) diffuse into or on the surface of the catalyst and from graphene lattice planes, (6) inactive species like hydrogen gets desorbed and (6) are removed by the bulk gas flow through the boundary layer. The mechanism of graphene growth on the surface of Cu is governed by two regions which is dependent on where the reaction occurs as mass transport region, depends on the diffusion through the boundary layer and surface reaction region. The surface process is mainly influenced by the temperature of the substrate. Therefore there exist two parameters that determine the growth rate: flow of carbon through the boundary region and the rate at which carbon is consumed at the surface of the catalyst to form the graphene lattice. It was mathematically shown that at growth temperature under ambient pressure conditions the mass transport through the boundary layer is the rate limiting factor and surface reaction at ultrahigh

vacuum. This essentially means that at ambient pressure conditions the surface geometry, position of the substrate and the amount of active species all varies the thickness of the boundary layer thus causing thickness non-uniformity on the surface. Also it was shown that due to the high rate of flow of gasses in the chamber gaseous reactions occur which deposits particulates on the surface of graphene/catalyst resulting in a higher defect density. Thus to control the thickness of graphene the only parameter which has to be changed is the rate of flow of active species (hydrogen and methane). To avoid this it is necessary to conduct the experiment in the surface reaction regime. This is achieved by lowering the pressure of the system. Lower pressure means there is less number of active species present which translates to a smaller boundary layer thus diffusion through the boundary layer in enhanced. So as long as the temperature is maintained constant throughout the surface the catalyst the thickness of the graphene is uniform.

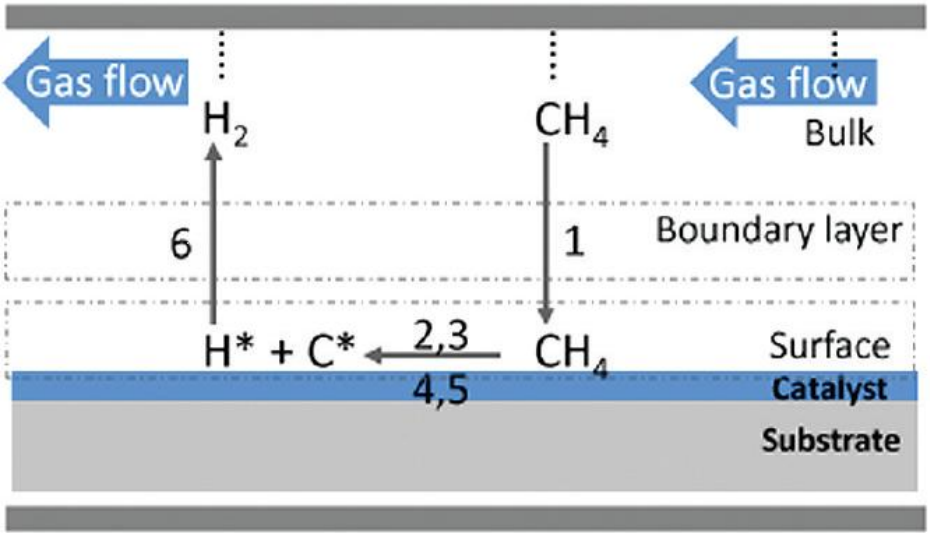

Figure 1.10 Schematic illustrating the different processes involved during graphene synthesis in Cu catalysts, which is a low solubility metal, in a CVD process [Source: Ref no.52].

Various other sources of carbon were also tried. The solid carbon source[53], in this case Poly-methyl meth acrylate (PMMA) ~100 nm, was spin coated on a thin film of Cu. At elevated temperatures and under low pressure conditions and on passing a reductive gas flow of hydrogen and argon, a single uniform layer of graphene was formed on the surface of the substrate. They showed that the thickness of graphene layers could be easily controlled by changing the growth temperature, thickness of the polymer solid carbon source and the pressure of the system. The same group went on to make graphene for "girls scout cookies". Another group coated a-Carbon on copper substrate and annealed it to grow graphene[53]. They studied the effect of hydrogen in the system at the growth temperature. It was showed that due to the presence of hydrogen the carbon feedstock that was on the surface of copper reacted and was activated. The active carbon species then reacted with the surface of the catalyst forming graphene lattices. They also placed a neat Cu foil upstream and downstream to the a-C coated Cu foil and found the presence of graphene in those pieces also. They postulated three possibilities for the reaction to occur: (1) carbon atom diffusion through the Cu foil, (2) carbon atoms/clusters being transported downstream and upstream as gaseous species and/or (3) hydrocarbon acting as the critical precursors. The first two solutions were highly unlikely because (1) the Cu foils are not in contact and (2) if a-C atoms or clusters are formed then it should rapidly react with hydrogen in stream forming CH_3^+ or CH_4^+ and serves as precursor for reaction to occur. All this shows that numerous other carbon sources could be used to synthesis graphene through the CVD process.

Once the graphene is grown on the catalyst the graphene sheets needs to be transferred to another substrate/insulator to do further processing. The procedure is almost the same for both Cu and Ni catalyst. The substrate, which has graphene on the surface after growth is completed, is spin coated with a very thin layer of polymers like poly (methyl methacrylate) (PMMA) or

polydimethylsiloxane (PDMS). The substrate is then baked for about 10 min in an oven maintained at 120 °C. The side that was not spin coated it blazed with oxygen plasma so that the graphene in the other side is etched away. This foil is then placed in a ferric chloride copper-etch solution. Once the copper is etched away the PMMA is scooped out of the solution and is rinsed with DI water a couple of time and is scooped out onto the required substrate. Once the substrate is dry then it is rinsed with acetone to dissolve the PMMA. Then the chip is dried to obtain a clean layer of graphene on the desired substrate.

1. 6 Thesis organization

In the first part of chapter 2, the theory of Raman scattering is introduced both in the classical and quantum picture. A detailed description of the different Raman modes of graphene is presented. Later the chapter goes into the theory of operation of Scanning Electron Microscope (SEM) and Raman spectrometer. The final part of the chapter discusses the CVD equipment used in the experiments. A detailed description of the standard "as obtained" equipment and the modified equipment is provided at the end of the chapter. Chapter 3 focuses on synthesis of graphene with copper substrate using standard growth procedure. Important results obtained by studying the effects of various parameters used in the CVD process are discussed. Chapter 4 provides an insight into the modified growth procedure which is introduced for the first time. Later part of the chapter presents the results for the two modified procedures: (A) fast cooling, (B) fast heating and fast cooling. Chapter 5 looks into synthesis of graphene using Ni as substrate. The modified procedure has been employed to this new material and the results are discussed. Finally, Chapter 6 summarizes the main results presented in the thesis and talks about the future work to be carried out in the synthesis of nano particles.

1.7 References

1. Novoselov, K. S., Geim, A. K., Morozov, S. V., Jiang, D., Zhang, Y., Dubonos, S. V., Grigorieva, I. V., and Firsov, A. A., 2004, "Electric Field Effect in Atomically Thin Carbon Films," Science, 306(5696), pp. 666-669.
2. Mermin, N. D., 1968, "Crystalline Order in Two Dimensions," Physical Review, 176(1), p. 250.
3. Venables, J. A., and et al., 1984, "Nucleation and growth of thin films," Reports on Progress in Physics, 47(4), p. 399.
4. Evans, J. W., Thiel, P. A., and Bartelt, M. C., 2006, "Morphological evolution during epitaxial thin film growth: Formation of 2D islands and 3D mounds," Surface Science Reports, 61(1-2), pp. 1-128.
5. Geim, A. K., and Novoselov, K. S., 2007, "The rise of graphene," Nat Mater, 6(3), pp. 183-191.
6. Zhang, Y., Small, J. P., Amori, M. E. S., and Kim, P., 2005, "Electric Field Modulation of Galvanomagnetic Properties of Mesoscopic Graphite," Physical Review Letters, 94(17), p. 176803.
7. Shioyama, H., 2001, "Cleavage of graphite to graphene," Journal of Materials Science Letters, 20(6), pp. 499-500.
8. Glotzer, S. C., 2004, "Some Assembly Required," Science, 306(5695), pp. 419-420.
9. Zhang, and Glotzer, S. C., 2004, "Self-Assembly of Patchy Particles," Nano Letters, 4(8), pp. 1407-1413.
10. Shevchenko, E. V., Talapin, D. V., Kotov, N. A., O'Brien, S., and Murray, C. B., 2006, "Structural diversity in binary nanoparticle super lattices," Nature, 439(7072), pp. 55-59.
11. Nakata, K., Hu, Y., Uzun, O., Bakr, O., and Stellacci, F., 2008, "Chains of Superparamagnetic Nanoparticles," Advanced Materials, 20(22), pp. 4294-4299.
12. DeVries, G. A., Talley, F. R., Carney, R. P., and Stellacci, F., 2008, "Thermodynamic Study of the Reactivity of the Two Topological Point Defects Present in Mixed Self-

Assembled Monolayers on Gold Nanoparticles," Advanced Materials, 20(22), pp. 4243-4247.

13. Khatri, O. P., Adachi, K., Murase, K., Okazaki, K.-i., Torimoto, T., Tanaka, N., Kuwabata, S., and Sugimura, H., 2008, "Self-Assembly of Ionic Liquid (BMI-PF6)-Stabilized Gold Nanoparticles on a Silicon Surface: Chemical and Structural Aspects," Langmuir, 24(15), pp. 7785-7792.
14. Khatri, O. P., Murase, K., and Sugimura, H., 2008, "Structural Organization of Gold Nanoparticles onto the ITO Surface and Its Optical Properties as a Function of Ensemble Size," Langmuir, 24(8), pp. 3787-3793.
15. Perepichka, D. F., and Rosei, F., 2007, "Metal Nanoparticles: From "Artificial Atoms" to "Artificial Molecules"," Angewandte Chemie International Edition, 46(32), pp. 6006-6008.
16. Mohanty, N., and Berry, V., 2008, "Graphene-Based Single-Bacterium Resolution Biodevice and DNA Transistor: Interfacing Graphene Derivatives with Nanoscale and Microscale Biocomponents," Nano Letters, 8(12), pp. 4469-4476.
17. Mohanty, N., Fahrenholtz, M., Nagaraja, A., Boyle, D., and Berry, V., 2011, "Impermeable Graphenic Encasement of Bacteria," Nano Letters, 11(3), pp. 1270-1275.
18. Morgan, A. E., and Somorjai, G. A., "Low energy electron diffraction studies of gas adsorption on the platinum (100) single crystal surface," Surface Science, 12(3), pp. 405-425.
19. Van Bommel, A. J., Crombeen, J. E., and Van Tooren, A., 1975, "LEED and Auger electron observations of the SiC (0001) surface," Surface Science, 48(2), pp. 463-472.
20. Stankovich, S., Piner, R. D., Chen, X., Wu, N., Nguyen, S. T., and Ruoff, R. S., 2006, "Stable aqueous dispersions of graphitic nanoplatelets via the reduction of exfoliated graphite oxide in the presence of poly (sodium 4-styrenesulfonate)," Journal of Materials Chemistry, 16(2), pp. 155-158.
21. Li, X., Zhang, G., Bai, X., Sun, X., Wang, X., Wang, E., and Dai, H., 2008, "Highly conducting graphene sheets and Langmuir-Blodgett films," Nat Nano, 3(9), pp. 538-542.

22. Reina, A., Jia, X., Ho, J., Nezich, D., Son, H., Bulovic, V., Dresselhaus, M. S., and Kong, J., 2008, "Large Area, Few-Layer Graphene Films on Arbitrary Substrates by Chemical Vapor Deposition," Nano Letters, 9(1), pp. 30-35.

23. Hass, J., Feng, R., Li, T., Li, X., Zong, Z., Heer, W. A. d., First, P. N., Conrad, E. H., Jeffrey, C. A., and Berger, C., 2006, Highly ordered graphene for two dimensional electronics, AIP.

24. Cano-Márquez, A. G., Rodríguez-Macías, F. J., Campos-Delgado, J., Espinosa-González, C. G., Tristán-López, F., Ramírez-González, D., Cullen, D. A., Smith, D. J., Terrones, M., and Vega-Cantú, Y. I., 2009, "Ex-MWNTs: Graphene Sheets and Ribbons Produced by Lithium Intercalation and Exfoliation of Carbon Nanotubes," Nano Letters, 9(4), pp. 1527-1533.

25. Kosynkin, D. V., Higginbotham, A. L., Sinitskii, A., Lomeda, J. R., Dimiev, A., Price, B. K., and Tour, J. M., 2009, "Longitudinal unzipping of carbon nanotubes to form graphene nano-ribbons," Nature, 458(7240), pp. 872-876.

26. Jiao, L., Zhang, L., Wang, X., Diankov, G., and Dai, H., 2009, "Narrow graphene nano-ribbons from carbon nanotubes," Nature, 458(7240), pp. 877-880.

27. Furtado, C. A., Kim, U. J., Gutierrez, H. R., Pan, L., Dickey, E. C., and Eklund, P. C., 2004, "Debundling and Dissolution of Single-Walled Carbon Nanotubes in Amide Solvents," Journal of the American Chemical Society, 126(19), pp. 6095-6105.

28. Giordani, S., Bergin, S. D., Nicolosi, V., Lebedkin, S., Kappes, M. M., Blau, W. J., and Coleman, J. N., 2006, "Debundling of Single-Walled Nanotubes by Dilution: Observation of Large Populations of Individual Nanotubes in Amide Solvent Dispersions," The Journal of Physical Chemistry B, 110(32), pp. 15708-15718.

29. Landi, B. J., Ruf, H. J., Worman, J. J., and Raffaelle, R. P., 2004, "Effects of Alkyl Amide Solvents on the Dispersion of Single-Wall Carbon Nanotubes," The Journal of Physical Chemistry B, 108(44), pp. 17089-17095.

30. Hasan, T., Scardaci, V., Tan, P., Rozhin, A. G., Milne, W. I., and Ferrari, A. C., 2007, "Stabilization and “Debundling” of Single-Wall Carbon Nanotube Dispersions in N-

Methyl-2-pyrrolidone (NMP) by Polyvinylpyrrolidone (PVP)," The Journal of Physical Chemistry C, 111(34), pp. 12594-12602.

31. Shane, D. B., and et al., 2007, "Exfoliation in ecstasy: liquid crystal formation and concentration-dependent debundling observed for single-wall nanotubes dispersed in the liquid drug γ-butyrolactone," Nanotechnology, 18(45), p. 455705.

32. Hernandez, Y., Nicolosi, V., Lotya, M., Blighe, F. M., Sun, Z., De, S., McGovern, I. T., Holland, B., Byrne, M., Gun'Ko, Y. K., Boland, J. J., Niraj, P., Duesberg, G., Krishnamurthy, S., Goodhue, R., Hutchison, J., Scardaci, V., Ferrari, A. C., and Coleman, J. N., 2008, "High-yield production of graphene by liquid-phase exfoliation of graphite," Nat Nano, 3(9), pp. 563-568.

33. Hernandez, Y., Nicolosi, V., Lotya, M., Blighe, F. M., Sun, Z., De, S., McGovern, I. T., Holland, B., Byrne, M., Gun'Ko, Y. K., Boland, J. J., Niraj, P., Duesberg, G., Krishnamurthy, S., Goodhue, R., Hutchison, J., Scardaci, V., Ferrari, A. C., and Coleman, J. N., 2008, "High-yield production of graphene by liquid-phase exfoliation of graphite," Nat Nano, 3(9), pp. 563-568..

34. Kim, K. S., Zhao, Y., Jang, H., Lee, S. Y., Kim, J. M., Kim, K. S., Ahn, J.-H., Kim, P., Choi, J.-Y., and Hong, B. H., 2009, "Large-scale pattern growth of graphene films for stretchable transparent electrodes," Nature, 457(7230), pp. 706-710.

35. Kwon, S.-Y., Ciobanu, C. V., Petrova, V., Shenoy, V. B., Bareño, J., Gambin, V., Petrov, I., and Kodambaka, S., 2009, "Growth of Semiconducting Graphene on Palladium," Nano Letters, 9(12), pp. 3985-3990.

36. Sutter, P. W., Flege, J.-I., and Sutter, E. A., 2008, "Epitaxial graphene on ruthenium," Nat Mater, 7(5), pp. 406-411.

37. Coraux, J., N`Diaye, A. T., Busse, C., and Michely, T., 2008, "Structural Coherency of Graphene on Ir (111)," Nano Letters, 8(2), pp. 565-570.

38. Li, X., Cai, W., An, J., Kim, S., Nah, J., Yang, D., Piner, R., Velamakanni, A., Jung, I., Tutuc, E., Banerjee, S. K., Colombo, L., and Ruoff, R. S., 2009, "Large-Area Synthesis of High-Quality and Uniform Graphene Films on Copper Foils," Science, 324(5932), pp. 1312-1314.

39. May, J. W., 1969, "Platinum surface LEED rings," Surface Science, 17(1), pp. 267-270.

40. Blakely, J. M., Kim, J. S., and Potter, H. C., 1970, Segregation of Carbon to the (100) Surface of Nickel, AIP.

41. Eizenberg, M., and Blakely, J. M., 1979, "Carbon monolayer phase condensation on Ni (111)," Surface Science, 82(1), pp. 228-236.

42. Eizenberg, M., and Blakely, J. M., 1979, Carbon interaction with nickel surfaces: Monolayer formation and structural stability, AIP.

43. Hamilton, J. C., and Blakely, J. M., 1978, Carbon layer formation on the Pt (111) surface as a function of temperature, AVS.

44. Hamilton, J. C., and Blakely, J. M., 1980, "Carbon segregation to single crystal surfaces of Pt, Pd and Co," Surface Science, 91(1), pp. 199-217.

45. Patil, H. R., and Blakely, J. M., 1974, Electron energy losses in thin graphite layers on the (111) face of nickel, AIP.

46. Shelton, J. C., Patil, H. R., and Blakely, J. M., 1974, "Equilibrium segregation of carbon to a nickel (111) surface: A surface phase transition," Surface Science, 43(2), pp. 493-520.

47. Pletikosić, I., Kralj, M., Pervan, P., Brako, R., Coraux, J., N'Diaye, A. T., Busse, C., and Michely, T., 2009, "Dirac Cones and Minigaps for Graphene on Ir(111)," Physical Review Letters, 102(5), p. 056808.

48. Chuhei Oshima and Ayato, N., 1997, "Ultra-thin epitaxial films of graphite and hexagonal boron nitride on solid surfaces," Journal of Physics: Condensed Matter, 9(1), p. 1.

49. Tontegode, A. Y., 1991, "Carbon on transition metal surfaces," Progress in Surface Science, 38(3-4), pp. 201-429.

50. Isett, L. C., and Blakely, J. M., 1976, "Segregation isosteres for carbon at the (100) surface of nickel," Surface Science, 58(2), pp. 397-414.

51. Yu, Q., Lian, J., Siriponglert, S., Li, H., Chen, Y. P., and Pei, S.-S., 2008, Graphene segregated on Ni surfaces and transferred to insulators, AIP.

52. Bhaviripudi, S., Jia, X., Dresselhaus, M. S., and Kong, J., 2010, "Role of Kinetic Factors in Chemical Vapor Deposition Synthesis of Uniform Large Area Graphene Using Copper Catalyst," Nano Letters, 10(10), pp. 4128-4133.

53. Ji, H., Hao, Y., Ren, Y., Charlton, M., Lee, W. H., Wu, Q., Li, H., Zhu, Y., Wu, Y., Piner, R., and Ruoff, R. S., 2011, "Graphene Growth Using a Solid Carbon Feedstock and Hydrogen," ACS Nano, 5(9), pp. 7656-7661.

54. Li, X., Cai, W., Colombo, L., and Ruoff, R. S., 2009, "Evolution of Graphene Growth on Ni and Cu by Carbon Isotope Labeling," Nano Letters, 9(12), pp. 4268-4272.

55. Conrad, J. H. a. W. A. d. H. a. E. H., 2008, "The growth and morphology of epitaxial multilayer graphene," Journal of Physics: Condensed Matter, 20(32), p. 323202.

Chapter 2 - Experimental setup

After synthesizing graphene it is very essential to unambiguously prove that it is graphene. It requires a combination of characterization techniques. There are three things which need to be determined to characterize the sample: (1) quality, (2) number of layers and (3) size of the sheet. Transmission electron microscopy (TEM) imaging and scanning electron microscopy (SEM) imaging provides the means to determine the size of the graphene sheets. But Raman spectroscopy is required to accurately determine the number of layers and degree of disorder in the sheets.

2.1 Raman spectroscopy

Raman spectroscopy provides a unique method for identifying a broad range of carbon material. It is the most important of the characterization techniques as it provides a unambiguous, high throughput, nondestructive identification of graphene layers. There are other methods of identifying the number of layer in graphene like atomic force microscopy and quantum hall probing. The former takes a lot of time to give results and gives inaccurate thickness due to edge effects and the later requires processing and ohmic contacts. This chapter briefly describes the science of Raman spectroscopy, followed by a description of the characteristic peaks in graphene.

2.1.1 Classical theory of Raman scattering

A photon is described as an electromagnetic wave with frequency υ_o which induces a dipole on the molecule. The strength, P, of the induced dipole moment is given by,

$$P = \alpha E \qquad (2.1)$$

Where α is called polarizability and E is the electric field produced by the incident electromagnetic wave. Polarisability depends on the shape, size of the molecule and the nature of the bond. In an electric field the electron cloud of a large molecule which has a large amount of electron is polarized more easily than a small and compact small molecule which has less number of electrons.

The electric field of an electromagnetic wave fluctuates with time, t:

$$E = E_0 \cos(2\pi\nu_0 t) \qquad (2.2)$$

Thus substituting eqn (2.1) in eqn (2.2) we get,

$$P = \alpha E_0 \cos(2\pi\nu_0 t) \qquad (2.3)$$

If the molecule is vibrating with a frequency of υ_m, the physical displacement dQ of the atoms about their equilibrium position is written as

$$dQ = Q_0 \cos(2\pi\nu_m t) \qquad (2.4)$$

If the displacement is small, the polarizability can be written as

$$\alpha = \alpha_0 + (\frac{\delta\alpha}{\delta Q})_o \, dQ \qquad (2.5)$$

Here, α_0 is the polarizability at equilibrium position, and $(\frac{\delta\alpha}{\delta Q})_0$ is the rate of change of α with respect to change in distance which is evaluated at equilibrium position.

Combining eqn (2.3) and eqn (2.4) into eqn (2.5), we get

$$P = \alpha_0 E_0 \cos(2\pi\nu_0 t) + \frac{1}{2}\frac{\delta\alpha}{\delta Q_0} Q_0 E_0 [\cos(2\pi(\nu_0 + \nu_m) t) \cos(\nu_0 - \nu_m)t)] \qquad (2.6)$$

The first term of the equation has the same frequency as that of the exited photon which accounts for Rayleigh scattering while the second term determines the anti-Stokes and Stokes processes of Raman scattering. From the equation it is clear that the $(\frac{\delta\alpha}{\delta Q})_o$ should be non-zero for Raman scattering. This means that only if the change is polarizable then the motion is Raman-active.

2.1.2 Quantum theory of Raman scattering

In quantum physics Raman scattering occurs when in an inelastic scattering process a photon is annihilated and creates a phonon and a Strokes photon. Inversely, it also happens when a photon together with a annihilated phonon creates an anti-Stokes photon. According to quantum theory, for a transition between two energy levels in an electronic band occurs due to an emission or absorption of photons. Thus the photons are considered to have energy and mass. An energy transfer occurs when the Bohr's frequency condition is satisfied

$$\Delta E = h\nu_m \qquad (2.7)$$

As a result, the electrons can pass only to the states which have a difference in energy equal to the transfer energy.

$$\Delta E = E - E_0 \qquad (2.8)$$

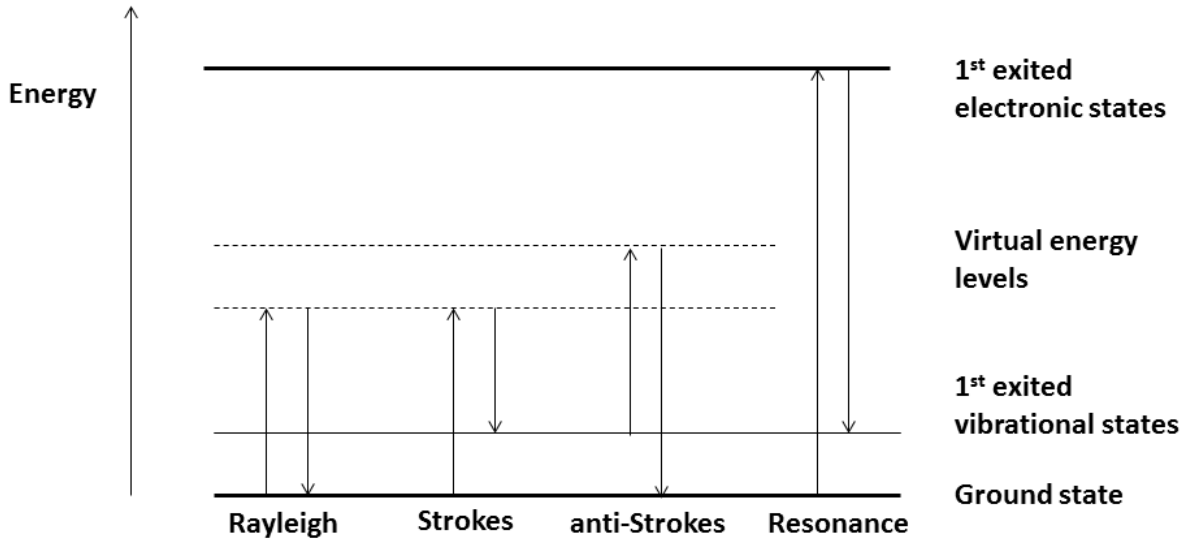

Figure 2.1 General picture of Rayleigh, Strokes, anti-Strokes and resonance scattering processes.

In the quantum picture that explains the Raman scattering, the virtual states are considered as intermediate states between the ground state and the first exited state. What happen in a Rayleigh scattering process is that the electrons gets energized and falls back to the ground state by emitting a photon with the same frequency as that of the incident radiation., whereas in a Strokes scattering the electron starts from the ground state and lands on a higher energy level, and vice-versa for anti-Strokes scattering. This Raman shift represents the different vibrational level

which corresponds to the phonon's energy which depends on the material and is independent on the frequency of the emitted photon.

2.2 Peaks in the plot of graphene

Graphene consists of sp^2 carbon hexagonal networks, in which the carbon atoms are bonded by strong covalent bonds. Raman spectroscopy makes use of the electron-phonon interaction to uniquely capture the electronic structure of single, bi and few-layer graphene.

The number of graphene layers in a flake can be determined by studying the 2D peak of the Raman spectrum. Ferrari *et al.,* showed that a flake of graphene which has few layer graphene exhibit similar 2D peak as that of HOPG [1, 2], while the bi-layer graphene exhibit an asymmetric peak which is at 2700 cm^{-1}. They also showed that for a single layer graphene exhibit a 2D peak that is symmetric and down-shifted to 2680 cm^{-1}.

Using Raman spectroscopy we can also determine the quality of graphene. This technique is used to determine the presence of disorder and defects in the graphene sheets. The two common Raman peaks D and G peak positioned near 1350 and 1580 cm^{-1} respectively is produced by all major allotropes of carbon like graphene, graphite, carbon nanotubes, carbon soot, carbon fiber, coal, etc[1, 4-10]. The structure and the position of these peaks provide information on the degree of disorder in the structure. In a typical HOPG crystal shows a minimal D peak at 1350 cm^{-1} and a sharp G peak at 1580 cm^{-1}.

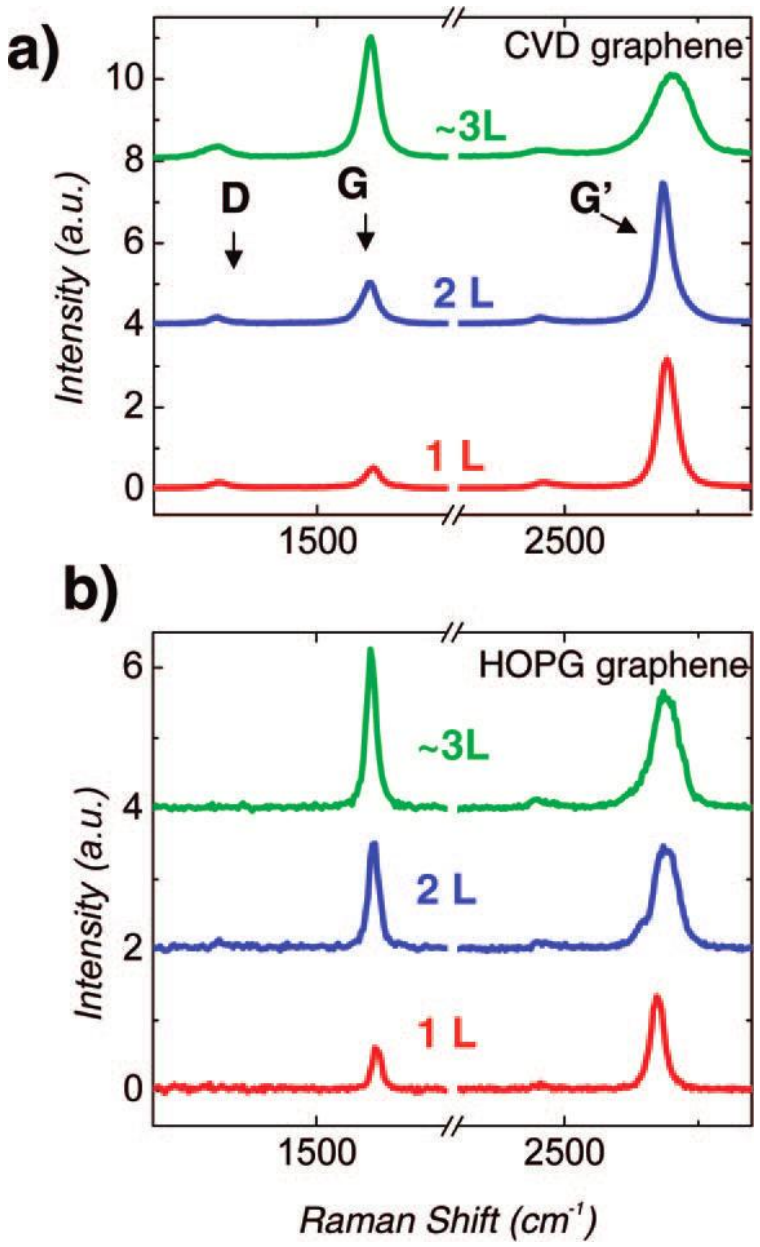

Figure 2.2 (a) Raman spectrum of 1-LG (one layer graphene-red), 2-LG (two layer graphene-blue), 3-LG (three layer graphene-red) synthesized by CVD process on Ni substrate and then transferred to a SiO_2/Si substrate. (b) Raman spectrum of 1-LG (one layer graphene-red), 2-LG (two layer graphene-blue), 3-LG (three layer graphene-red) prepared by mechanical exfoliation technique from HOPG, shown for comparison. (Source Ref no. 13)

The letter D denotes defects in the graphitic structure[5]. As the amount of defect increases, so does the intensity of the D peak[4-10]. This increases the ration of intensities of the D and G peak also (I_D / I_G). In addition to that the Full Width and Half Maximum (FWHM) of the D peak increases but the peak remain at 1350 cm^{-1}, while the FWHM of G peak also increases and displaces to higher values in excess of 1600 cm^{-1} as the number of defects increases. Pristine graphene which is mechanically exfoliated from HOPG show no D peak and a sharp and narrow G peak[1] and thus a pure sheet of graphene should have the (I_D / I_G) ratio of zero. Graphene sheets synthesized by other approaches which do not yield pristine graphene has shown strong and broadened D peak, wide and upshifted G peak and (I_D / I_G) ratio that is close to one or greater than one.

2.3 Raman instrumentation

The Raman spectra were obtained by using a LabRAM ARMIS Raman spectrometer operated by the Bioengineering Research Center, University of Kansas, Lawrence, KS. The instrument was manufactured by HORIBA Jobin Yvon (Edison, New Jersey). The laser source was a HeNe laser (l = 633 nm, a laser power of 17 mW) was used. The instrument setup was as follows: 200 µm confocal hole, 150 µm wide entrance slit, 600 gr/mm grating and 100x objective lens. The data processing was performed using LabSPEC 5 (HORIBA Jobin Yvon) software. The samples were mounted onto the sample holder in the microscope which was in a computer controlled, high-precision x-y stage.

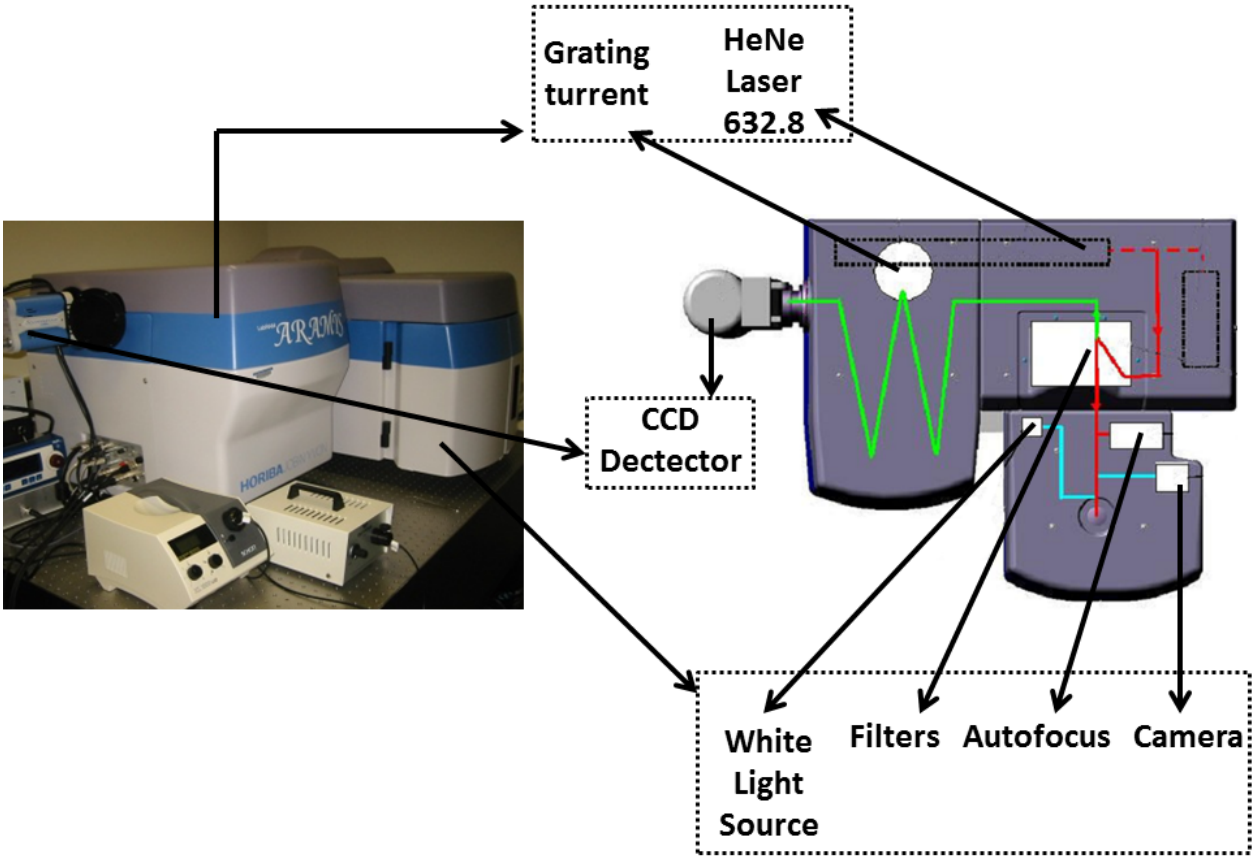

Figure 2.3 General schematic showing individual components of Raman spectrometer used to characterize graphene specimen in this work.

2.4 SEM imaging

Once the quality of the graphene sheets and the number of layers had been identified by Raman spectroscopy determining the size of the sheets is the next step in characterizing the graphene sheets. There are three imaging techniques used to image the structure Transmission Electron Microscopy (TEM), Scanning Electron Microscopy (SEM) and optical microscopy. Scanning electron microscopy provides a fast and easy method of determining the size of the graphene sheet.

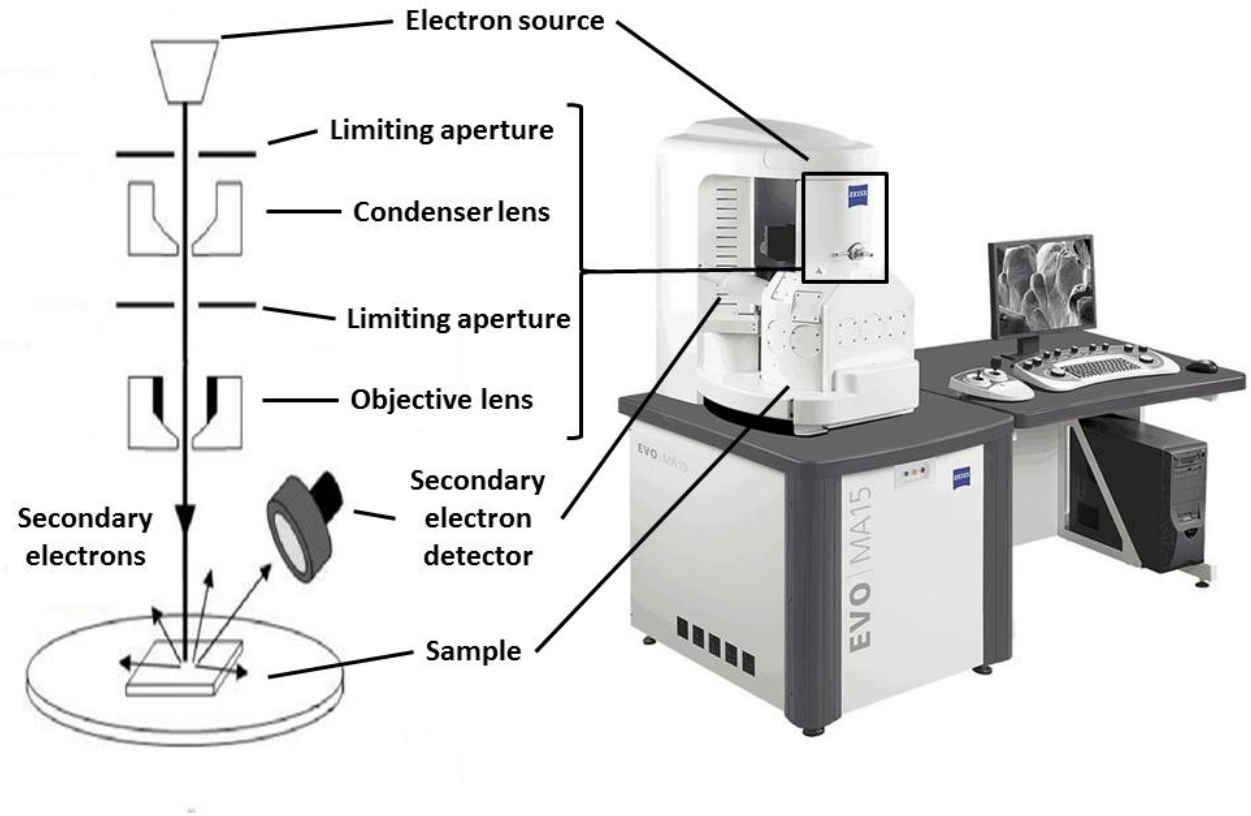

Figure 2.4 General schematic showing individual components of EVO MA15 Scanning Electron Microscope. The high energy electrons emitted from the electron source are collimated into a narrow beam by a series of condenser and objective lenses.

The principle of operation of SEM is by electron rastering across the sample surface and collecting either secondary electrons or back scattered electrons. The electron beam is controlled by a series of lenses which are as shown in the Figure 2.4. The intensity of the incident electron beam could be anywhere from a few hundred eV to 30KeV. When an electron is incident on the sample, secondary electrons are generated by inelastic collisions between the electron beam and electrons surrounding atoms in the sample. These collisions result in low energy electrons to

escape from the surface of the sample and are detected by the detector. The secondary electrons are low energy electrons, so only electrons from the top few nm of sample escape the surface. This means that these electrons are very sensitive changes in the composition and topography of the sample surface.

Backscattered electrons are basically incident electrons that are reflected back from the nuclei of atoms in the sample. A backscattered electron is a high energy electron and it can penetrate very deep into the sample. Also the amount of backscattered electrons is equal to the atomic number of the substance. Thus if the sample has heavy elements in them then it would appear bright.

2.5 SEM instrumentation

Images of the synthesized materials were obtained using a Carl Zeiss EVO MA10 system. The electron source is a tungsten electrode. The incident voltage of the electron could be varied from 5 KV to 30 KV. The chamber is kept at a constant low pressure of 5×10^{-7} Torr using a combination of two vacuum pumps. The image accusation and processing was performed in SmartSEM (Carl Zeiss) software. Even though the system was equipped with both back scattered electron detector and secondary electron detector, only the back scattered electron detector was used to obtain the images.

2.6 Chemical vapor deposition (CVD)

A Chemical Vapor Deposition (CVD) is a chemical process in which hot volatile precursors are exposed to a catalytic substrate thus producing the desired deposit. The precursors usually chemically react and/or decompose at elevated temperatures. The catalyst also becomes active at high a temperature which leads to volatile by-products being produced, which are removed by the carrier gasses that flow through the tube furnace. The atmosphere for the reaction is usually kept inert using noble gasses as the substrate or the reaction gasses will react with gasses in atmosphere like oxygen, etc. Thus there lies three main parts in a CVD process: (1) substrate, (2) precursor gasses and (3) inert carrier gas. The substrate temperature is a critical condition in the reaction because the substrate acts as a catalyst which requires appropriate temperature to activate. There are many CVD processes available which are used extensively in semiconductor industry. Of these the once which are prominently used in the field of nanotechnology are (1) Atmospheric Pressure Chemical Vapor Deposition (APCVD), (2) Low Pressure Chemical Vapor Deposition (LPCVD), Plasma Assisted Chemical Vapor Deposition (PACVD) or Plasma Enhanced Chemical Vapor Deposition (PECVD). APCVD is the process that is used to synthesize graphene in this work. The advantage of APCVD over others is that it is a simple setup. But it involves strict control over the process parameters like the gas flow rate, growth time and temperature because of the high volume of reactions gasses present at the growth temperature.

2.6.1 Description of the chemical vapor deposition reactor before modifications

A general structure of a CVD reactor consists of the following parts: (1) gas delivery system- for supply of precursors to the reaction chamber, (2) reactor chamber- within which deposition takes place, (3) substrate loading mechanism- a system of introducing and removing substrate from the reaction chamber, (4) energy source- energy that is required to get the precursor to react and decompose, (5)vacuum system- a system for removal of all other gaseous species other than those required for the reaction/deposition, (6) exhaust system- a system for removal of volatile by-products from the reactor chamber, (7) exhaust treatment system- in some situation the by-products may not be suitable for release into the atmosphere and may require some treatment and/or conversion to safe/harmless compounds, and (8) process control equipment- gauges, controls, etc., to monitor process parameters such as pressure, temperature and time. Alarms and safety devices would also be included in this category.

In this system, as it is an APCVD, there are three gas flow controllers for the three gasses, hydrogen, methane and argon, each with a maximum range of 500, 200 and 10000 respectively. The flow controllers are manufactured by MKS systems with an accuracy of ±1%. The controller has a stop valve which is operated by a pneumatic system which is actuated with compressed nitrogen. It has a solenoid operated pressure control valve, which delivers the right amount of gas as specified in the program.

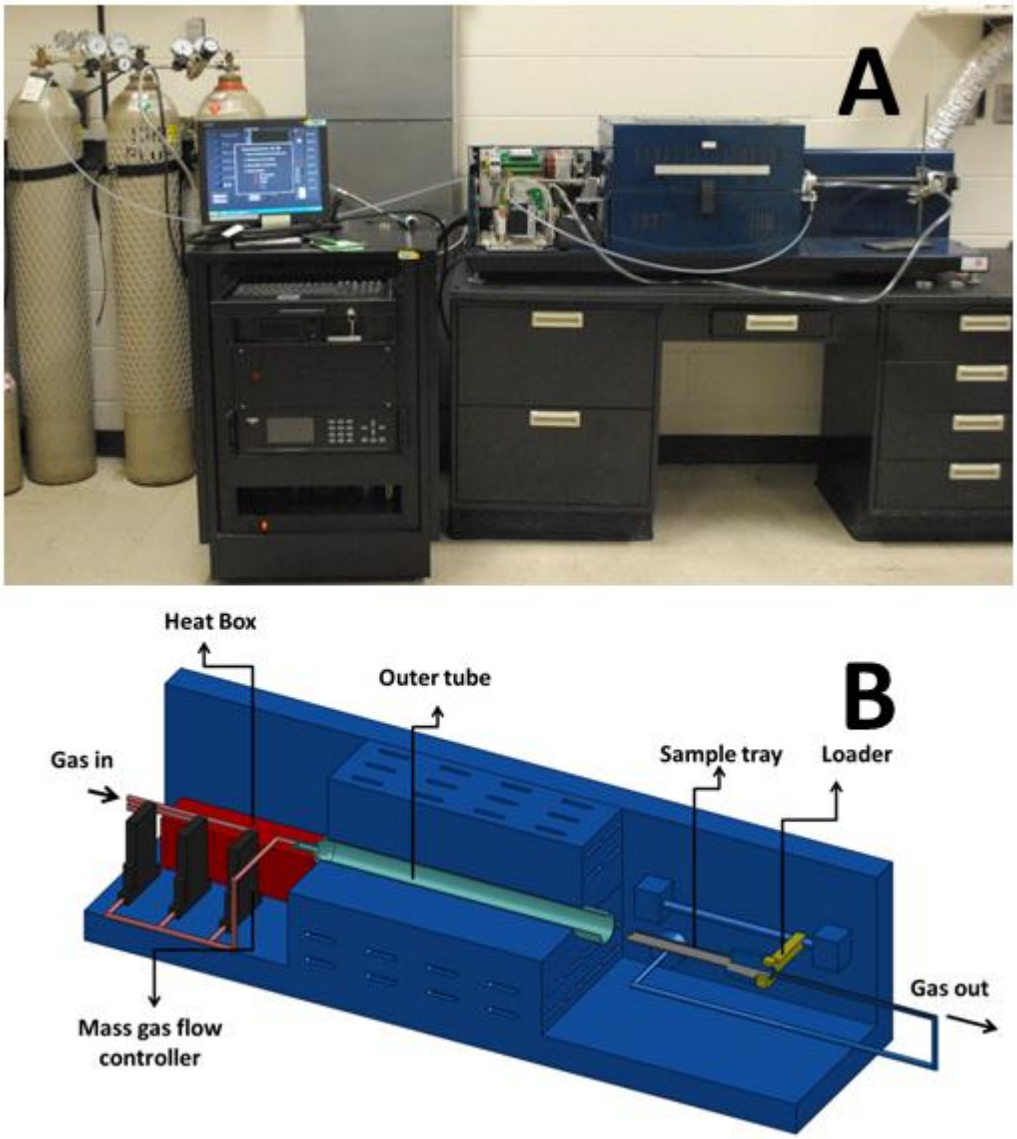

Figure 2.5 (A) Chemical Vapor Deposition setup used in the experiment to synthesize graphene. (B) Graphical representation of the actual CVD furnace used in the experiments. The quartz tube is placed inside a box furnace. The sample is placed in the sample tray that slides into the tube using a loader. The furnace is fitted with specific fixtures to install the mass gas flow controller and all other electronic control system which makes the furnace a complete stand-alone CVD system.

The reactor chamber is an alumina insulated cylindrical chamber with a quartz tube of 48 cm internal diameter which is supported only at the ends. The means of heating inside the chamber is convection heating and the reactor chamber is completely insulated which helps in maintaining the temperature in a steady constant rate inside the chamber during reaction.

The energy source is thermal energy produced by the resistance heating of the current carrying coils inside the reactor. The amount of current is constantly monitored. According to the temperature inside the chamber and the target input temperature the current in the coil it varied thus heating the furnace. The next component is the loader assembly. In this system the loader is operated by a stepper motor with limit switches at the ends. As for the vacuum system, it is not required as it is an APCVD. The pressure inside the furnace is at the ambient pressure. The reactants decompose and they mainly form hydrogen and carbon which are harmless but hydrogen is volatile. Also because the volume of these gasses in the chamber is not so large it is perfectly safe to keep the exhaust open to the atmosphere for it to reduce the concentration of the gasses. But as the system is place in a closed room in this condition the exhaust is safely removed through the fume hood. Ass these different components are controlled by a program which is written in labview. There are various different safety locks in the software for each of the components which are used to prevent any mishap from occurring.

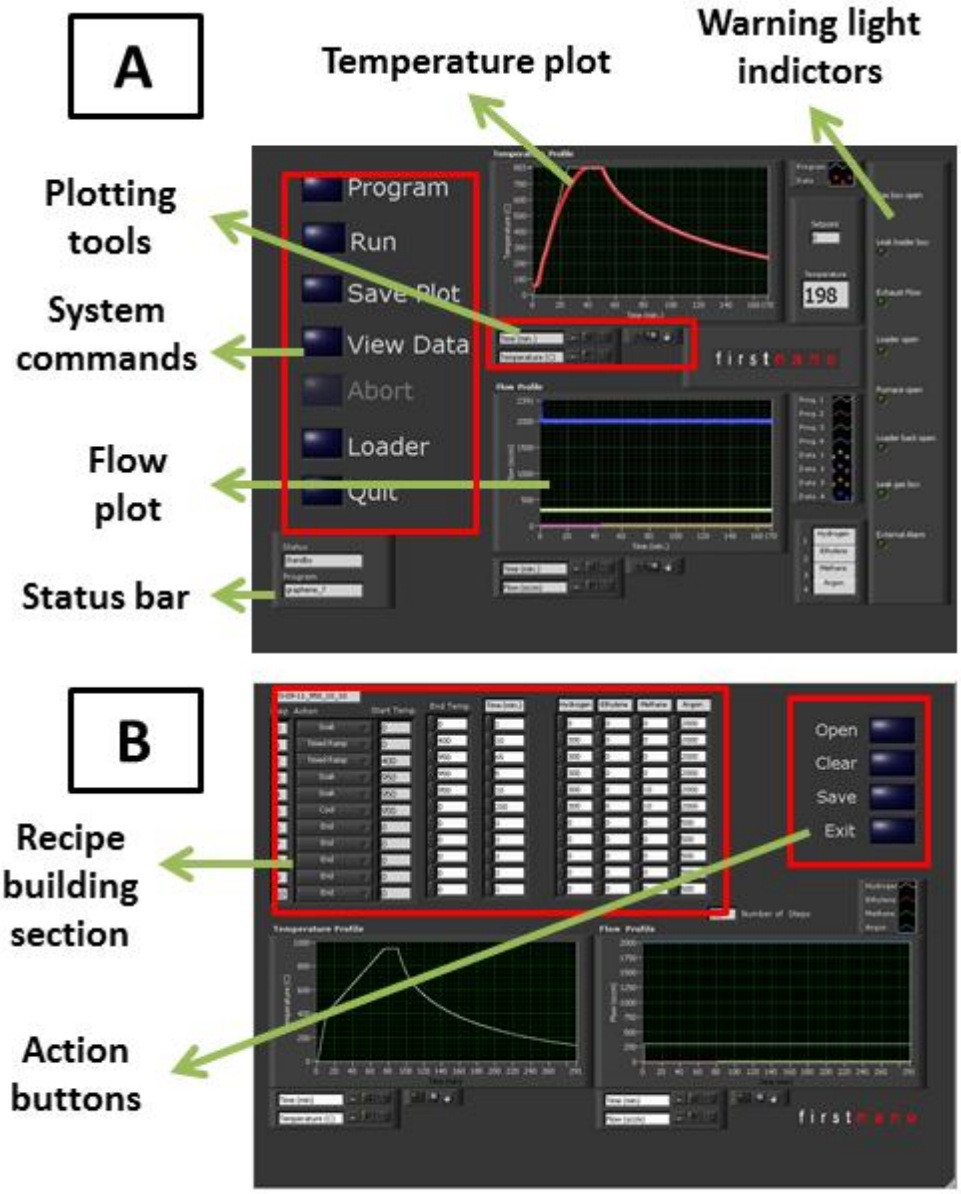

Figure 2.6 (A) Picture of a typical graphical user interface (GUI) in the CVD furnace. Image (A) is the front page of the GUI with the warning lights located at the right of the screen. (B) The recipe build area allows operator to build a new recipe by identifying the steps. It also offers to save and use the recipe for the future use.

2.6.2 Description of the chemical vapor deposition reactor after modifications

The system is almost the same as the stock system that was purchased from the company. But instead of a flat loader the system is provided with a cylinder which has a smaller diameter than the quartz tube in de furnace.

This provides an opportunity to introduce or remove the substrate from the reactor at any given time. Due to this a very high cooling and/or heating rate is achieved which opens new areas of studying the mechanism of reaction in the synthesis of graphene. To achieve this, the direction of flow in the furnace has been changed. This is done to ensure that the full volume of gasses flow through the substrate and no amount of gas is leaked before the substrate to give a precise control over the flow.

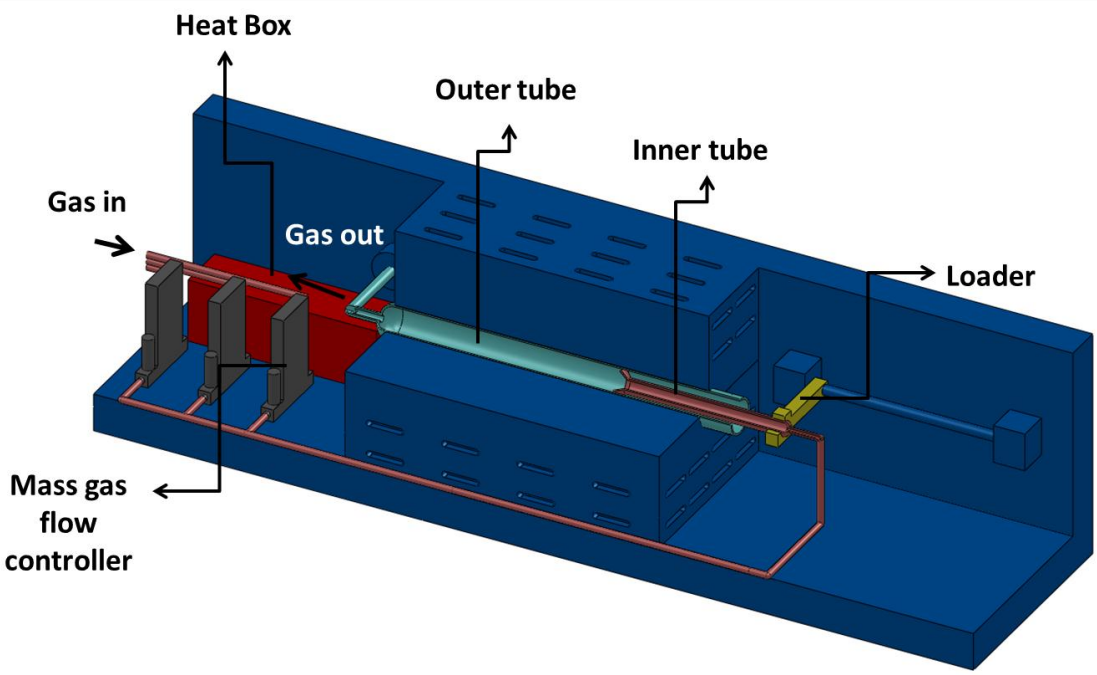

Figure 2.7 Graphical representation of the modified furnace. Instead of the sample tray the system is fitted with another smaller inner tube which acts as the sample holder. The gas delivery and the exhaust system were modified to accommodate the changes. This makes it easy to cool the sample as the inner tube slides out of the hot zone while still maintaining the inert atmosphere around the specimen.

2.7 References

1. Ferrari, A. C., 2007, "Raman spectroscopy of graphene and graphite: Disorder, electron-phonon coupling, doping and nonadiabatic effects," Solid State Communications, 143(1-2), pp. 47-57.
2. Ferrari, A. C., Meyer, J. C., Scardaci, V., Casiraghi, C., Lazzeri, M., Mauri, F., Piscanec, S., Jiang, D., Novoselov, K. S., Roth, S., and Geim, A. K., 2006, "Raman Spectrum of Graphene and Graphene Layers," Physical Review Letters, 97(18), p. 187401.
3. Casiraghi, C., Pisana, S., Novoselov, K. S., Geim, A. K., and Ferrari, A. C., 2007, Raman fingerprint of charged impurities in graphene, AIP.
4. Ferrari, A. C., and Robertson, J., 2000, "Interpretation of Raman spectra of disordered and amorphous carbon," Physical Review B, 61(20), p. 14095.
5. Cuesta, A., Dhamelincourt, P., Laureyns, J., Martínez-Alonso, A., and Tascón, J. M. D., 1994, "Raman microprobe studies on carbon materials," Carbon, 32(8), pp. 1523-1532.
6. Bacsa, W. S., de Heer, W. A., Ugarte, D., and Châtelain, A., 1993, "Raman spectroscopy of closed-shell carbon particles," Chemical Physics Letters, 211(4-5), pp. 346-352.
7. Gruber, T., Zerda, T. W., and Gerspacher, M., 1994, "Raman studies of heat-treated carbon blacks," Carbon, 32(7), pp. 1377-1382.
8. Jawhari, T., Roid, A., and Casado, J., 1995, "Raman spectroscopic characterization of some commercially available carbon black materials," Carbon, 33(11), pp. 1561-1565.
9. Ivleva, N. P., Messerer, A., Yang, X., Niessner, R., and Pöschl, U., 2007, "Raman Microspectroscopic Analysis of Changes in the Chemical Structure and Reactivity of Soot in a Diesel Exhaust Aftertreatment Model System," Environmental Science & Technology, 41(10), pp. 3702-3707.
10. Stankovich, S., Dikin, D. A., Piner, R. D., Kohlhaas, K. A., Kleinhammes, A., Jia, Y., Wu, Y., Nguyen, S. T., and Ruoff, R. S., 2007, "Synthesis of graphene-based nanosheets via chemical reduction of exfoliated graphite oxide," Carbon, 45(7), pp. 1558-1565.
11. Kudin, K. N., Ozbas, B., Schniepp, H. C., Prud'homme, R. K., Aksay, I. A., and Car, R., 2007, "Raman Spectra of Graphite Oxide and Functionalized Graphene Sheets," Nano Letters, 8(1), pp. 36-41.

12. Reina, A., Jia, X., Ho, J., Nezich, D., Son, H., Bulovic, V., Dresselhaus, M. S., and Kong, J., 2008, "Large Area, Few-Layer Graphene Films on Arbitrary Substrates by Chemical Vapor Deposition," Nano Letters, 9(1), pp. 30-35.
13. Malard, L. M., Pimenta, M. A., Dresselhaus, G., and Dresselhaus, M. S., 2009, "Raman spectroscopy in graphene," Physics Reports, 473(5-6), pp. 51-87.

Chapter 3 - Synthesis of graphene: Chemical vapor deposition using copper as catalyst

The preferred way to synthesize pristine graphene with minimum defects is mechanical exfoliation of highly oriented pyrolytic graphite (HOPG). Even though these are pristine the size of graphene sheets cannot be scaled up above a certain limit. To obtain graphene in sheets of large size, suitable for industrial production, chemical vapor deposition (CVD) is used. Initially only single crystal transition metals like Pt were used as catalyst [1, 2]. Alternatively poly crystalline materials like nickel [3, 4] and copper [3, 5] foils have been used as substrate to produce large scale graphene sheets through CVD.

This chapter focuses on synthesis of graphene on copper substrate. First the experimental procedures like cleaning and process flow charts are discussed. This is followed by discussion on initial results of graphene which is grown following a similar procedure provided by Reina *et al.,* [3]. This chapter ends with a discussion of the transfer techniques from metallic to insulating substrate.

3.1 Literature review

In 2009, Ruoff and co-workers[6] were the first to successfully develop a graphene chemical vapor deposition (CVD) growth process on copper foils. The graphene that they synthesized were predominantly monolayer with only < 5 % of the area having two- or three-layer graphene flakes. Towards the end of 2010, Tour and co-workers[8] showed a controllable growth of pristine PMMA-derived graphene films on Cu substrate. The also used other carbon sources like fluorine

and sucrose. In 2011 Ruoff and co-workers[7] explored the possibility of synthesizing graphene from amorphous carbon on a thin Cu foil. They studied the effect of hydrogen flow in the graphene growth process. They concluded that the mechanism of graphene growth on Cu is by surface chemistry on the catalyst. The presence of hydrogen converts the carbon source to hydrocarbons like CH_4 or CH_3^+ and then later these hydrocarbons reacts with the Cu catalyst forming graphene. Cho *et al.,* [9] investigated the effects of thermal annealing on ex-situ chemically vapor deposited sub-monolayer graphene islands. They showed that low-temperature annealing of graphene islands on Cu foil showed striped Moiré patterns, which proved the week interaction between graphene and its underlying substrate. These experiments showed the impenetrable nature of graphene and its potential application as a material that prevents corrosion. In the same year Chen *et al.,* [10] showed experimentally the excellent performance of graphene as a passivation layer. They proved that the layer of graphene is inert to oxidation and liquid solutions which opened a wide variety of applications.

3.2 Experimental procedure

3.2.1 Cleaning procedure

The cleaning procedure involves two parts: (1) cleaning the quartz tube and (2) cleaning the substrate. Before running the CVD system, the quartz tube has to be cleaned to reduce the amount of contaminants in the system. This process has to be repeated after four or five cycles to get consistent results as contaminants are known to affect the growth process. Due to the chemical process that occurs during the process, there is a possibility of carbon residue being

collected on the surface of the quartz tube. Thus to ensure optimum results, cleaning must be performed after a couple of runs.

The tube is first cleaned with acetone to remove any solid impurities. Then the clean cycle is executed. This is a preinstalled application in the system. In the clean cycle the quartz tube is baked in air at a temperature of 1000 °C and cooled down to room temperature. The loader is kept open during this process.

Commercially available Cu foil (Alfa Aesar item no. 13382) is used as the catalyst. To remove contaminates like packing residue, oil and dust particles the substrate is cleaned with acetone or isopropanol by ultra-sonication. After this the substrate is blown dry in air.

3.2.1 Steps involved in growth of graphene using CVD

The first step is to key in a program in the software. Values for different parameters like rate of heating, time of annealing and the flow rate for various gasses involved in the different steps of the process are keyed in. Once the program is keyed in the loader open command is executed using the software. Then a clean Cu foil is placed on the loader and closed. Once the loader is closed the run command is executed.

Table 3.1 Typical growth parameters used in the standard procedure.

Process	Start temperature (°C)	End temperature (°C)	Time (min)	Argon (SCCM)	Methane (SCCM)	Hydrogen (SCCM)
Soak	0	0	5	2000	0	0
Timed ramp	0	950	65	2000	0	300
Soak	950	950	20	2000	0	300
Soak	950	950	10	1000	10	300
Cool	950	0	200	3000	10	300

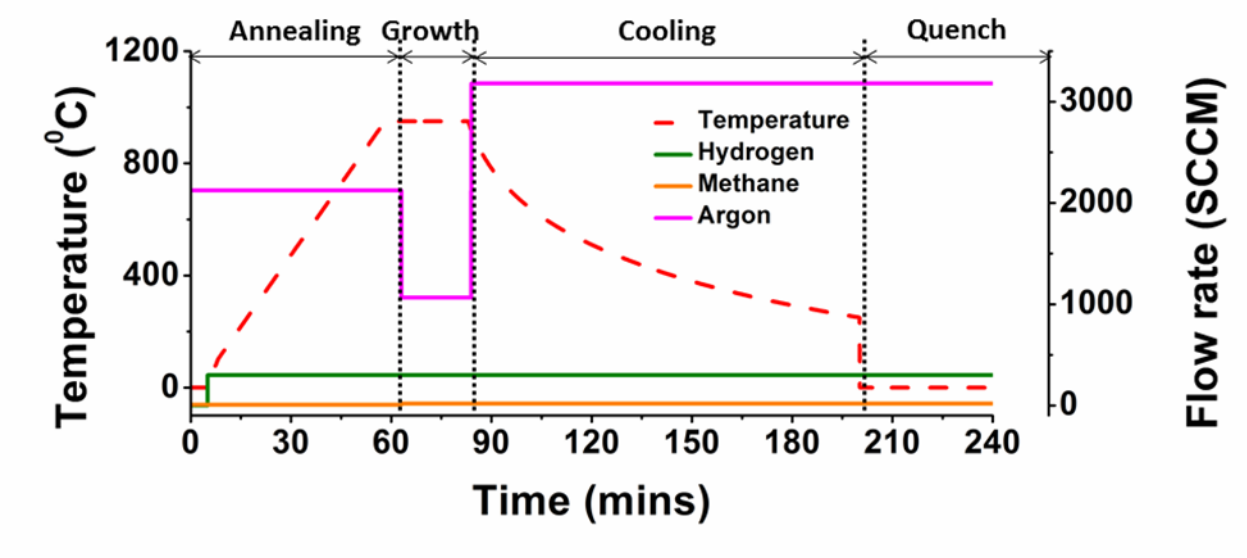

Figure 3.1 Plot of the growth parameters in the standard growth procedure used for synthesis of graphene on Cu substrate (temperature and flow rate) as a function of time.

At this point the valves for the gasses are opened and the system is checked to see if the different interlocks are in place. A typical growth procedure starts with purging of argon gas into the tube

for 5 mins. This effectively creates an inert atmosphere inside the quartz tube. Then the furnace is heated up to desired temperature, up to 1000 °C in the presence of argon and hydrogen. The temperature is stabilized for 5 mins to facilitate the actual temperature inside the furnace to become constant. At this growth temperature the precursor gas, CH_4, is passed into the furnace. And after a specified amount of time the furnace is cooled down to room temperature in presence of hydrogen, argon and hydrogen. It should be noted that cooling rate is not a critical factor for graphene growth on Cu.

3.3 Methodology

The quality and the coverage of graphene sheets vary from one CVD system to another. The main growth parameters that contribute to the CVD process are:

(1) Precursor used,

(2) Gas flow rate,

(3) Growth temperature,

(4) Pressure before, during and after growth,

(5) Growth period,

(6) Type of catalyst.

Of these, this chapter focuses on the effect of growth temperature, duration and gas flow rate. The samples are characterized using Raman spectroscopy and SEM.

3.4 Effect of growth temperature

One of the critical factors in synthesis of graphene is temperature because high energy is necessary to dissociate methane so that it reacts with the catalyst. Figure 3.3 shows the effect of temperature on the growth of graphene while keeping time and flow rates of gasses constant. The SEM images show that density and size of growth domains increases because of increase in the activity of the precursor at high temperature.

The Raman spectroscopy for each growth temperature is shown in Figure 3.2. It is noticed that the 2D peak is blue-shifted with increasing growth temperature while the G peak remains at the same place. This is a result of the uniform biaxial strain due to compression of Cu during cooling process which causes stress on the graphene sheet. This hypothesis is referred from the report by Novoselov *et al.,* [11], where uniaxial strain is applied on exfoliated graphene. In Raman spectroscopy, tension and compression induces a shift in 2D peak and also, the G peak splits into two due to the distortion of the hexagonal lattice structure. The two possible phonon modes of the in-plane bond stretching of a pair of carbon atoms are represented by the G peak.

Table 3.2 Parameters used to study the effect of change in growth temperatures.

Temperature (°C)	Time (min)	CH_4 rate (SCCM)	H_2 rate (SCCM)	I_D/I_G	I_{2D}/I_G
1000	20	30	300	0.46	0.39
950	20	30	300	0.20	0.19

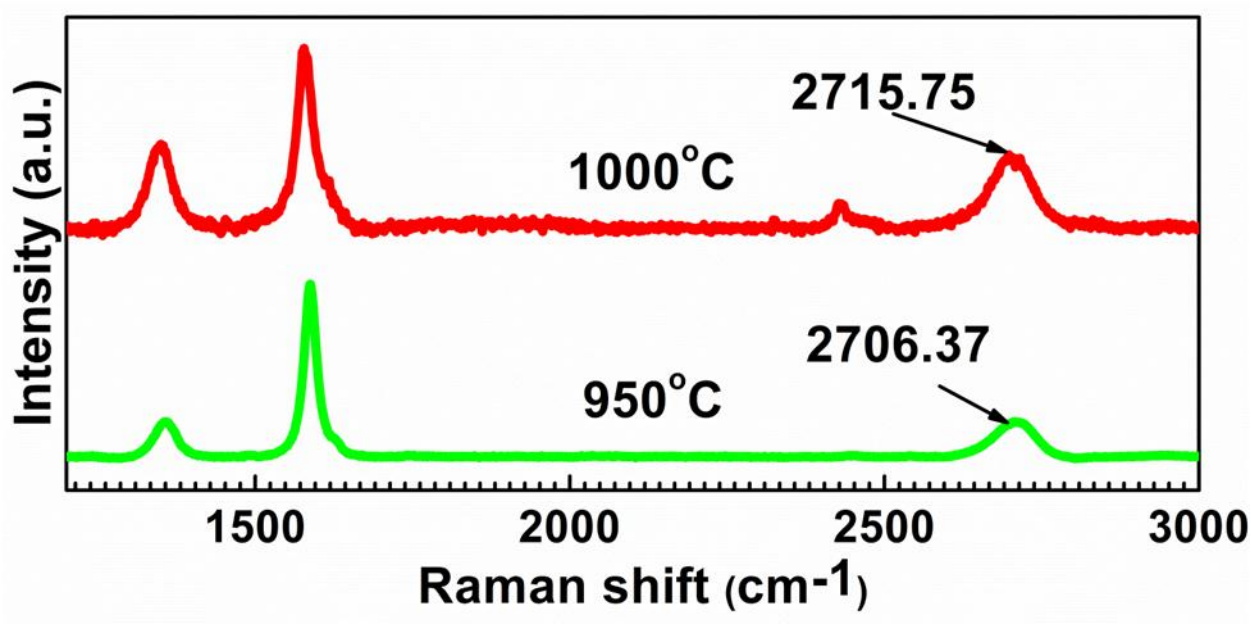

Figure 3.2 Raman spectra for each growth temperature. The samples were prepared using parameters stated in Table 3.2. The shift in location of the 2D peak is due to the strain on the graphene sheet due to shrinkage of copper when cooling.

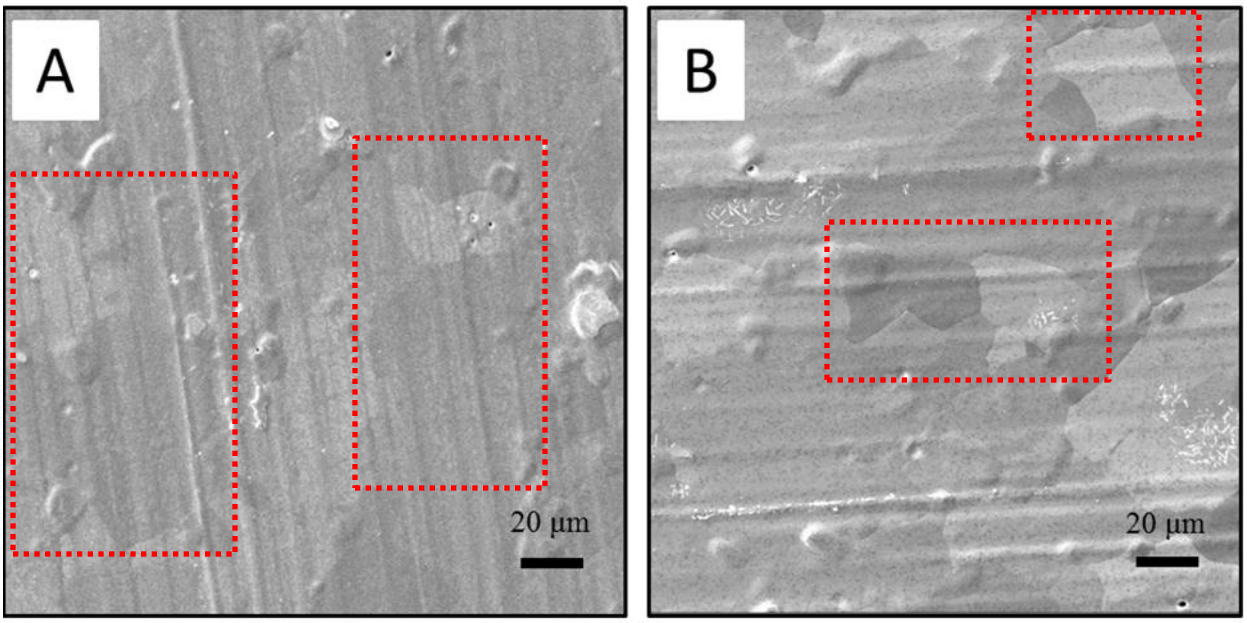

Figure 3.3 SEM images of synthesized graphene for (A) 950 °C and (B) 1000 °C. The change in contrast between the two images shows the increase in number of layers due to the high activity of carbon at higher temperatures. Other growth parameters are as shown in Table 3.2.

It is known that compression induces a larger Brillion zone as well as a narrow cone in the linear dispersion resulting in a low Fermi velocity. Including this the double resonance process is employed to explain the induced shift in the 2D peak. Figure illustrates the Raman process of unstrained graphene and compared it with compressed graphene. In an unstrained graphene, the 2D peak arises due to the emission of two phonons with a frequency of q_o. Under compression the frequency of phonon increases to q^* which results in a shift of the 2D peak to a higher frequency. As for the G peak, the hexagonal structure is kept intact under uniform biaxial strain which results in no shifting or splitting of G peak.

For unstrained graphene the 2D peak is located at 2680 cm^{-1}. In the data recorded the 2D peaks are located well above this value. Which is quiet normal as there is bound to be a certain amount of strain at any given temperature.

3.5 Effect of growth period

With experimental conditions as shown in Table 3.3, it is seen that the graphene growth is a quick process. The Figure 3.4 shows the evolution of graphene growth with respect to time of growth ranging from 3 minutes to 20 minutes at 950 °C with methane flow rate of 10 SCCM and hydrogen flow rate of 300 SCCM. The Raman spectrum proves that the majority of growth domains have coalesced to form graphene in 3 minutes.

But from the SEM images it is seen that the layers formed are all not uniform and there are spots where the bare copper is exposed. These empty spots seem to get covered as the duration of growth increases and at 20 minutes the entire surface of the copper foil is covered with graphene. This shows that the carbon atoms actively move in and out of the edges of the graphene sheet till all the growth domains are linked, forming a solid and stable graphene sheet. Longer growth durations give similar results. The Raman spectrum shows that the density of defects decreases as the time increases suggesting that it takes almost 10 minutes for the graphene to cover the entire area. But at higher duration the density of defects starts to increase suggesting that multiple layers starts to grow which is typical of an APCVD device. Thus the optimum growth duration is from 10 to 15 minutes.

Table 3.3 Parameters to study the effect of various growth time.

Time (min)	Temperature (°C)	CH_4 rate (SCCM)	H_2 rate (SCCM)	I_D/I_G	I_{2D}/I_G
3	950	10	300	0.28	0.38
10	950	10	300	0.23	0.44
20	950	10	300	0.51	0.26

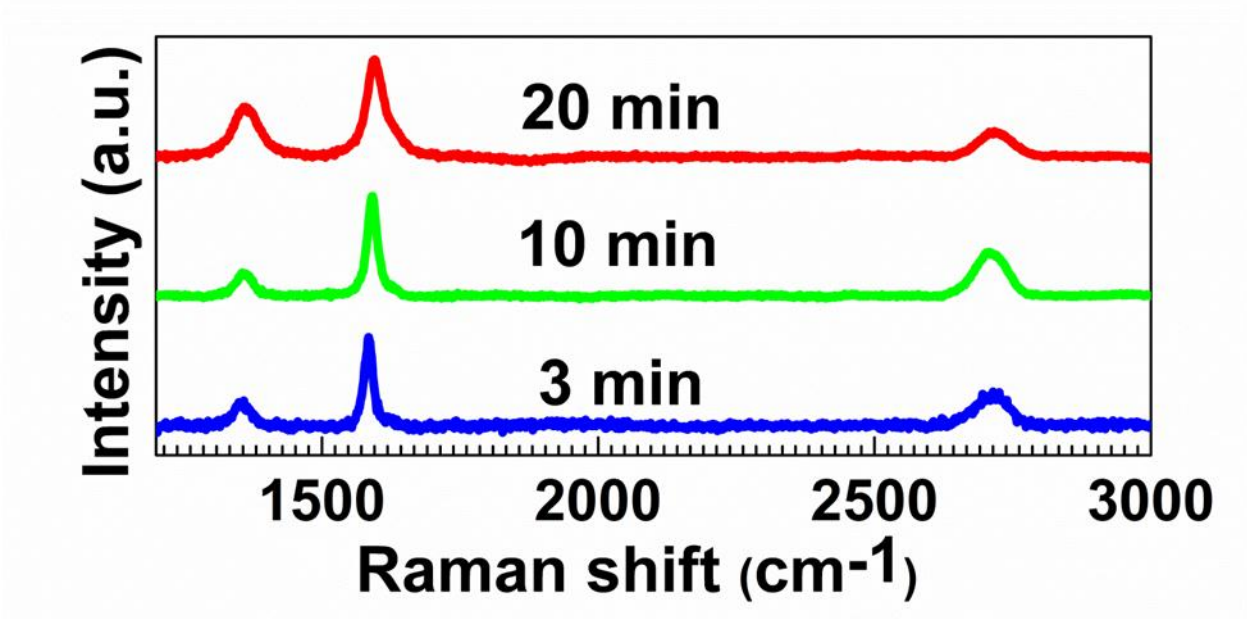

Figure 3.4 Raman spectra corresponding to each growth period. The samples were prepared using parameters as stated in Table 3.3. Complete coverage was observed for as little as 10 minutes.

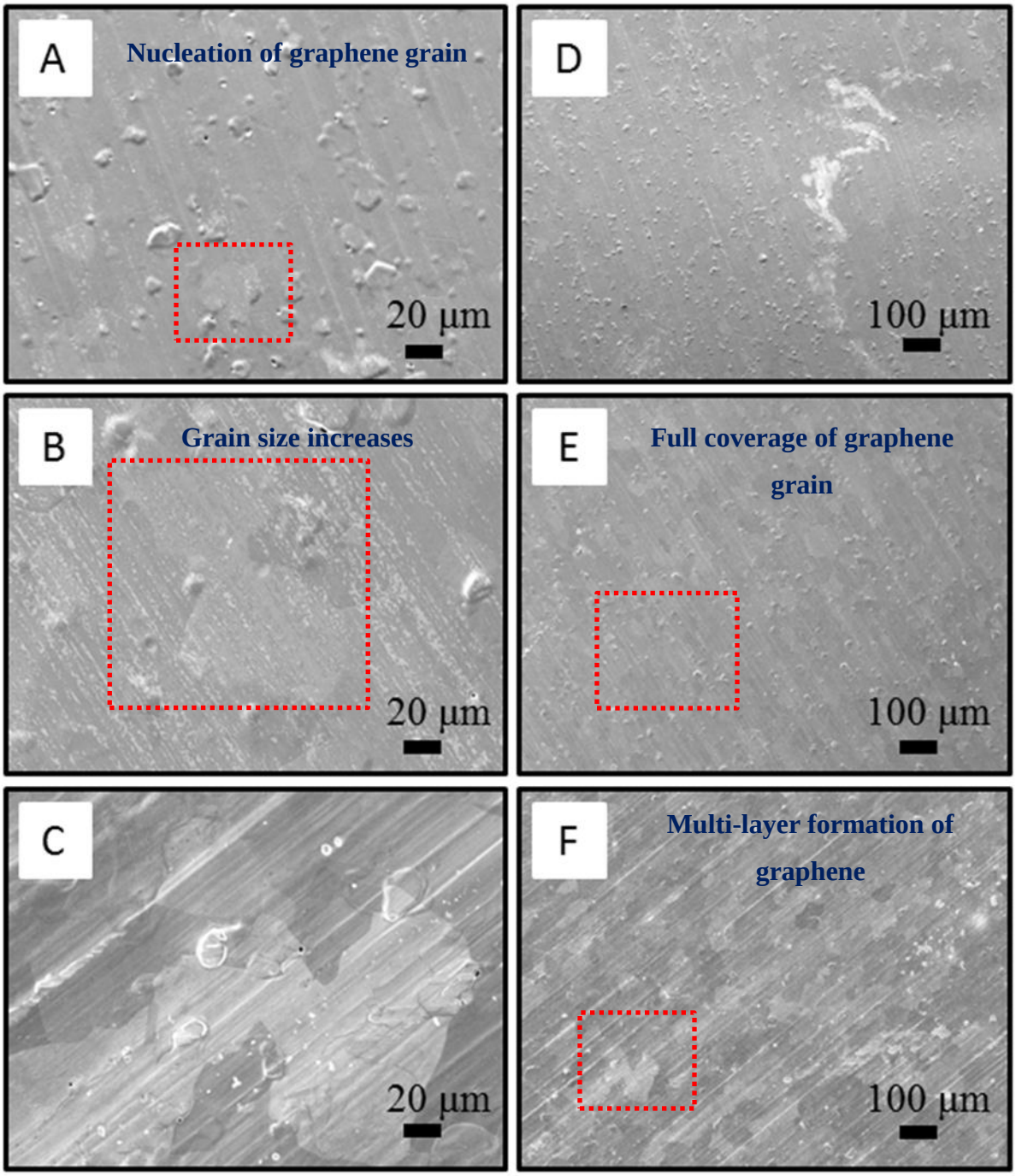

Figure 3.5 SEM images of synthesized graphene layers on Cu substrate grown for (A, D) 3 minutes, (B, E) 10 minutes and (C, F) 20 minutes with growth parameters as indicated in the Table 3.3. The grain size and the number of graphene layers increases as the time increases.

3.6 Effect of gas flow rate

The Raman spectrum shown in Figure 3.7 shows the effect of flow rate of CH_4 when the temperature and time are kept constant. To study this, the growth conditions used were as indicated in the Table 3.4.

The amount of precursor present actively greatly determines the quality of graphene produced. The Raman spectrum shows that as the flow rate increases the intensity of the 2D peak decreases. A possible explanation for this could be that as the flow rate of CH_4 increases, the gas density in the mixture increases. This increases the rate of catalytic reaction on the surface of copper thus forming multiple layers.

Table 3.4 Parameters to study the effect of different rate of flow of CH_4 keeping flow rate of H_2 constant at 300 SCCM.

CH_4 rate (SCCM)	Temperature (°C)	Time (min)	H_2 rate (SCCM)	I_D/I_G	I_{2D}/I_G
10	950	10	300	0.229973	0.44
20	950	10	300	0.535587	0.31
30	950	10	300	0.462042	0.2

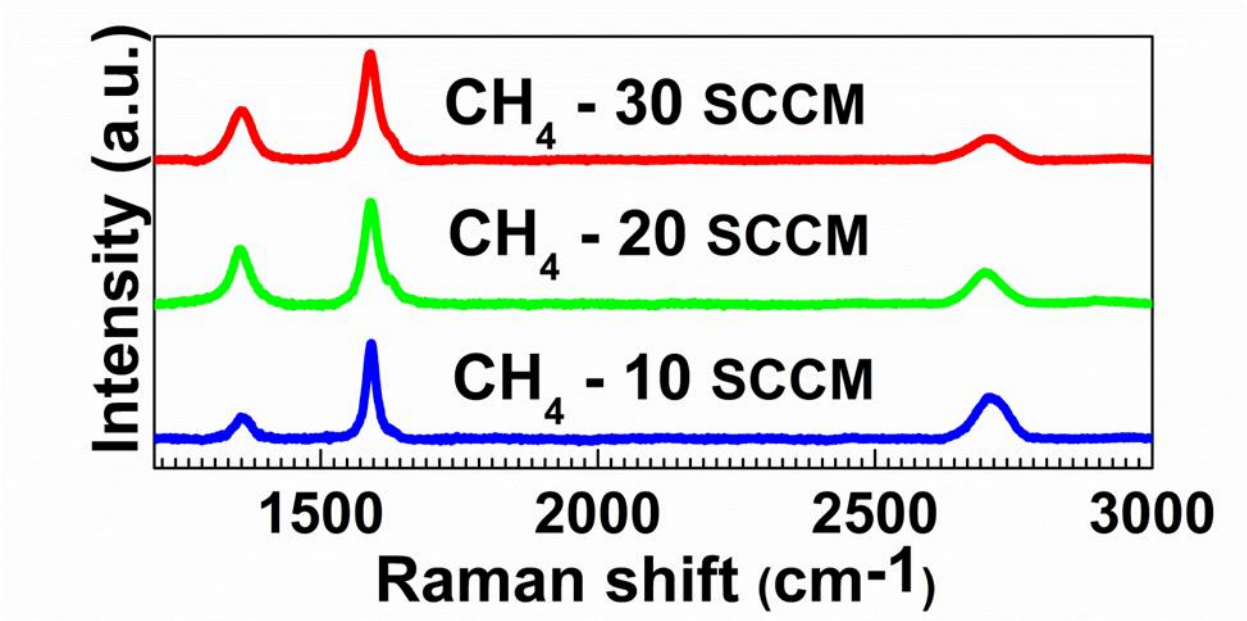

Figure 3.6 Representative Raman spectra collected for samples grown under varying CH_4 flow rates ranging from 10 SCCM to 30 SCCM (rate of flow of H_2 was constant). The samples were grown using parameters stated in Table 3.4 with standard growth procedure. Higher concentration of CH_4 increased the number of layers of graphene formed. This is indicated by the decrease in intensity of 2D peak as the flow rate of Ch_4 increases.

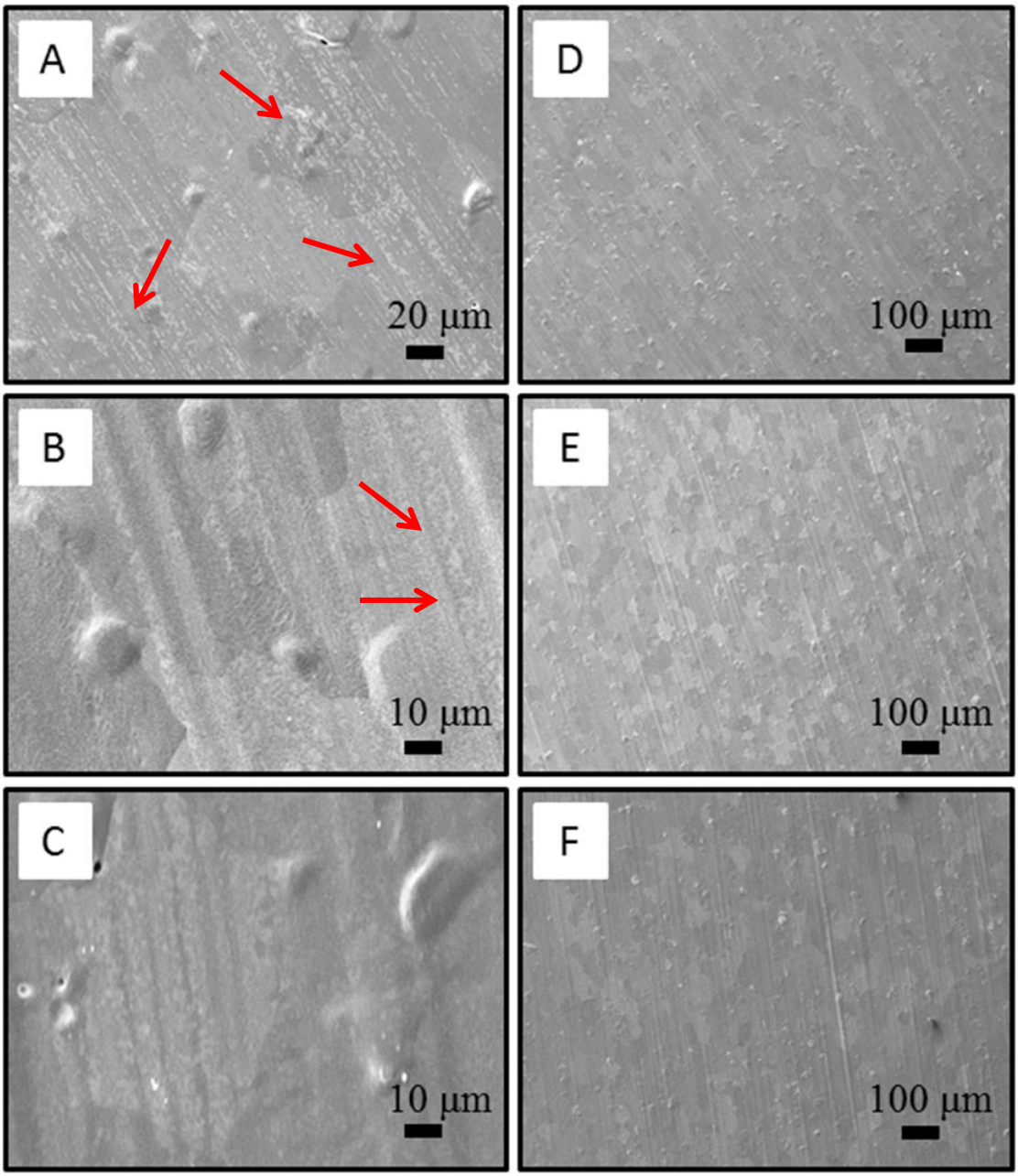

Figure 3.7 SEM images showing an evolution of multi-layer formation of graphene with increasing CH_4 flow rates. The bright empty spots are clearly seen which are indicated by the arrow. The amount of empty spots decreased as the flow rate increased. The graphene films were synthesized with (A, D) 10 SCCM, (B, E) 20 SCCM and (C, F) 30 SCCM of CH_4 with all other parameters as state in table 3.4.

Table 3.5 Parameters to study the effect of various flow rates of H_2.

H_2 rate (SCCM)	Temperature (°C)	Time (min)	CH_4 rate (SCCM)
0	950	3	10
100	950	3	10
300	950	3	10
500	950	3	10

To observe the effect of H_2, the flow rate of CH_4 is kept constant at 10 SCCM. The growth conditions are as indicated in the Table 3.5. H_2 is employed to prevent the Cu from oxidizing due to the oxygen found in CH_4. The SEM images show the effect of rate of hydrogen flow rate in the experimental procedure. Whit no CH_4 flow during cooling cycle the H_4 etched away the carbon atoms starting from the graphene edges and serves as secondary nuclei to coalesce the graphene islands. This is shown in the SEM images where the bare copper shows up as bright spots in the image. With low rate of H_2 flow, the effect of etching is very less and it results in formation of multiple layers of graphene. The fourth image shows the effect of surplus amount of hydrogen that leads to a dominant etching effect, preventing the synthesis of graphene. The first and the fourth image are similar with more bare copper than graphene. This proves that not only the presence of hydrogen is essential in maintaining chemical equilibrium in the reaction at the surface of the catalyst but also that surplus hydrogen etches the synthesized graphene.

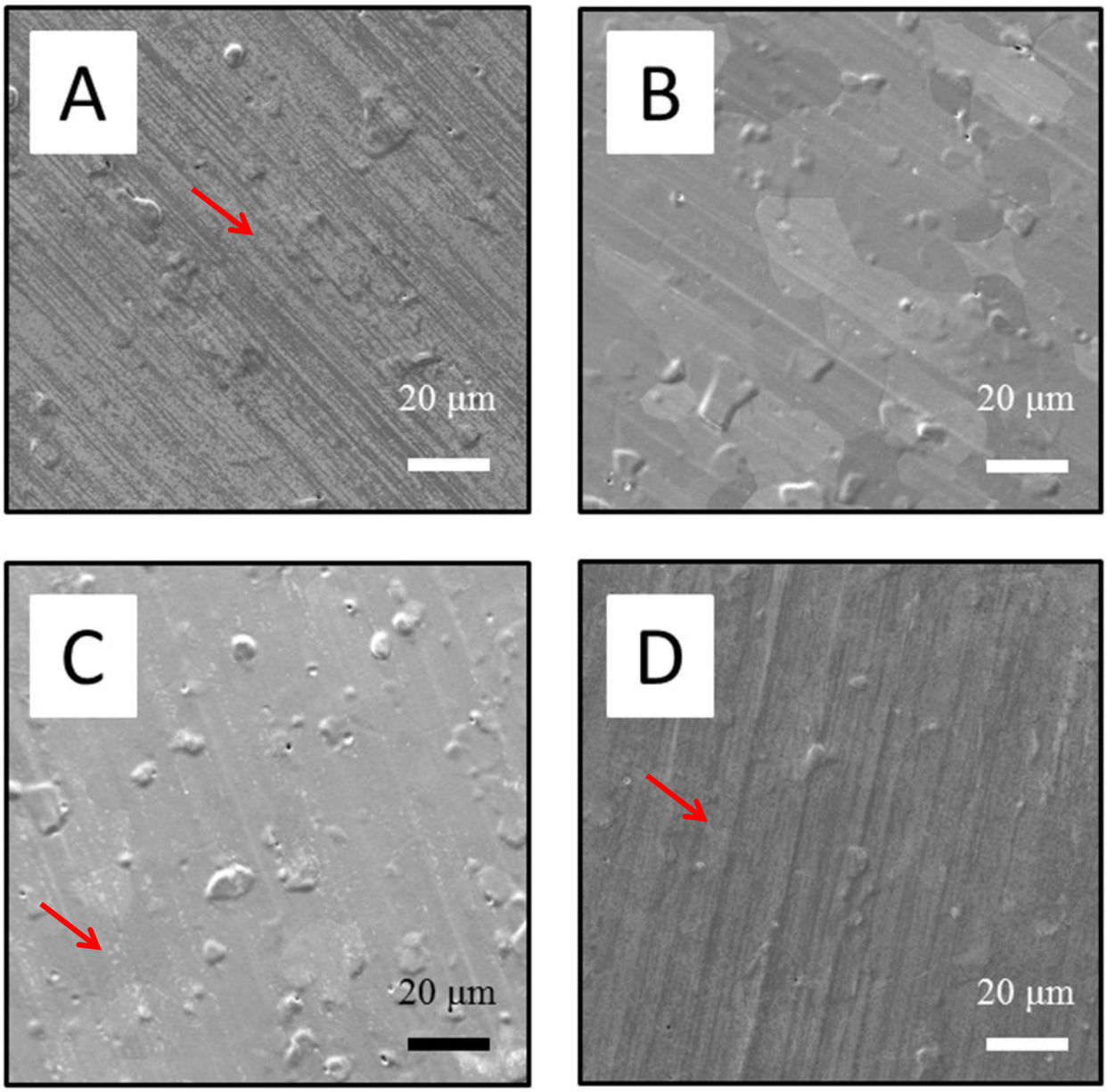

Figure 3.8 SEM images showing the effect of hydrogen flow rate in synthesis of graphene using CVD. The graphene films were synthesized with (A) 0 SCCM, (B) 100 SCCM, (C) 300 SCCM and (D) 500 SCCM.

3.7 Steps involved in transfer of graphene to non-metallic substrates

Graphene on metallic surfaces is not suitable for any interesting application. Thus it is very necessary to transfer the material to an insulating or non-metallic surface. Graphene cannot remain on its own without any supporting layer or it will curl up. The substrate, which has graphene on the surface after growth is completed, is spin coated with a very thin layer of polymers like poly(methyl methacrylate) (PMMA) or Polydimethylsiloxane (PDMS). The substrate is then baked for about 10 min in an oven maintained at 120°C. The side that was not spin coated it blazed with oxygen plasma so that the graphene in the other side is etched away. This foil is then placed in a ferric chloride copper-etch solution. Once the copper is etched away the PMMA is scooped out of the solution and is rinsed with DI water a couple of time and is scooped out onto the required substrate. Once the substrate is dry then it is rinsed with acetone to dissolve the PMMA. Then the chip is dried to obtain a clean layer of graphene on the desired substrate.

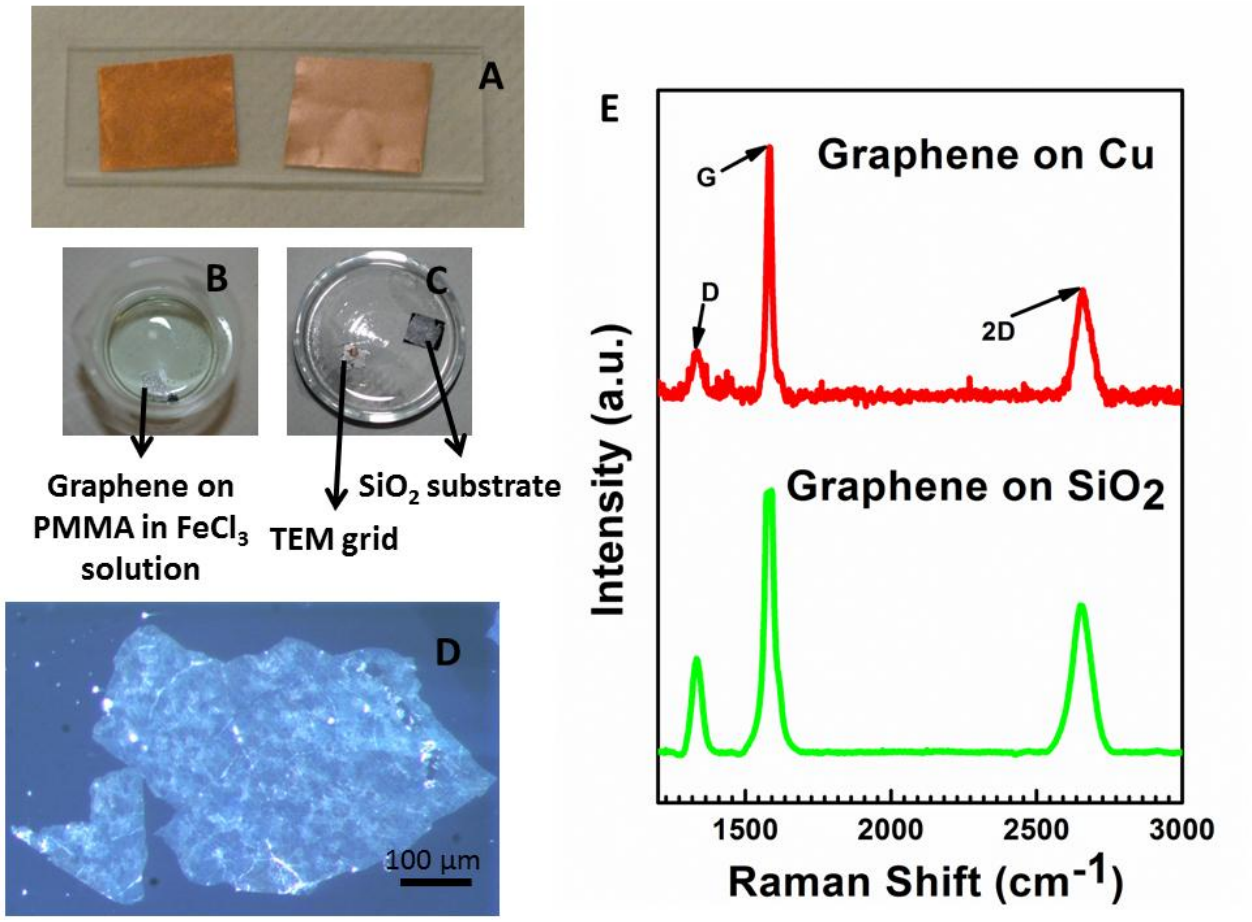

Figure 3.9 (A) Image showing the surface of copper before and after synthesis: Specimen on the right is bare copper and the specimen on the left has a layer of graphene on it. (B) Digital image of graphene coated with PMMA floating in $FeCl_3$ etchant solution after the under lying copper was etched. (C) The image shows a layer of graphene + PMMA after it was transferred to SiO_2 for optical imaging and copper grid for TEM imaging. (D) Optical image of the transferred graphene. The variation in contrast in the film is due to the difference in number of layers of graphene. (E) Raman spectrum of the transferred graphene.

3.8 References

1. Starodubov, A., Medvetskii, M., Shikin, A., and Adamchuk, V., 2004, "Intercalation of silver atoms under a graphite monolayer on Ni(111)," Physics of the Solid State, 46(7), pp. 1340-1348.

2. Johann, C., and et al., 2009, "Growth of graphene on Ir(111)," New Journal of Physics, 11(2), p. 023006.

3. Reina, A., Jia, X., Ho, J., Nezich, D., Son, H., Bulovic, V., Dresselhaus, M. S., and Kong, J., 2008, "Large Area, Few-Layer Graphene Films on Arbitrary Substrates by Chemical Vapor Deposition," Nano Letters, 9(1), pp. 30-35.

4. Kim, K. S., Zhao, Y., Jang, H., Lee, S. Y., Kim, J. M., Kim, K. S., Ahn, J.-H., Kim, P., Choi, J.-Y., and Hong, B. H., 2009, "Large-scale pattern growth of graphene films for stretchable transparent electrodes," Nature, 457(7230), pp. 706-710.

5. Bae, S., Kim, H., Lee, Y., Xu, X., Park, J.-S., Zheng, Y., Balakrishnan, J., Lei, T., Ri Kim, H., Song, Y. I., Kim, Y.-J., Kim, K. S., Ozyilmaz, B., Ahn, J.-H., Hong, B. H., and Iijima, S., 2010, "Roll-to-roll production of 30-inch graphene films for transparent electrodes," Nat Nano, 5(8), pp. 574-578.

6. Li, X., Cai, W., An, J., Kim, S., Nah, J., Yang, D., Piner, R., Velamakanni, A., Jung, I., Tutuc, E., Banerjee, S. K., Colombo, L., and Ruoff, R. S., 2009, "Large-Area Synthesis of High-Quality and Uniform Graphene Films on Copper Foils," Science, 324(5932), pp. 1312-1314.

7. Ji, H., Hao, Y., Ren, Y., Charlton, M., Lee, W. H., Wu, Q., Li, H., Zhu, Y., Wu, Y., Piner, R., and Ruoff, R. S., 2011, "Graphene Growth Using a Solid Carbon Feedstock and Hydrogen," ACS Nano, pp. null-null.

8. Sun, Z., Yan, Z., Yao, J., Beitler, E., Zhu, Y., and Tour, J. M., 2010, "Growth of graphene from solid carbon sources," Nature, 468(7323), pp. 549-552.

9. Cho, J., Gao, L., Tian, J., Cao, H., Wu, W., Yu, Q., Yitamben, E. N., Fisher, B., Guest, J. R., Chen, Y. P., and Guisinger, N. P., 2011, "Atomic-Scale Investigation of Graphene Grown on Cu Foil and the Effects of Thermal Annealing," ACS Nano, 5(5), pp. 3607-3613.

10. Chen, S., Brown, L., Levendorf, M., Cai, W., Ju, S.-Y., Edgeworth, J., Li, X., Magnuson, C. W., Velamakanni, A., Piner, R. D., Kang, J., Park, J., and Ruoff, R. S., 2011, "Oxidation Resistance of Graphene-Coated Cu and Cu/Ni Alloy," ACS Nano, 5(2), pp. 1321-1327.

11. Novoselov, K. S., Geim, A. K., Morozov, S. V., Jiang, D., Zhang, Y., Dubonos, S. V., Grigorieva, I. V., and Firsov, A. A., 2004, "Electric Field Effect in Atomically Thin Carbon Films," Science, 306(5696), pp. 666-669.

Chapter 4 - Synthesis of graphene: Chemical vapor deposition using copper as catalyst II

The effect of change in temperature, gas flow rate and growth duration on synthesis of graphene has been studied extensively. In this chapter we study the effect of cooling rate on graphene growth on Cu foil and effect which also includes change in annealing temperature. The first part of the chapter deals with the effect of rate of cooling in the graphene CVD process. In this the rate of cooling is reduced exponentially i.e. the Cu foil is quenched after the duration of growth is complete. And the second part of the chapter we discuss the effect of rate of cooling along with reduction in the annealing time.

4.1 Experimental procedure

4.1.1 Steps involved in growth of graphene using CVD II

The steps for this experiment are very similar to that of the normal CVD growth of graphene on Cu foil but with minor variations. In the first experiment the typical growth procedure used in the experiment is shown in the Figure 4.1.

Table 4.1 Typical growth parameters used in the modified procedure (Type I).

Process	Start temperature (°C)	End temperature (°C)	Time (min)	Argon (SCCM)	Methane (SCCM)	Hydrogen (SCCM)
Soak	0	0	5	2000	0	0
Timed ramp	0	950	65	2000	0	300
Soak	950	950	20	2000	0	300
Soak	950	950	10	1000	10	300
Cool	950	0	5	3000	10	300

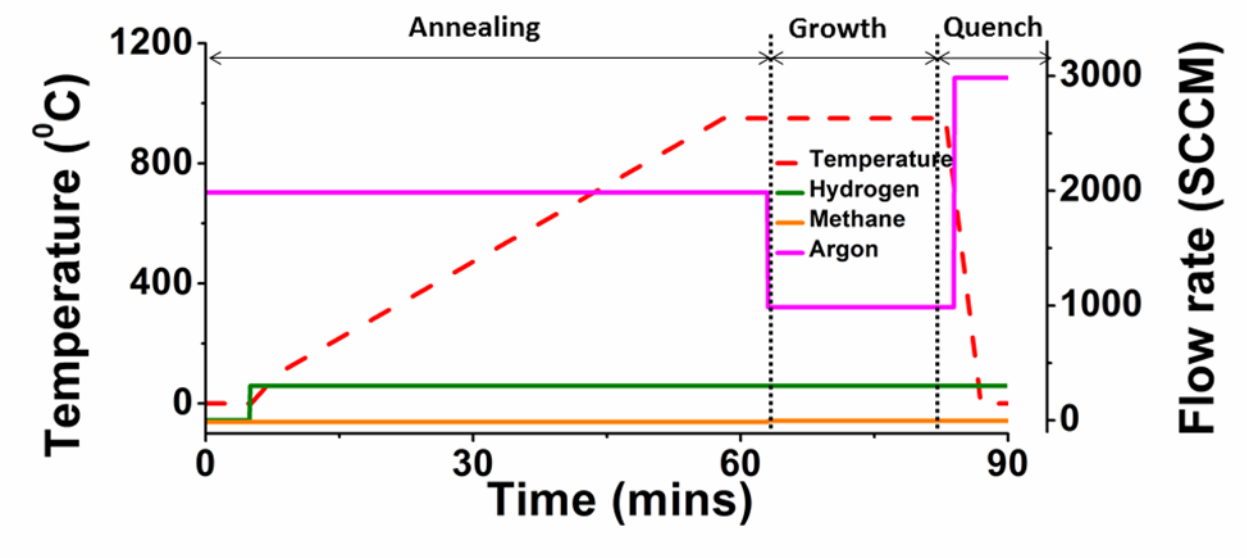

Figure 4.1 Plot of growth parameters following the modified growth procedure (Type I) for synthesis of graphene on Cu substrate (temperature and flow rate) as a function of time.

The only difference between this procedure and the standard growth procedure is the rate of cooling. The sample is quenched after the growth process is complete. The cooling rate is kept at approximately 4 °C/sec.

Table 4.2 Typical growth parameters used in the modified procedure (Type II).

Process	Start temperature (°C)	End temperature (°C)	Time (min)	Argon (SCCM)	Methane (SCCM)	Hydrogen (SCCM)
Soak	950	950	5	2000	0	300
Soak	950	950	20	2000	0	300
Soak	950	950	10	1000	10	300
Cool	950	0	5	2000	10	300

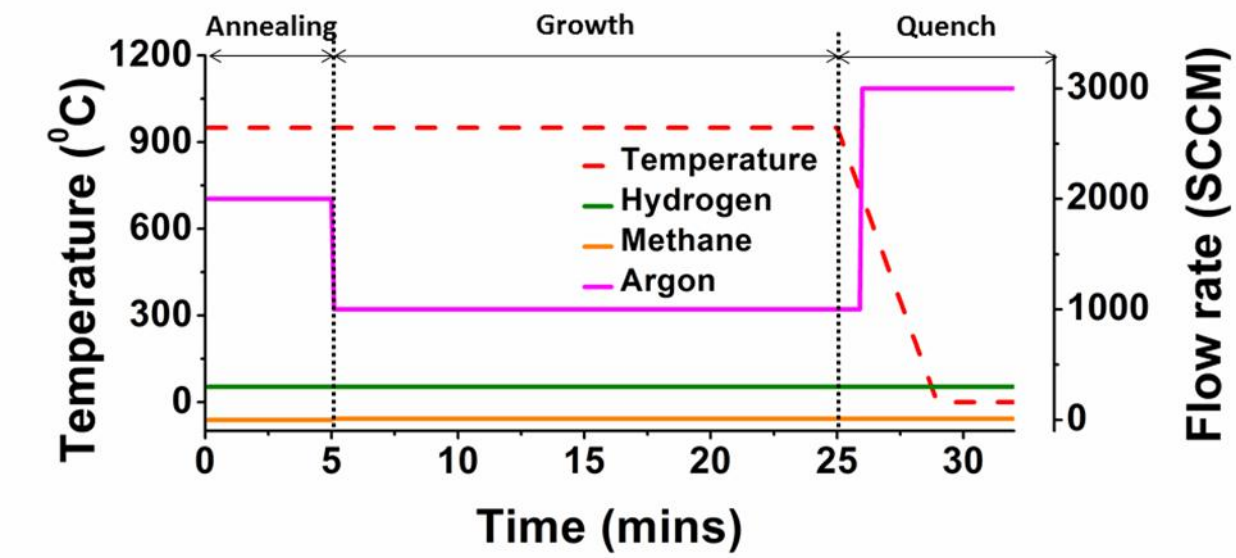

Figure 4.2 Plot of growth parameters the modified growth procedure (Type II) for synthesis of graphene on Cu substrate (temperature and flow rate) as a function of time.

In the second experiment the typical growth procedure used in the experiment is shown in the Figure 4.2. In this procedure the duration of annealing is eliminated or is reduced very less. The sample is introduced into the furnace at the elevated temperature of 950 °C. And after the growth process is completed the sample is quenched. Because the temperature of the furnace remains constant all through the cycle there is no time lag between multiple consecutive samples.

4.2 Methodology

This chapter focuses on the effect of growth period and gas flow rate. The rate of cooling is kept as a constant. The samples are characterized using Raman spectroscopy and SEM.

4.2.1 Graphene grown on Cu with a fast rate of cooling (Modified procedure type I)

4.2.1.1 Effect of growth period

As stated in the previous chapter, the growth period is a very important factor in the synthesis procedure of graphene. The Figure 4.4 shows evolution of graphene growth from 3 minutes to 20 minutes. In the standard CVD process as discussed earlier it was stated that the optimum graphene growth period is from 10 to 15 minutes. But the Raman spectra show that the intensity of D peak and that of the 2D peak does not vary much with respect to the G peak over time. One reason for this phenomenon could be that the quality (density of defects) and the number of layer of graphene do not change much over time.

Table 4.3 Parameters to study the effect of varying duration of growth.

Time (min)	Temperature (°C)	CH_4 rate (SCCM)	H_2 rate (SCCM)	I_D/I_G	I_{2D}/I_G
3	950	10	300	0.45	0.33
10	950	10	300	0.5	0.39
20	950	10	300	-	-

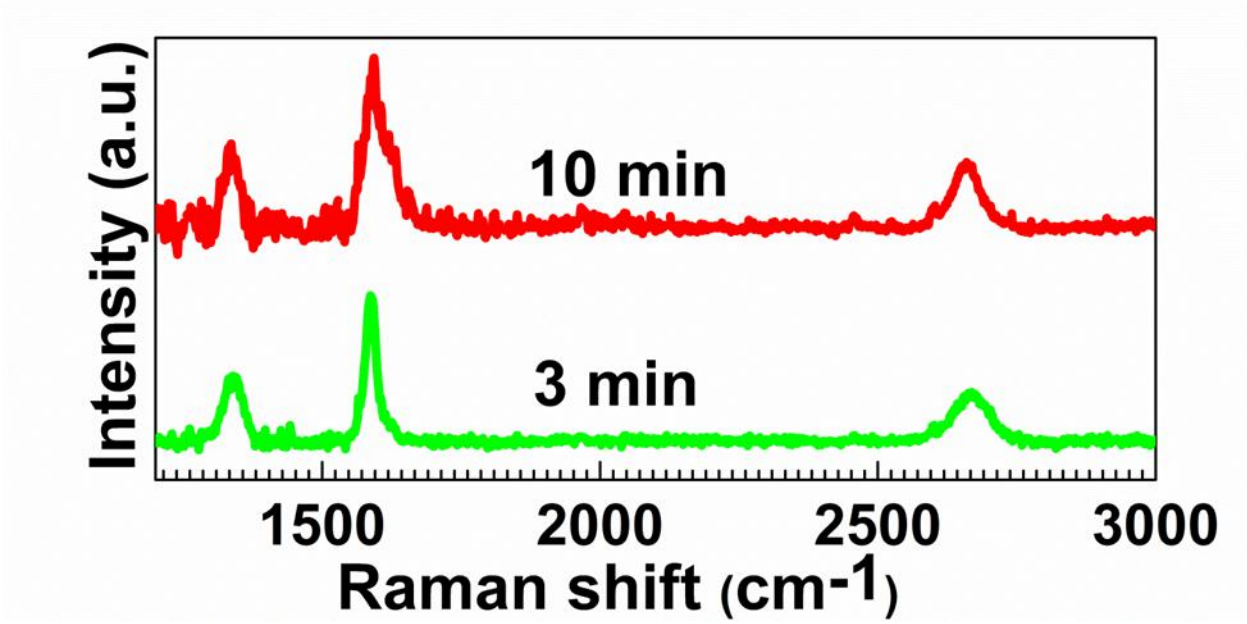

Figure 4.3 Representative Raman spectra showing the effect of growth time. The samples were prepared using parameters as stated in Table 4.3 with modified growth procedure (Type I). The intensity of the 2D peak did not vary much with time indicating that number of layers remained constant.

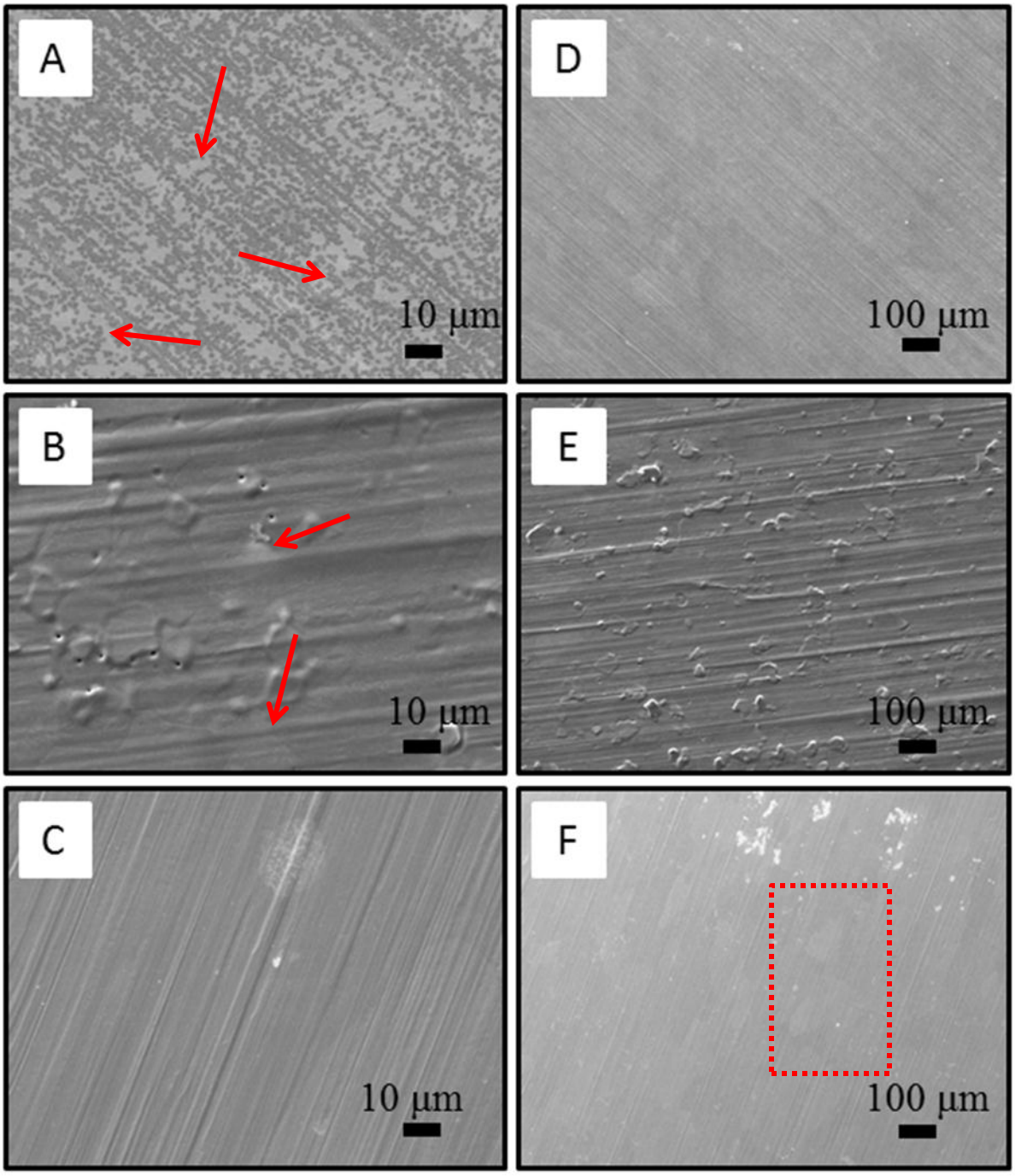

Figure 4.4 SEM images of the synthesized graphene layers on Cu substrate, showing evolution of graphene growth for (A, D) 3 minutes, (B, E) 10 minutes and (C, F) 20 minutes. Other growth parameters are as stated in Table 4.3. The arrows indicate empty spots which get covered as the growth time increases.

But in the SEM images it could be seen that there are more bright empty spots on the copper surface at 3 minutes, which means smaller grain size. This results in the formation of thinner layer with empty spots. But as the time increases the grain size increases as there is time for more amount of carbon to react with the surface. But these empty spots seem to be covered at 10 minutes growth time. But in the standard experimental procedure complete coverage was achieved at around 15 minutes of growth. One possible explanation could be the absence of cooling cycle. In the standard experiment cooling cycle is a long period and at lower temperatures the carbon atoms are not so active but the hydrogen continues to etch away the deposited carbon.

But the number of layers does not seem to change which is shown in the 2D peak of the Raman spectra which is constant for both the growth period. This suggests that at the nucleation stage itself the carbon forms multiple layers and as the graphene sheet grows it covers the entire surface with the same number of layers. Thus for the new experimental procedure the optimum growth period is around 6 or 7 minutes which is approximately half than that of the standard procedure.

4.2.1.2 Effect of gas flow rate

The Raman spectrum shown in Figure 4.5 shows the effect of flow rate of CH_4 when the temperature and time are kept constant. To study this, the growth conditions used were as indicated in the Table 4.4. In the previous chapter it was discussed that the as the flow rate of CH_4 increases, the gas density in the mixture increases.

Table 4.4 Parameters to study the effect of varying CH_4 flow rates.

CH_4 rate (SCCM)	Temperature (°C)	Time (min)	H_2 rate (SCCM)	I_D/I_G	I_{2D}/I_G
10	950	10	300	0.5	0.4
20	950	10	300	0.30	0.25
30	950	10	300	0.41	0.34

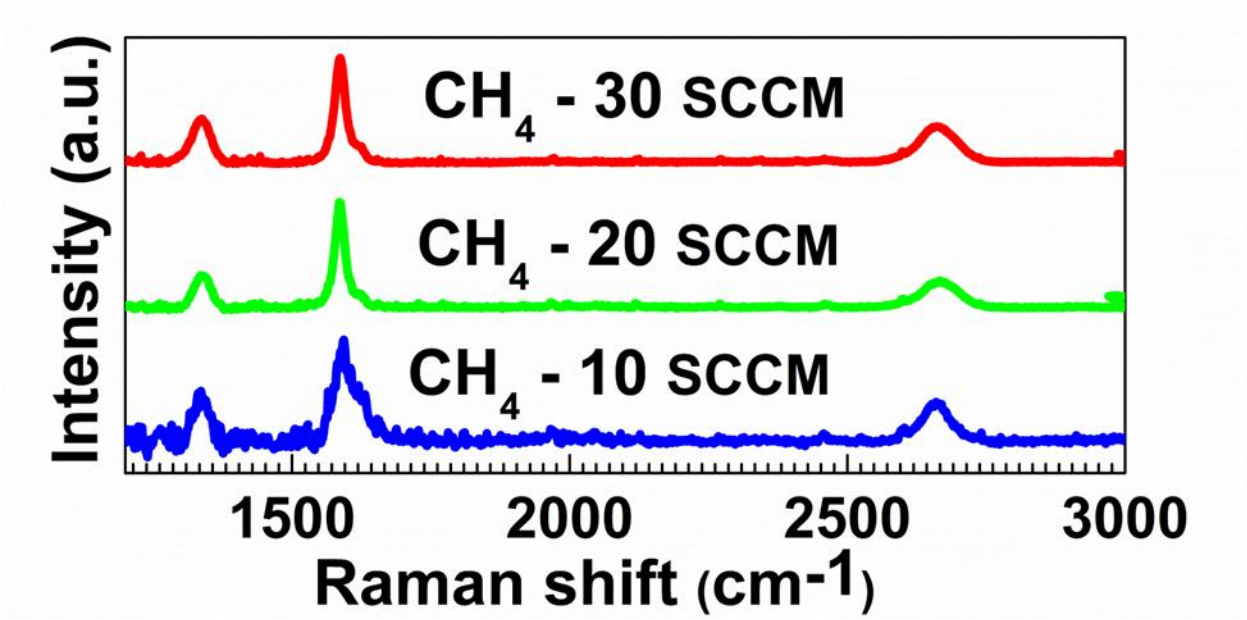

Figure 4.5 Representative Raman spectra collected for samples under varying CH_4 flow rates ranging from 10 SCCM to 30 SCCM (flow of H_2 constant). The samples were grown using parameters stated in Table 4.4 with the modified growth procedure (Type I). The decrease in intensity of the 2D peak as the flow rate increases. This indicates that it forms more layers as the concentration increases.

This increases the rate of catalytic reaction on the surface of copper thus forming multiple layers. But in the Raman spectra shown in Figure 4.6, the intensity of the 2D peak relative to the G peak remains constant, which is also noticed in the SEM images in Figure 4.6. That is, the number of layers remains constant. But this was not the case with standard procedure where the number of layers increases with increase in CH_4 flow rate. This suggests that the CH_4 flow rate does not have a predominant effect in determining the number of layers. This is because the duration of gas flow is very less when compared to that of the standard procedure. Thus the optimum flow rate is below 10 SCCM for around 10 minutes. Because anything above 10 SCCM for as little as 10 minutes gives complete coverage and similar results.

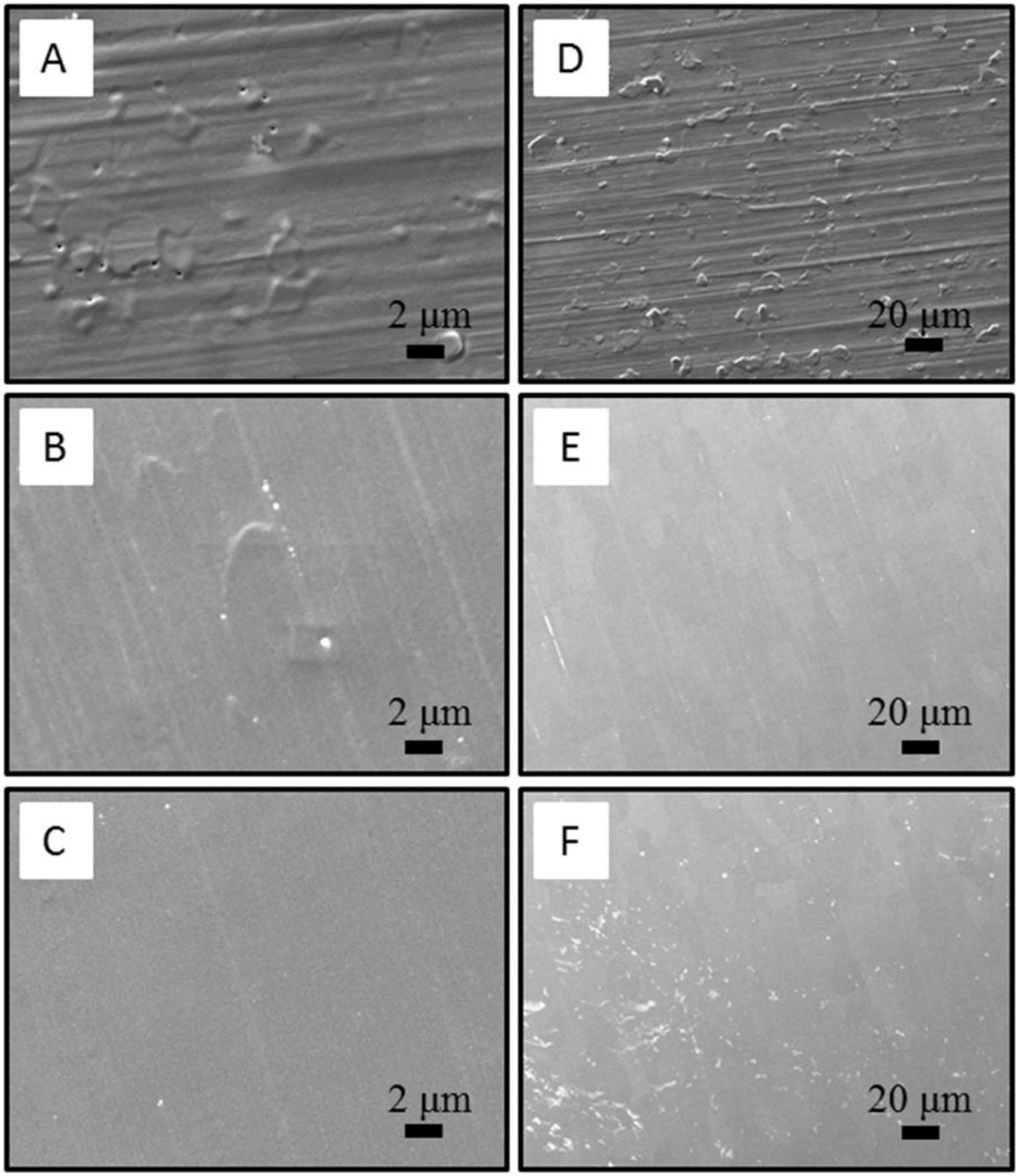

Figure 4.6 SEM images showing the synthesized graphene with varying CH_4 flow rates of (A, D) 10 SCCM, (B, E) 20 SCCM and (C, F) 30 SCCM with other growth parameters stated in Table 4.4. The coverage and the number of graphene layers remains the same.

4.2.2 Graphene grown on Cu with a fast rate of cooling and fast rate of heating (Modified procedure type II)

4.2.2.1 Effect of growth period

In this procedure as previously stated, the sample is introduced for at the growth temperature which effectively decreases the annealing time. The Raman spectra were obtained for samples with experimental conditions as shown in Table 4.5. It was previously stated in the first part of the chapter that increase in growth time increases the number of layers after a certain period of time because of the decreased effect of hydrogen etching due to the absence of a cooling cycle. But in this procedure it is seen that the 2D peak intensity when compared to that of the G peak intensity is higher for the sample with 20 minutes of growth time than that of the sample with 10 minutes of graphene growth. This is contradictory at first to that stated in the first part of the chapter. But it should be noted that this procedure is completely different form that of the previous one.

Table 4.5 Parameters to study the effect of varying growth times.

Time (min)	Temperature (°C)	CH_4 rate (SCCM)	H_2 rate (SCCM)	I_D/I_G	I_{2D}/I_G
10	950	30	300	0.24	0.24
20	950	30	300	0.51	0.66

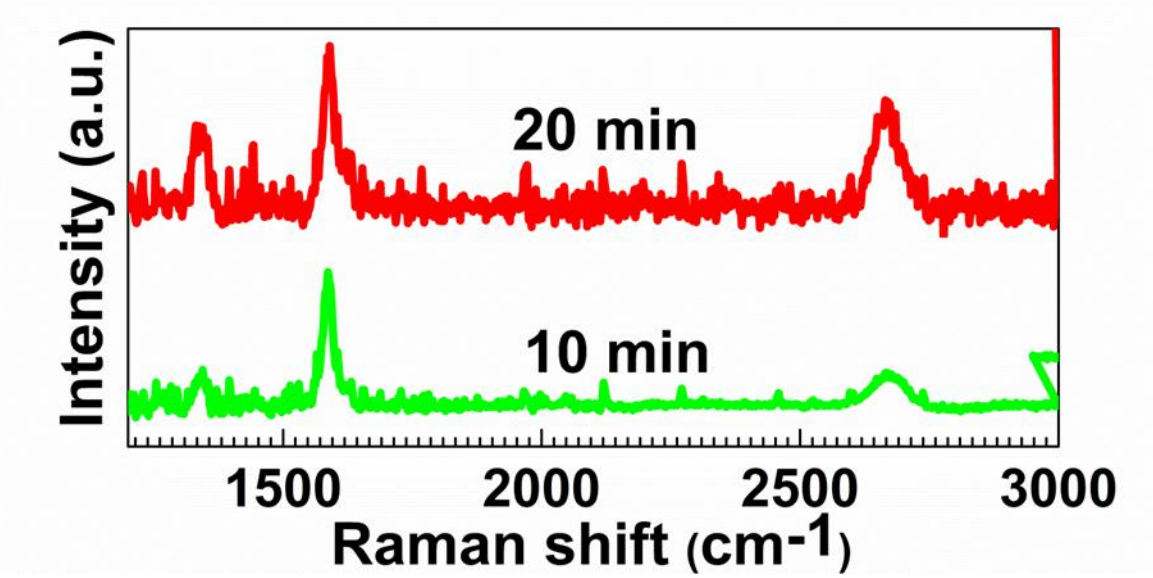

Figure 4.7 Representative Raman spectra showing the effect of growth time ranging from 10 minutes to 30 minutes. The samples were grown using parameters stated in Table 4.5 with the modified procedure (Type II).

In the modified procedure type I, there was hydrogen flow all through the cycle of annealing which cleaned the copper surface prior to that of the growth time. But in the modified procedure type II there is no period of annealing. So annealing occurs during the period of growth. This could be one of the possible reasons for the increase in quality of graphene with extended period of time. This is also proved by the SEM images. In the Figure (B) it can be seen that the size of graphene grain is very small even for 20 minutes which could be greatly due to the presence of impurities which are indicated by the arrows. At 10 minutes there are only certain numbers of graphene grains which are limited greatly by the presence of impurities. But at 20 minutes the size of graphene sheets increases as more copper surface becomes available for graphene growth. And the surface also looks more rugged and course because of the complete absence of annealing.

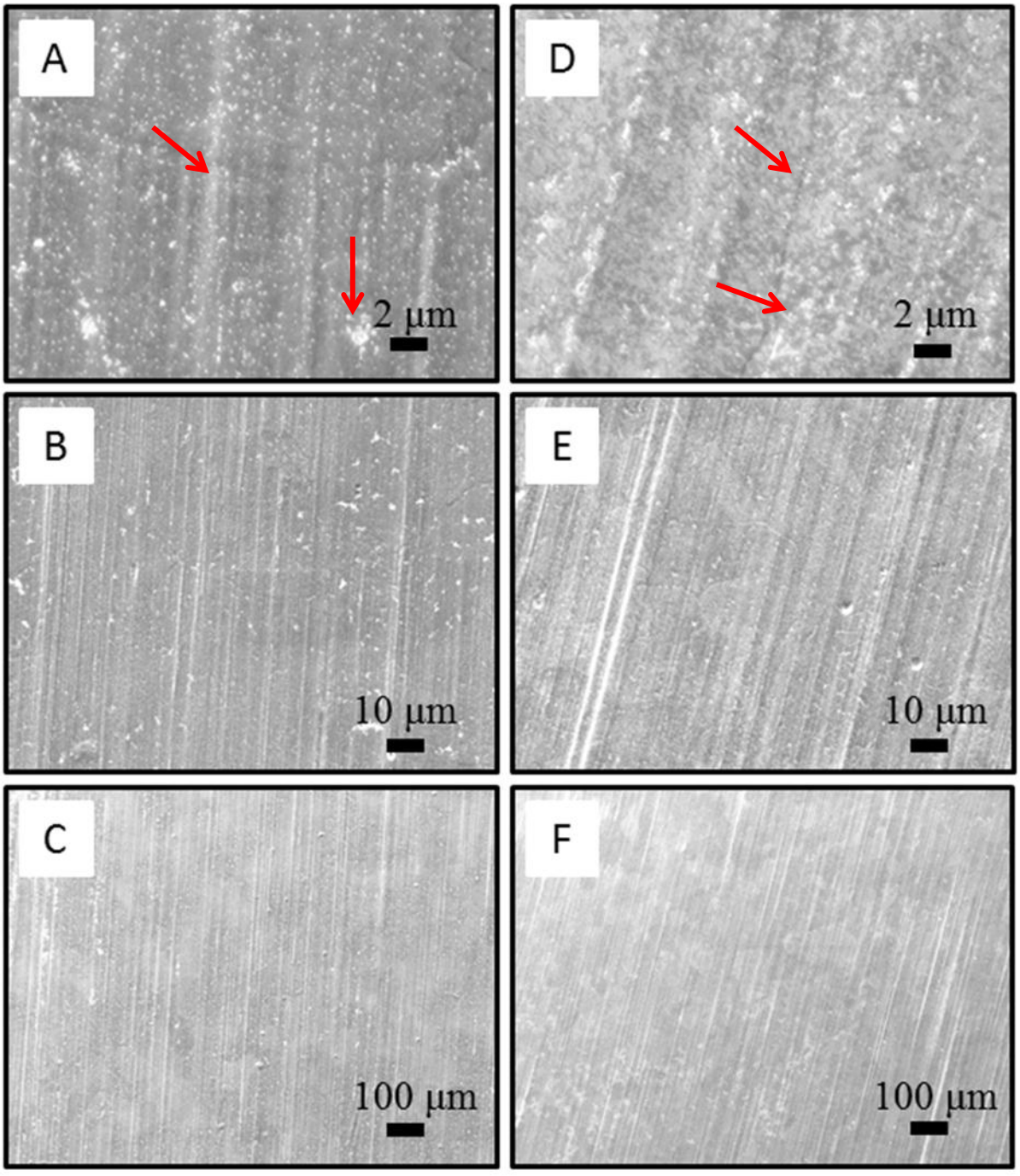

Figure 4.8 SEM images of the synthesized graphene layers on Cu substrate, show evolution of graphene growth by modified procedure (Type II) for (A, C, E) 10 minutes and (B, D, F) 20 minutes with other parameters as stated in Table 4.5.

4.2.2.2 Effect of gas flow rate

The growth parameters used to study this effect are as stated in the Table 4.6. The Raman spectra of these samples show a trend that is opposite to the one shown by samples which have the same parameters as in the ones in the standard procedure. In the Raman spectra, the ratio of intensity of 2D peak with respect to the G peak (I_{2D}/I_G) decreases as the rate of flow of CH_4 increases. This means that the number of layer of graphene decreases as the flow rate increases. In the SEM images shown in the Figure 4.10, the image A and D are ones with 10 SCCM. There is nucleation of graphene but a major part of the substrate remains empty. In the second set of images the grain size of graphene increases thus providing the proof of higher flow rate. In the third set of images there are very few empty spots on the surface. This is also proved by the intensity of D peak with respect to the G peak (I_D/I_G) in the Raman spectra. The Raman spectra of graphene will have higher intensity of D peak also when the size of the grain is small due to edge effect. As the grain size is small the intensity of D peak is high in the lower flow rate and the intensity decreases as the flow rate increases indicating that the grain size gradually increases.

Table 4.6 Parameters to study the effect of different flow rates of CH_4.

CH_4 rate (SCCM)	Temperature (°C)	Time (min)	H_2 rate (SCCM)	I_D/I_G	I_{2D}/I_G
10	950	20	300	0.55	0.29
20	950	20	300	0.63	0.39
30	950	20	300	0.51	0.66

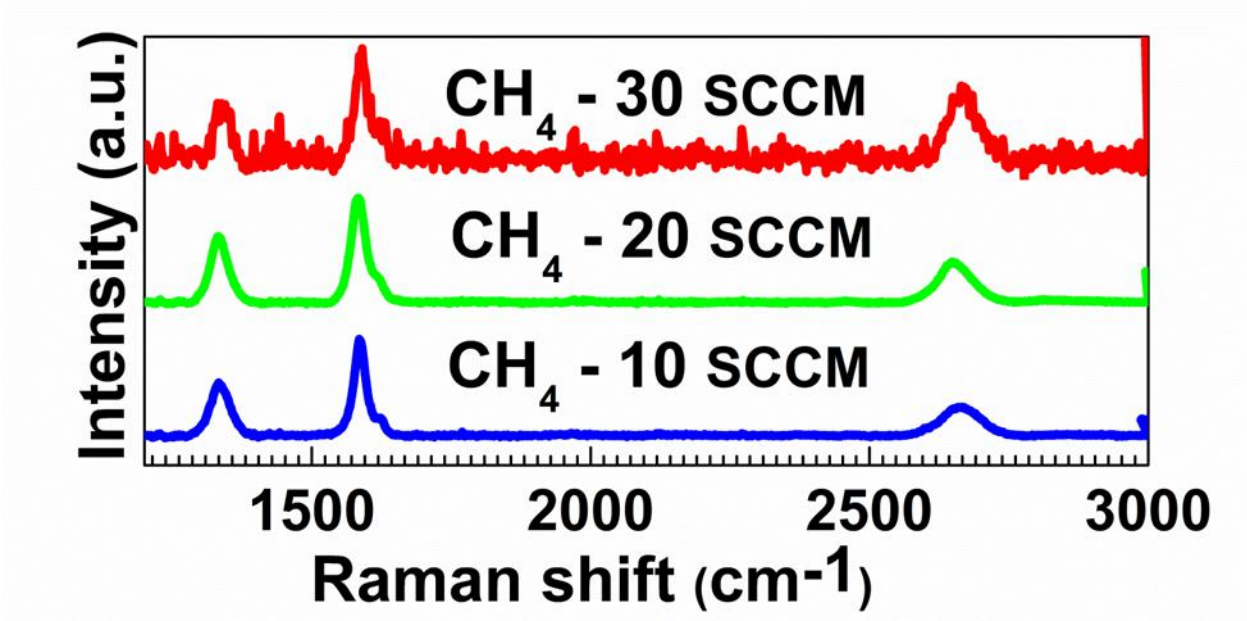

Figure 4.9 Representative Raman spectra collected for samples grown under varying CH_4 gas ranging from 10 SCCM to 30 SCCM (flow of H_2 constant). The samples were grown using parameters stated in Table 4.6 with the modified procedure (Type II). As the CH_4 flow rate increases the 2D peak intensity increases indicating that fewer layers of graphene as obtained for higher concentrations. This pattern is opposite to the one observed in the previous procedure.

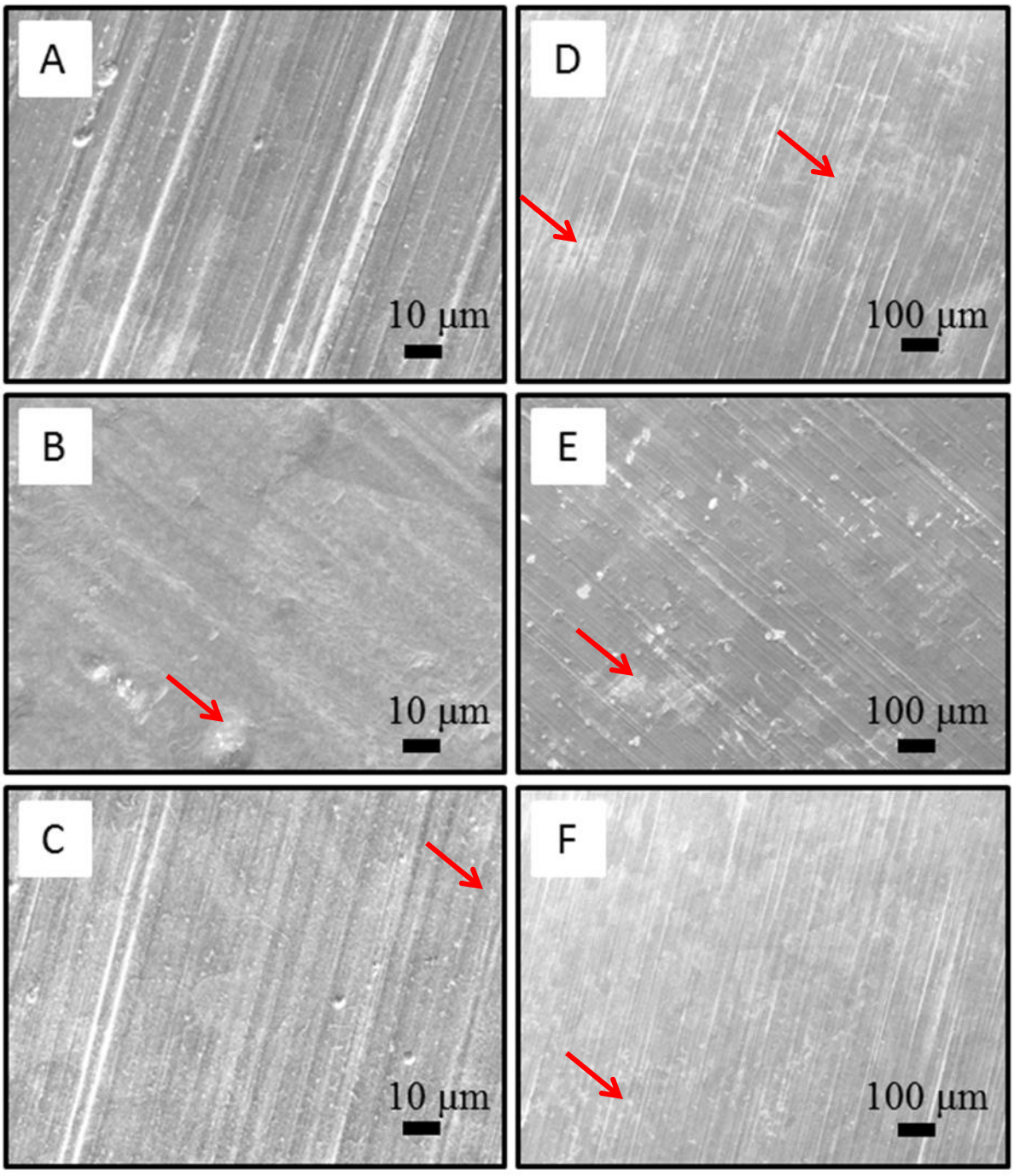

Figure 4.10 SEM images showing the synthesized graphene with varying CH_4 flow rates of (A, D) 10 SCCM, (B, E) 20 SCCM and (C, F) 30 SCCM using the modified procedure (Type II) with other growth parameters as stated in Table 4.6. The empty spots are indicated by the arrows.

Chapter 5 - Synthesis of graphene: Chemical vapor deposition using nickel as catalyst

It has been known for a long time that CVD of hydrocarbons on reactive nickel or transmission metal carbides can produce layers of graphene. The mechanism of synthesis of graphene on nickel is very different from copper. The technique of synthesis of graphene on nickel was studied before that of copper. The study of graphene growth on nickel lost interest because of the lack of control over the number of layers on the substrate. But today it has again come under the spot light because of the new found knowledge that the rate of cooling plays an important role in the segregation process. This chapter focuses on the synthesis of graphene on nickel substrate. First the experimental procedures like process flow charts are discussed. This is followed by discussion on the initial results of graphene which is grown following the standard procedure of heating, growth and cooling. This is followed by the discussion on the results of graphene growth on nickel whose duration of annealing is very low. This chapter ends with a discussion of the transfer techniques from metallic to insulating substrate.

5.1 Literature review

Segregation of graphene on nickel surface has been studied for a long time[1]. It has been proved that thin graphite with well controlled thickness (including monolayers) and low defect density can segregate from metals and metal carbides[2, 3], held at high temperatures in an equilibrium segregation process. In 2008 Pei and co-workers[4] showed the effect of rate of cooling and how is it important in forming the graphene sheet on the surface of nickel. Li *et al.,* [5] in 2009 postulated the mechanism of graphene growth on nickel surfaces by carbon isotope labeling. In the same

year Kim *et al.,* [6] synthesized graphene on a thin layer of graphene deposited on SiO_2/Si substrates using an electron-beam evaporator. This was done to reduce the number of graphene layers that were formed on the surface as thicker nickel implies more carbon absorbed and more will be the occurrence of segregation of carbon on the surface.

5.2 Experimental procedure

5.2.1 Steps involved in growth of grapheme using CVD

The steps are very similar to that of the graphene growth on Cu. But because the segregation process is dependent on the rate of cooling, the substrate is cooled at a rate of ~4 °C/sec after the growth process is completed. The growth parameters used would be similar to Figure 5.1.

Table 5.1 Typical growth parameters used in the standard procedure.

Process	Start temperature (°C)	End temperature (°C)	Time (min)	Argon (SCCM)	Methane (SCCM)	Hydrogen (SCCM)
Soak	0	0	5	2000	0	0
Timed ramp	0	950	65	2000	0	300
Soak	950	950	20	2000	0	300
Soak	950	950	10	1000	120	300
Cool	950	0	5	3000	120	300

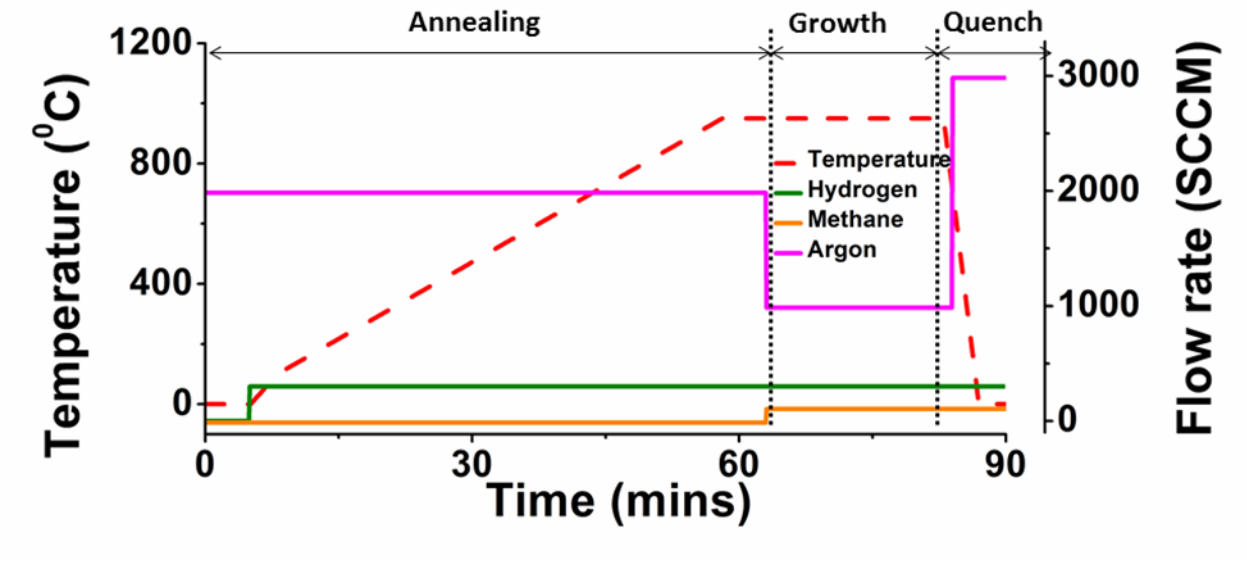

Figure 5.1 Plot of growth parameters following the traditional growth procedure for synthesis of graphene on Ni substrate (temperature and flow rate) as a function of time.

In the second experiment that is discussed in the second part of the chapter, the sample is introduced at the growth temperature. The cooling rate is the same as the previous procedure (~4 °C/sec) but the heating rate is increased to ~8 °C/sec. The growth procedure used in the experiment is shown in the Figure 5.2. This practically removes the process of annealing on the sample. Because the temperature of the furnace remains constant all through the cycle there is no time lag between multiple consecutive samples.

Table 5.2 Typical growth parameters used in the standard procedure.

Process	Start temperature (°C)	End temperature (°C)	Time (min)	Argon (SCCM)	Methane (SCCM)	Hydrogen (SCCM)
Soak	950	950	5	2000	0	0
Soak	950	950	20	2000	0	300
Soak	950	950	10	1000	120	300
Cool	950	0	5	3000	120	300

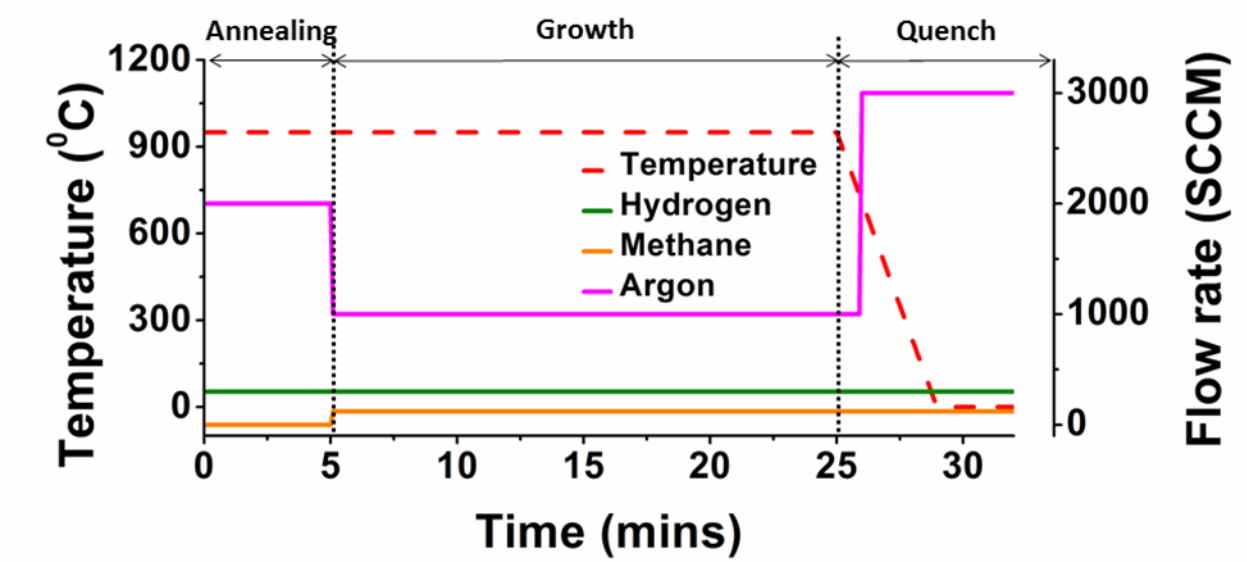

Figure 5.2 Plot of growth parameters following the modified growth procedure used for synthesis of graphene on Ni substrate (temperature and flow rate) as a function of time.

5.3 Methodology

The methodology for Ni is not very much different from that of Cu. The main growth parameters that contribute to the CVD process are: (1) Precursor used, (2) Gas flow rate, (3) Growth temperature, (4) Growth period, (5) Type of catalyst, (6) Rate of cooling.

Of these, this chapter focuses on the effect of growth period and gas flow rate. Rate of cooling is a very important parameter which determines the quality of grapheme. The samples are characterized using Raman spectroscopy and SEM.

5.3.1 Graphene grown on Ni using Traditional growth procedure

5.3.1.1 Effect of growth period

The period of growth is an important parameter in synthesis of grapheme using Ni substrate also. As previously stated the method of graphene growth on Ni is by segregation. The parameters for studying this effect are as stated in the Table 5.3.

Table 5.3 Parameters to study the effect of varying duration of growth.

Time (min)	Temperature (°C)	CH_4 rate (SCCM)	H_2 rate (SCCM)	I_D/I_G	I_{2D}/I_G
10	950	120	200	0	1.03
20	950	120	200	0	0.55
30	950	120	200	0	0.78

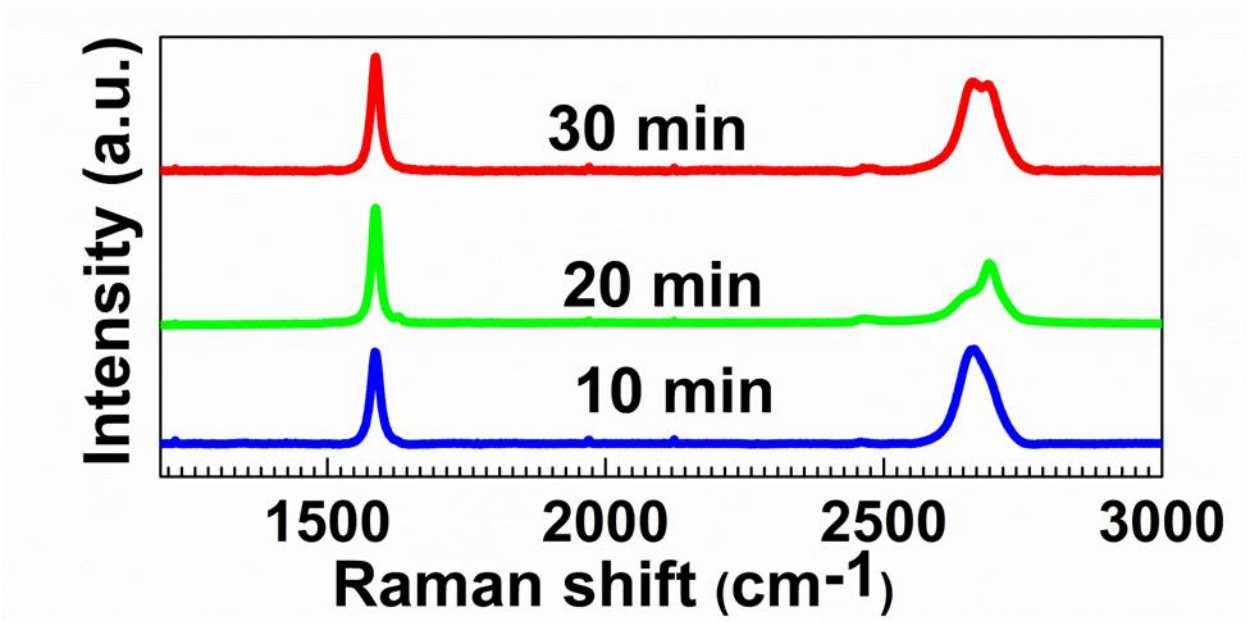

Figure 5.3 Representative Raman spectra showing the effect of time ranging from 10 minutes to 30 minutes. The samples were grown using parameters as stated in Table 5.3 with standard procedure of growth. The number of layers decreased for lesser amount of time which is indicated by the increasing intensity of the 2D peak.

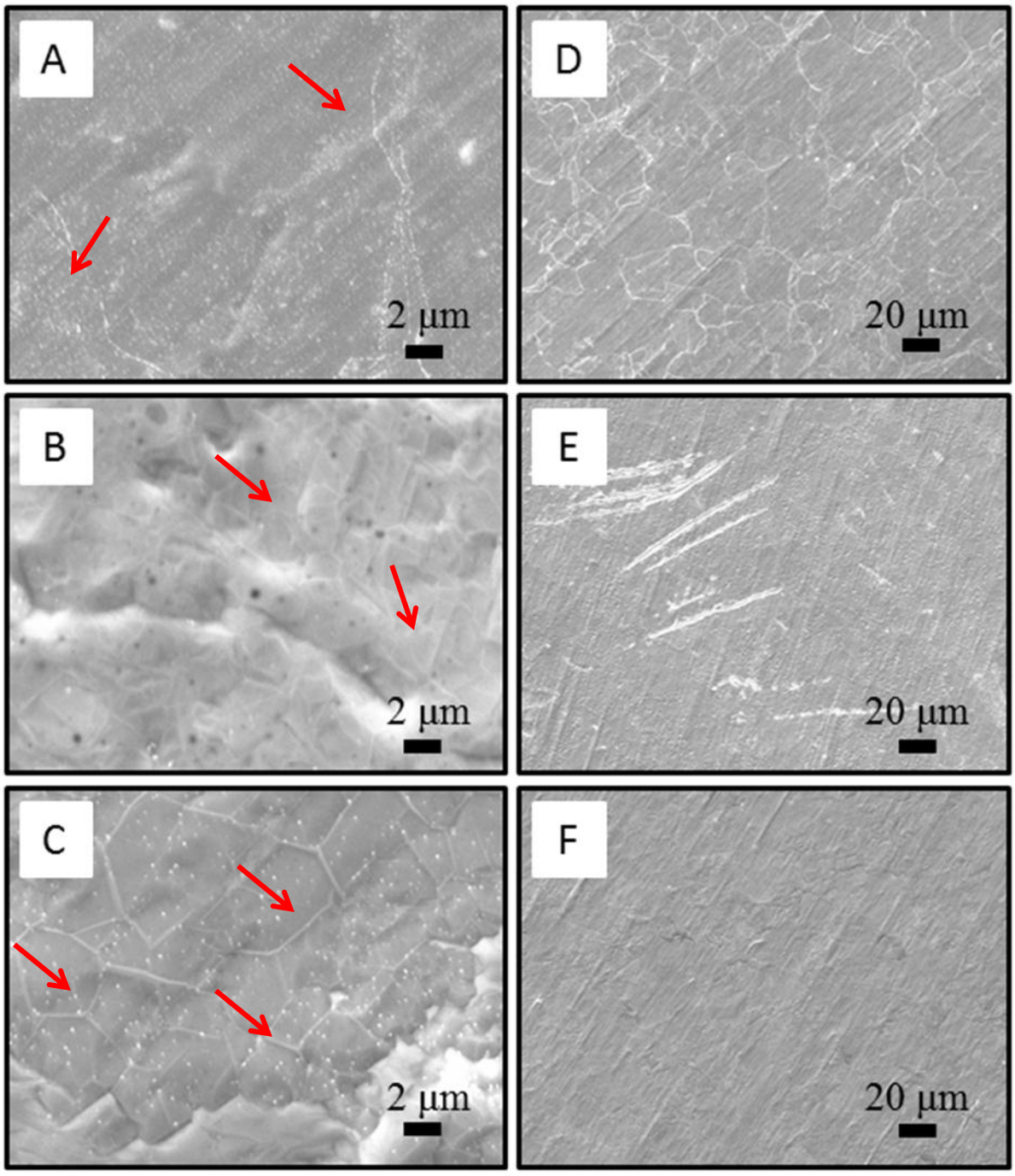

Figure 5.4 SEM images showing the synthesis of graphene on Ni-substrate grown for (A, D) 10 minutes, (B, E) 20 minutes and (C, F) 30 minutes with growth parameters as stated in Table 5.3. The grain boundaries are indicated by arrows.

The experiment is conducted by changing the time of growth while keeping temperature and the rate of flow of H_2 and CH_4 constant. The Raman spectra as shown in the Figure 5.3 show a trend in which with increasing growth time, the peak position of the 2D peak up-shifts, while the intensity of the 2D band decreases. One possible explanation is that more time of growth leads to more absorption of carbon into the substrate which leads to more number of layers of graphene being formed. The SEM images shown in the Figure 5.4 also prove that as the time of growth increases the layers of carbon increases which is revealed by the increase in prominence of graphene boundary layer. Thus to minimize the amount of carbon being absorbed into the substrate, the time of growth has to be 10 minutes or less.

5.3.1.2 Effect of gas flow rate

The Raman spectrum shown in Figure 5.5 shows the effect of flow rate of CH_4 when the temperature and time are kept constant. To study this, the growth conditions used were as indicated in the Table 5.4. Unlike to copper, the increase in CH_4 decreases the number of layers formed. The Raman spectra, as shown in the Figure 5.5, the 2D peak increases with increase in CH_4 flow rate. This is because the rate of cooling determines greatly the number of layers segregated to the surface. It is also noticed from the SEM images in Figure 5.6 that increase in flow rate increases the grain size.

Table 5.4 Parameters to study the effect of different rate of flow of CH_4 keeping H_2 flow rate constant.

CH_4 rate (SCCM)	Temperature (°C)	Time (min)	H_2 rate (SCCM)	I_D/I_G	I_{2D}/I_G
10	950	10	200	0	0.68
50	950	10	200	0	0.87
120	950	10	200	0	1.03

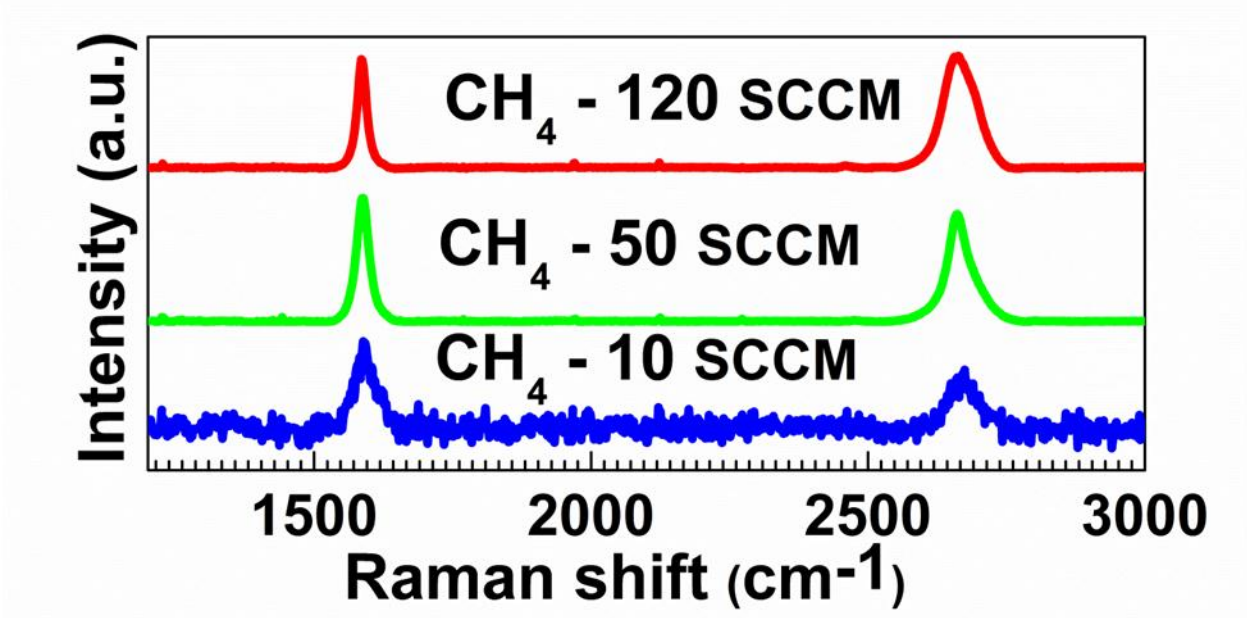

Figure 5.5 Representative Raman spectra collected for samples grown under varying CH_4 flow rate ranging from 10 SCCM to 120 SCCM keeping the rate of flow of H_2 constant. The samples were grown using parameters as stated in Table 5.4 with standard growth procedure. The relative intensity of 2D peak indicates formation of bi-layer graphene for a CH_4 flow rate of 120 SCCM. It also shows that the number of layers decreases as the flow rate increases indicating lesser number of layers are formed for increasing concentration of CH_4.

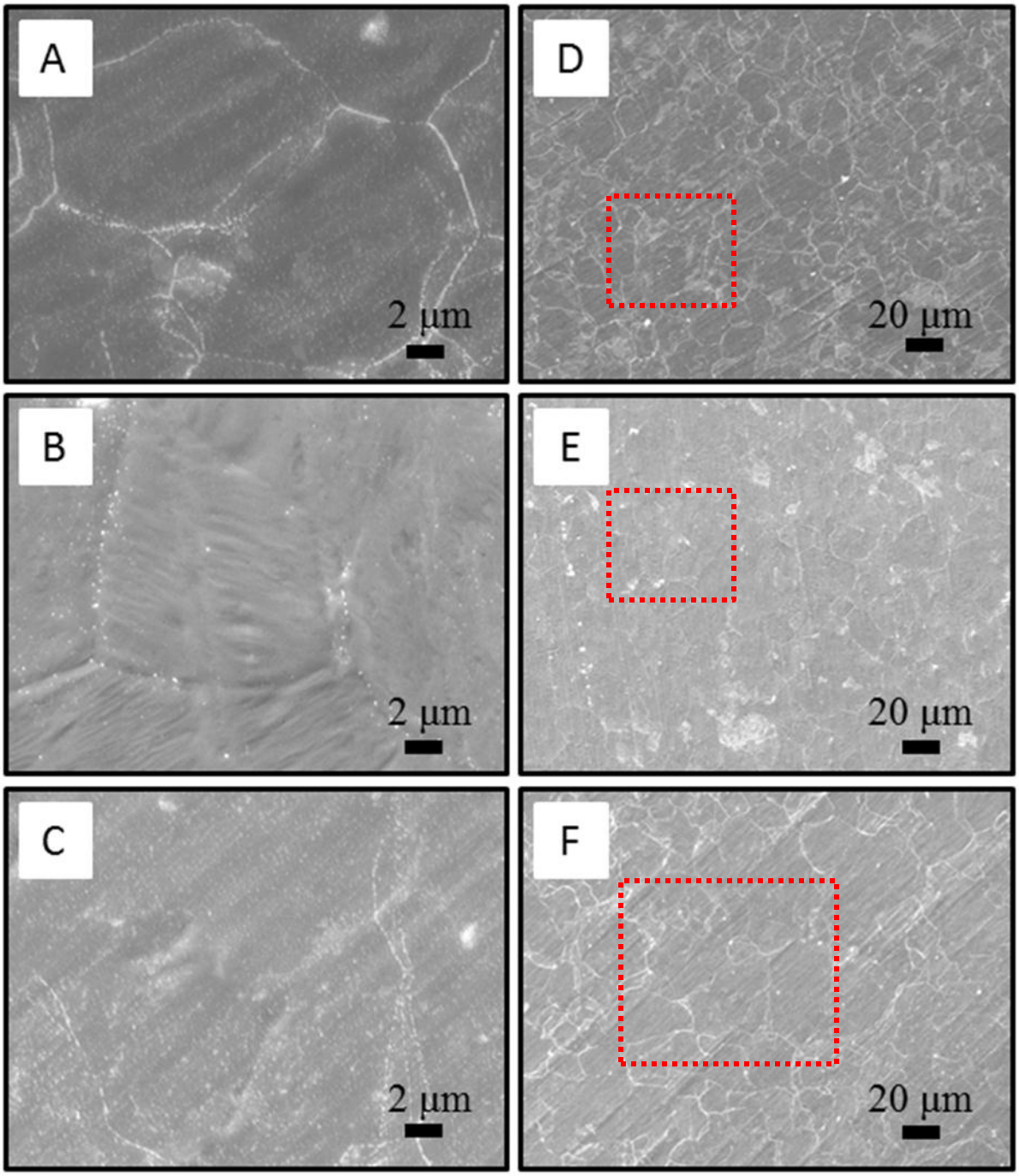

Figure 5.6 SEM images of synthesized graphene layers on Ni-substrate grown with varying CH_4 flow rates of (A, D) 10 SCCM, (B, E) 50 SCCM and (C, F) 120 SCCM with growth parameters as stated in Table 5.4. The increase in grain size (~10 µm to ~100 µm) is indicated by the dotted line.

5.3.2 Graphene grown on Ni using modified growth procedure

5.3.2.1 Effect of growth period

With experimental conditions as shown in Table 5.5, it is seen that the graphene growth is a quick process. The Figure 5.8 shows the evolution of graphene growth with respect to time of growth ranging from 10 minutes to 30 minutes at 950 °C with methane flow rate of 120 SCCM and hydrogen flow rate of 300 SCCM.

Changing the duration of growth seems to have no effect on the number of layers of graphene which is shown by the intensity of the 2D peak in the Raman spectra as shown in the Figure 5.5. Similar to the first part of the chapter, where graphene is grown on Ni using standard procedure, the prominence of grain boundary increases with time. This is because with more time more carbon is absorbed into the substrate and during cooling process more carbon is segregated to the surface. This is interesting because there is a period of annealing before the growth process starts in the standard procedure but not in the modified procedure. It is also noted that the surface of the substrate is found to be rough when compared to the sample used in the normal procedure. This is also because of the absence of period of annealing before growth.

Table 5.5 Parameters to study the effect of varying growth times.

Time (min)	Temperature (°C)	CH_4 rate (SCCM)	H_2 rate (SCCM)	I_D/I_G	I_{2D}/I_G
10	950	120	200	0	0.51
20	950	120	200	0	0.34
30	950	120	200	0	0.78

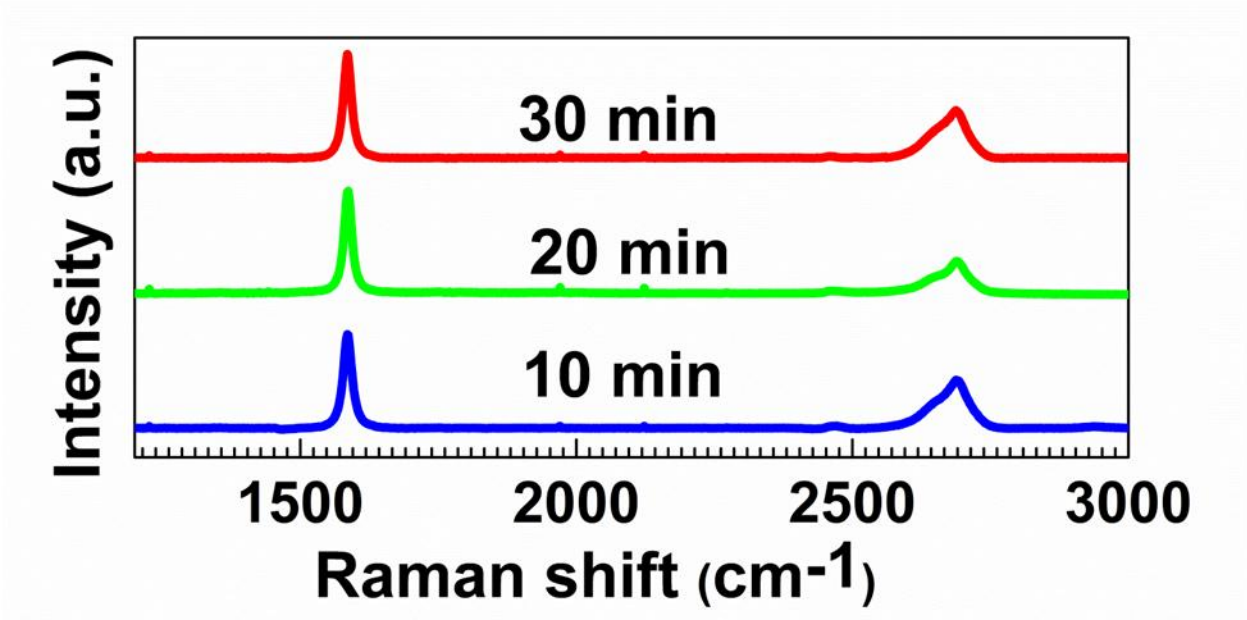

Figure 5.7 Representative Raman spectra collected for samples grown under varying time ranging from 10 minutes to 30 minutes. The samples were grown using parameters as stated in Table 5.5 with modified procedure. The shape of the 2D peak indicates that this procedure yielded only multilayer graphite instead of graphene for all flow rates.

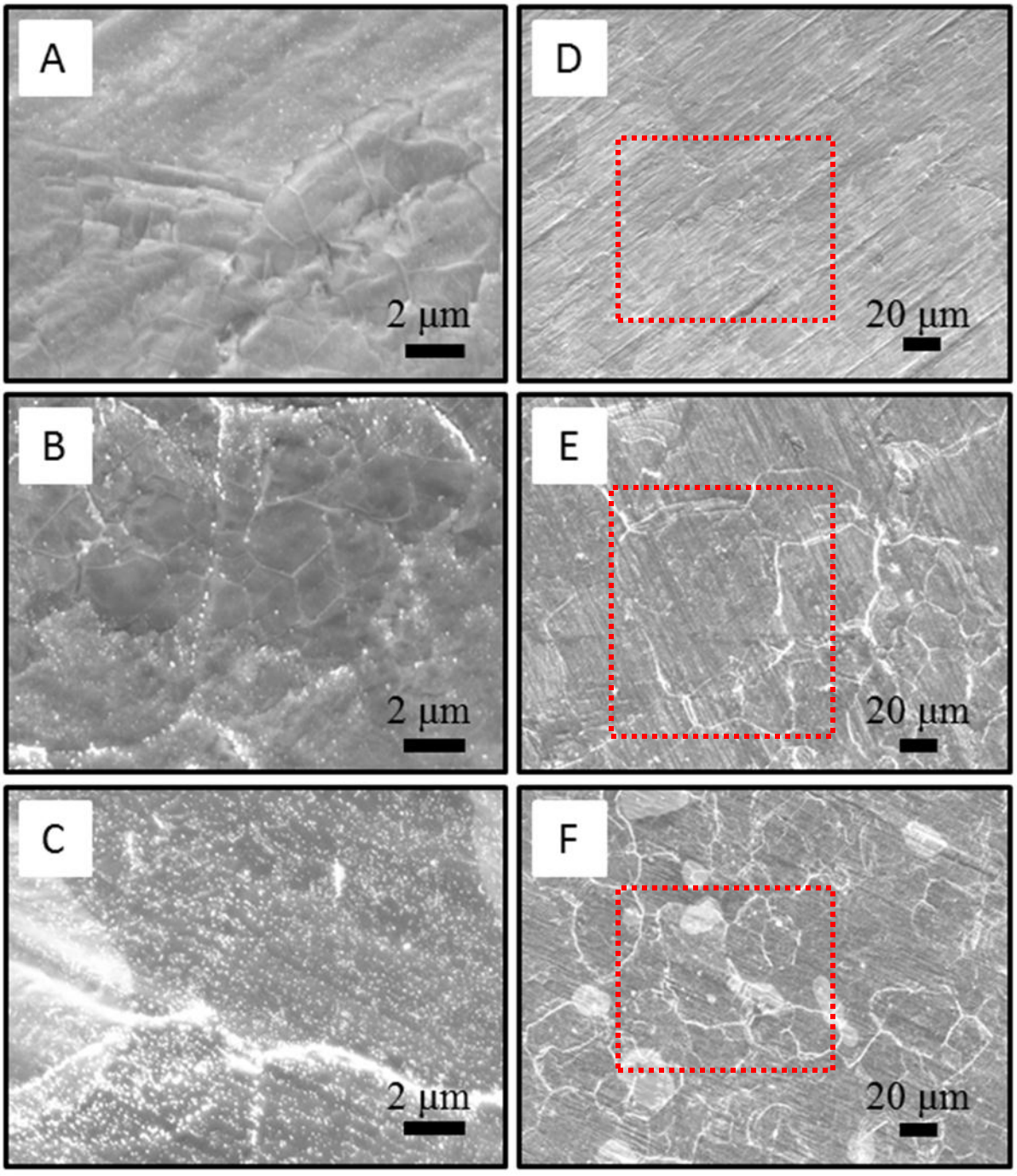

Figure 5.8 SEM images showing synthesis of graphene on Ni-substrate grown for (A, D) 10 minutes, (B, E) 20 minutes and (C, F) 30 minutes with growth parameters as stated in Table 5.5. The prominence of graphene grain is indicated by the structure of grain.

5.3.2.2 Effect of gas flow rate

The Raman spectrum Figure 5.9 shows the effect of flow rate of CH_4 when the temperature and time are kept constant. The growth conditions used were as indicated in the Table 5.6.

The intensity of the 2D peak in the Raman spectra as shown in the Figure 5.9 are very low when compared to that of the G peak suggesting that the graphene formed is composed multiple layers. This suggests that the segregation of carbon is so extensive that instead of forming few layers of graphene they combine and form graphite. One possible explanation could be the very low rate of H_2 used in the experiment and the second one could be the presence of impurities on the surface. As it is a surface segregation process, the presence of impurities affects the growth in nickel more radically when compared to growth over copper. The impurities cause the graphene to grow as islands thus segregating more carbon at the same area forming graphite. Also the amount of carbon segregating to the surface is determined by the rate of cooling and not the flow rate of CH_4 during the growth process. Thus minimum flow rate is optimum as the results are the same for increasing carbon rates.

Table 5.6 Parameters to study the effect of different rate of flow of CH_4.

CH_4 rate (SCCM)	Temperature (°C)	Time (min)	H_2 rate (SCCM)	I_D/I_G	I_{2D}/I_G
10	950	10	200	0	0.49
50	950	10	200	0	0.41
80	950	10	200	0	0.15
120	950	10	200	0	0.51

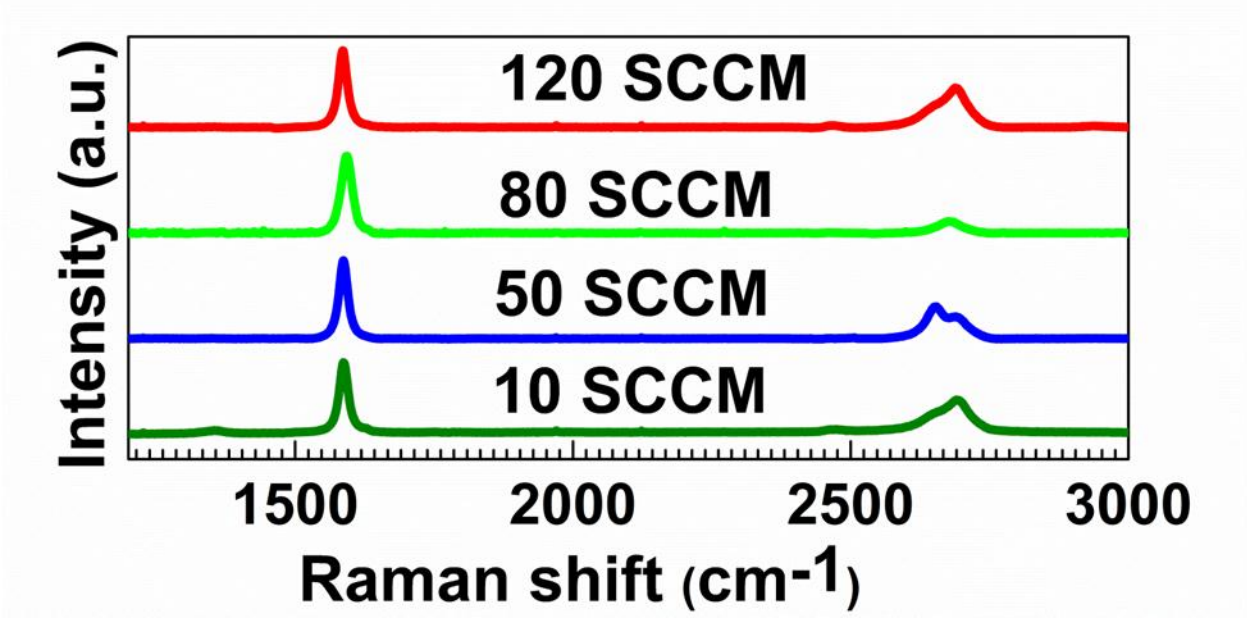

Figure 5.9 Representative Raman spectra collected for samples grown under varying CH_4 flow rates ranging from 10 SCCM to 120 SCCM (flow rate of H_2 was constant). The samples were grown using parameters as stated in Table 5.6 with the modified procedure. The relative intensity of the 2D peak indicates that this procedure yielded only multilayer graphite instead of graphene for all flow rates.

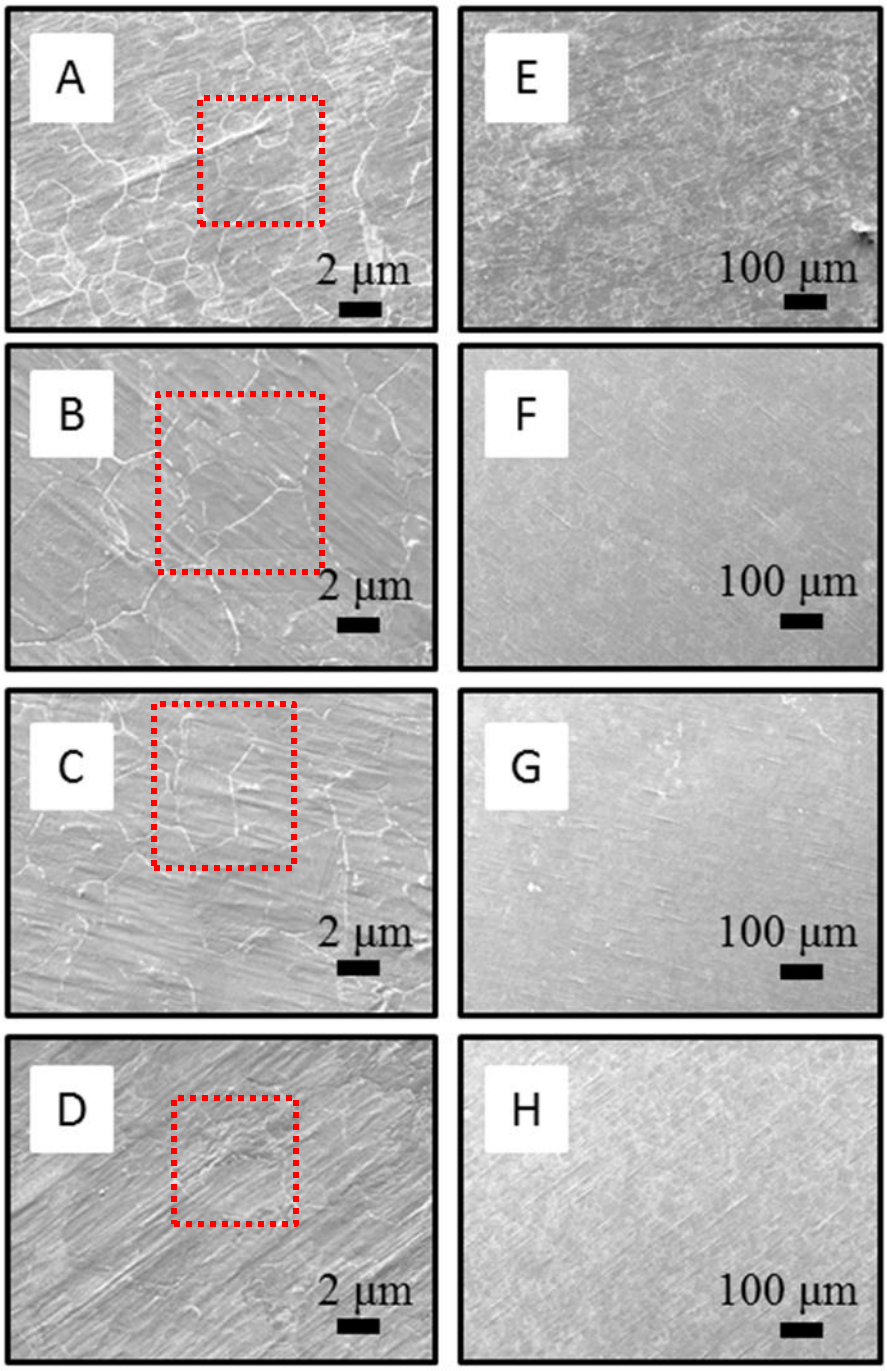

Figure 5.10 SEM images of synthesized graphene layers on Ni-substrate grown with varying CH_4 flow rates of (A, E) 10 SCCM, (B, F) 50 SCCM, (C, G) 80 SCCM and (D, H) 120 SCCM with growth parameters as stated in Table 5.6. The images show that the grain size, indicated by box, did not show dependence on CH_4 flow rate.

5.4 Steps involved in transfer of graphene to non-metallic substrates

Transfer of grapheme from Ni to an insulating substrate is very similar to that of transfer from Cu substrate. In a similar method as that of the copper process the substrate, which has graphene on the surface after growth is completed, is spin coated with a very thin layer of polymers like poly(methyl methacrylate) (PMMA) or Polydimethylsiloxane (PDMS).

The substrate is then baked for about 10 min in an oven maintained at 120 °C. The side that was not spin coated it blazed with oxygen plasma so that the graphene in the other side is etched away. This foil is then placed in a ferric chloride etch solution. Once the nickel is etched away the PMMA is scooped out of the solution and is rinsed with DI water a couple of time and is scooped out onto the required substrate. Once the substrate is dry then it is rinsed with acetone to dissolve the PMMA. Then the chip is dried to obtain a clean layer of graphene on the desired substrate. The difference is the use of ferric chloride for etching the nickel.

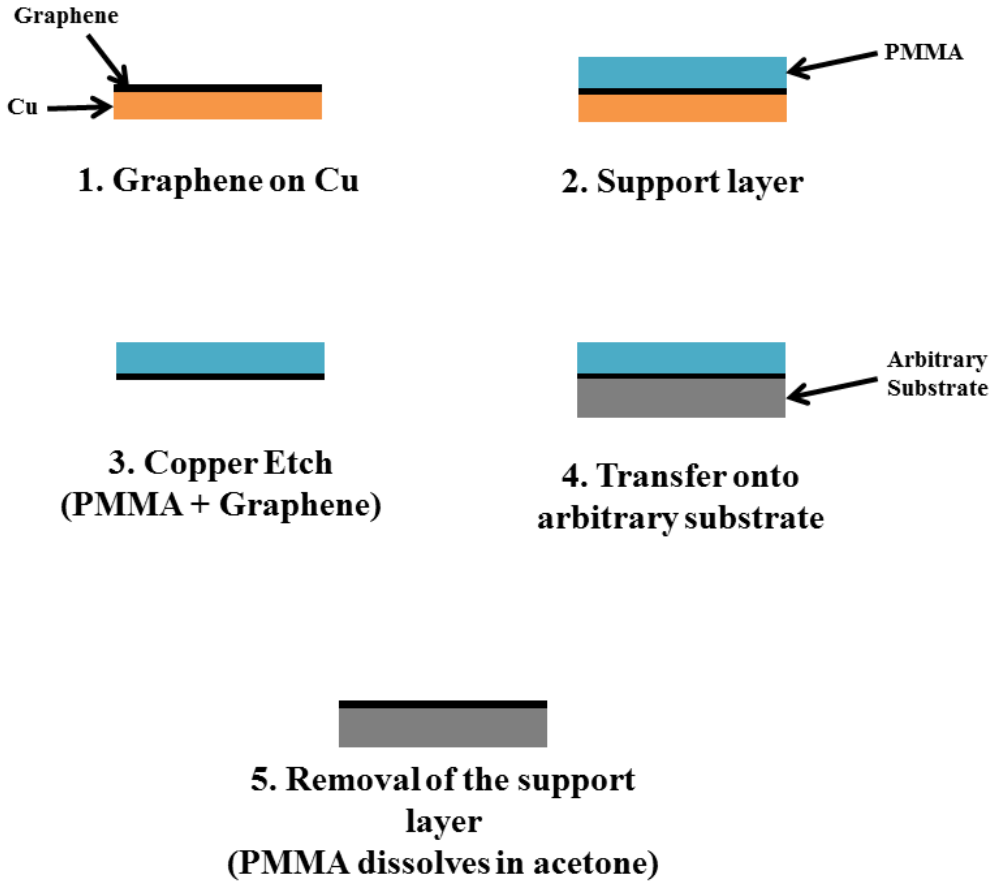

Figure 5.11 The schematic illustrates transfer process of graphene from copper to an arbitrary substrate.

5.5 References

1. Hayes and J. Chipman, Trans. Am. Inst. Min., Metall. Pet. Eng. 135, 85 , 1939.
2. Chuhei Oshima and Ayato, N., 1997, "Ultra-thin epitaxial films of graphite and hexagonal boron nitride on solid surfaces," Journal of Physics: Condensed Matter, 9(1), p. 1.
3. A.Ya, T., 1991, "Carbon on transition metal surfaces," Progress in Surface Science, 38(3-4), pp. 201-429.
4. Yu, Q., Lian, J., Siriponglert, S., Li, H., Chen, Y. P., and Pei, S.-S., 2008, Graphene segregated on Ni surfaces and transferred to insulators, AIP.
5. Li, X., Cai, W., Colombo, L., and Ruoff, R. S., 2009, "Evolution of Graphene Growth on Ni and Cu by Carbon Isotope Labeling," Nano Letters, 9(12), pp. 4268-4272.
6. Kim, K. S., Zhao, Y., Jang, H., Lee, S. Y., Kim, J. M., Kim, K. S., Ahn, J.-H., Kim, P., Choi, J.-Y., and Hong, B. H., 2009, "Large-scale pattern growth of graphene films for stretchable transparent electrodes," Nature, 457(7230), pp. 706-710.

Chapter 6 - Conclusion and Future work

The thesis provides a reference for growth of large-area graphene films and their characterization. It acts as a good starting point in producing high quality graphene using APCVD. All through the thesis Raman spectroscopy was utilized to ascertain the quality of graphene as well as to confirm the presence of strain and disorder in the graphene sheet. In this work, a carbon nanotube CVD furnace was modified to mass produce, large area graphene using fast heating and fast cooling hence reducing the overall time required for graphene synthesis.

Experiments on CVD grown graphene showed the importance of different growth parameters. First set of experiments involved synthesis of graphene using standard growth procedures available in the literature. Graphene synthesized at higher temperature caused an increase in density and size domains of graphene. Raman of the samples had a blue shift of the 2D peak which was attributed to isotropic compressive strain induced by copper while cooling. Double resonance theory was also employed to explain this effect. Secondly, under prevailing conditions the growth of graphene had achieved coverage of the entire area at around 15 minutes of growth. Longer growth time ended with similar results. Finally, the effect of flow rate of gasses was discussed. It was shown that higher flow rates of CH_4 resulted in an increase in the number of layers which was correlated by Raman spectroscopy. The effect of flow rate of hydrogen was also discussed. Very high flow rate resulted in etching of carbon atoms from the ends of graphene.

Second set of experiments were conducted following fast heating/cooling. The growth period for the modified procedure (type I) in which the sample was quenched from 950^0C to room

temperature as soon as the growth period is completed was studied. It was found that the carbon forms multiple layers at the stage of nucleation itself and as the time of growth increases the size of grain increases. Thus the optimum growth time was around 6 minutes. The gas flow rate do not have a predominant effect in determining the number of layers of graphene. Because of the lack of period of cooling, the time of flow of gasses is reduced down to the period of growth only. The Raman spectra and also SEM images did not show any difference in the number of layers or the grain size of graphene. A flow rate of below 10 SCCM is enough to cover the entire surface of the catalyst.

Next the growth of graphene on copper using the modified procedure-type II (fast heating/cooling) was studied. The results were not at all similar to previously obtained results. Because of the reduction of annealing time in the new modified procedure annealing of substrate occurs during the period of growth. Because of the presence of impurities the growth of graphene layers gets interrupted and they form small islands of multiple layers. Because of the absence of annealing cycle and also cooling cycle the growth period is the only time at which the gasses are reactive, which results in lack of gasses during the growth process. Thus higher flow rate of CH_4 is required to optimize the growth of graphene.

In the fifth chapter of the thesis, nickel a material well known to be capable of synthesizing graphene using CVD was studied. In the first part of the chapter, standard procedure which involved annealing the substrate was studied. Results showed that high temperature, high hydrogen-gas content of sources and shorter growth times were the key factors for low-defect, few layer graphene growth. Later, the modified procedure was employed to study the effect of duration of growth and CH_4 flow rate for samples that did not go through the annealing cycle in

the CVD process. It was observed that the above mentioned parameters had little or no effect on the quality of graphene synthesized using the modified procedure. This may be due to the fact that the method of synthesis of graphene on Ni is by surface segregation and the presence of impurities on the surface of the substrate, unlike Cu substrate, greatly affected the synthesis process.

Thus, in conclusion we have studied synthesis of graphene on copper extensively using the standard procedure and two modified procedures and have shown that the growth of graphene on copper is actually a very short process. The optimum process parameters for few layer controlled growth of graphene were found to be as follows.

- Procedure – Modified procedure (Type II)
- Temperature – 950 °C
- Time – 30 minutes
- CH_4 flow rate – 20 SCCM
- H_2 flow rate – 300 SCCM

This knowledge provides a fast method which could be used to synthesize graphene on an industrial basis using batch process by which high quality graphene films can be mass produced.

In terms of graphene growth on nickel, it was found that it was very important for nickel substrate to be annealed before the growth process could begin. So, more experiments have to be

carried out to study the effect of change in parameters in the modified procedure to produce high quality graphene films.

Based on the modified procedures, the study on growth of graphene can be expanded to include other source of carbon like ethylene or solid carbon sources like sugars, carbon black, etc. Each of these new sources would provide the knowledge that might lead to a large scale production of graphene using the modified procedure. It has been known that synthesis of graphene under low pressure yields mono-layered graphene. With this knowledge, the modified procedure could be extended to the Low Pressure Chemical (LPCVD) to synthesis mono-layered graphene in industrial quantities. Effect of fast heating and cooling will also be studied on Cu and Ni based alloys.